
From: Jennifer Becket [jbecket@owenbird.com]
Sent: Wednesday, November 28, 2012 10:23 AM
To: Commission Secretary BCUC:EX
Subject: FW: FortisBC AMI, Project No. 3698682 - CEC IR #2 (Email #4)
Attachments: DOC.PDF; DOC.PDF; DOC.PDF

It has come to our attention that the four attachments for Appendix H sent in our email below may have been all the same document. In that regard, attached please find Appendix H (in three parts) to the CEC's IR #2 for the above-noted proceeding.

Can you kindly confirm that the attached Appendix H will replace the document filed in our email below.

Thank you,

Jennifer Becket,
Legal Assistant to Christopher P. Weafer,
J. David Dunn and Jocelyn Le Dressay
c/o Owen Bird Law Corporation
2900 - 595 Burrard Street
Vancouver, B.C.
V7X 1J5

Direct Line: (604) 697-5610
Direct Fax: (604) 641-4707
E-mail: jbecket@owenbird.com

From: Jennifer Becket **On Behalf Of** Christopher P. Weafer
Sent: Friday, November 23, 2012 5:11 PM
To: Commission Secretary (Commission.Secretary@bcuc.com)
Cc: dwcraig@allstream.net; 'alex.atamanenko.c1@parl.gc.ca'; 'alex.atamanenko@parl.gc.ca'; 'ashadra@telus.net'; 'bchydroregulatorygroup@bchydro.com'; 'bcjoey68@gmail.com'; 'bharper@econanalysis.ca'; 'bmerwin@mercerint.com'; 'curtis@thermoguy.com'; 'david@legalmind.ca'; 'Dennis.Swanson@fortisBC.com'; 'ekung@bcpiac.com'; 'electricity.regulatory.affairs@fortisbc.com'; 'fredweislaw@gmail.com'; 'guylerox2@gmail.com'; 'jerryjgf@shaw.ca'; 'kemiles@telus.net'; 'lerouxconsulting@shaw.ca'; 'ngabana@gmail.com'; 'rhobbs@shaw.ca'; 'shonnahayes@shaw.ca'; 'support@bcpiac.com'; 'tbraithwaite@bcpiac.com'; 'thackney@shaw.ca'; 'wjandrews@shaw.ca'; 'zerowaste@shaw.ca'
Subject: FortisBC AMI, Project No. 3698682 - CEC IR #2 (Email #4)

Attachment 4: Appendix H (Part 1 of 4)
Attachment 5: Appendix H (Part 2 of 4)
Attachment 6: Appendix H (Part 3 of 4)
Attachment 7: Appendix H (Part 4 of 4)

Best regards,

Christopher P. Weafer
Owen Bird Law Corporation
2900, 595 Burrard Street
P.O. Box 49130
Vancouver, B.C.
V7X 1J5

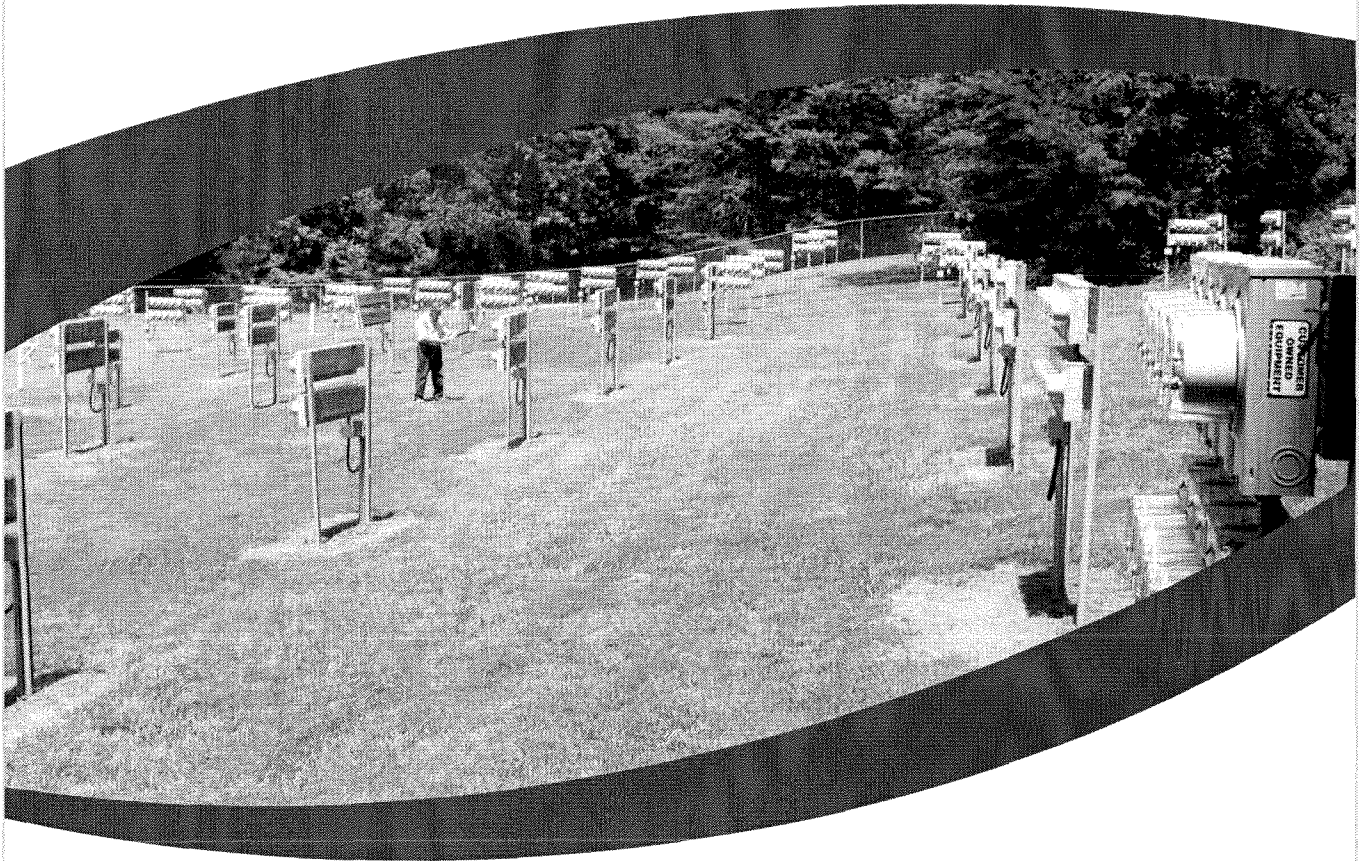
Direct Tel: 604-691-7557
Direct Fax: 604-632-4482
Email: cweafer@owenbird.com

This e-mail may contain privileged and confidential material and its transmission is not a waiver of that privilege. It is intended for the sole use of the person to whom it is addressed. Any copying, disclosure, distribution or reliance on this material by anyone other than the intended recipient is strictly prohibited. We assume no responsibility to persons other than the intended recipient. If you have received this transmission in error, please notify Owen Bird Law Corporation immediately and destroy any hard copies you may have printed and remove all copies of the e-mail from your mailbox and hard drives.
*** Do not remove to ensure timely delivery OBLCXAUTHHDR ***

APPENDIX H
Electrical Power Research Institute, An Investigation of Radio Frequency Fields
Associated with the Itron Smart Meter, Technical Report 2010

See attached.

An Investigation of Radiofrequency Fields Associated with the Itron Smart Meter



An Investigation of Radiofrequency Fields Associated with the Itron Smart Meter

EPRI Project Manager
G. Mezei



3420 Hillview Avenue
Palo Alto, CA 94304-1338
USA

PO Box 10412
Palo Alto, CA 94303-0813
USA

800.313.3774
650.855.2121

askepri@epri.com

www.epri.com

1021126

Final Report, December 2010

DISCLAIMER OF WARRANTIES AND LIMITATION OF LIABILITIES

THIS DOCUMENT WAS PREPARED BY THE ORGANIZATION(S) NAMED BELOW AS AN ACCOUNT OF WORK SPONSORED OR COSPONSORED BY THE ELECTRIC POWER RESEARCH INSTITUTE, INC. (EPRI). NEITHER EPRI, ANY MEMBER OF EPRI, ANY COSPONSOR, THE ORGANIZATION(S) BELOW, NOR ANY PERSON ACTING ON BEHALF OF ANY OF THEM:

(A) MAKES ANY WARRANTY OR REPRESENTATION WHATSOEVER, EXPRESS OR IMPLIED, (I) WITH RESPECT TO THE USE OF ANY INFORMATION, APPARATUS, METHOD, PROCESS, OR SIMILAR ITEM DISCLOSED IN THIS DOCUMENT, INCLUDING MERCHANTABILITY AND FITNESS FOR A PARTICULAR PURPOSE, OR (II) THAT SUCH USE DOES NOT INFRINGE ON OR INTERFERE WITH PRIVATELY OWNED RIGHTS, INCLUDING ANY PARTY'S INTELLECTUAL PROPERTY, OR (III) THAT THIS DOCUMENT IS SUITABLE TO ANY PARTICULAR USER'S CIRCUMSTANCE; OR

(B) ASSUMES RESPONSIBILITY FOR ANY DAMAGES OR OTHER LIABILITY WHATSOEVER (INCLUDING ANY CONSEQUENTIAL DAMAGES, EVEN IF EPRI OR ANY EPRI REPRESENTATIVE HAS BEEN ADVISED OF THE POSSIBILITY OF SUCH DAMAGES) RESULTING FROM YOUR SELECTION OR USE OF THIS DOCUMENT OR ANY INFORMATION, APPARATUS, METHOD, PROCESS, OR SIMILAR ITEM DISCLOSED IN THIS DOCUMENT.

The following organization, under contract to EPRI, prepared this report:

Richard Tell Associates, Inc.

NOTE

For further information about EPRI, call the EPRI Customer Assistance Center at 800.313.3774 or e-mail askepri@epri.com.

Electric Power Research Institute, EPRI, and TOGETHER...SHAPING THE FUTURE OF ELECTRICITY are registered service marks of the Electric Power Research Institute, Inc.

Copyright © 2010 Electric Power Research Institute, Inc. All rights reserved.

Acknowledgments

The following organization, under contract to the Electric Power Research Institute (EPRI), prepared this report:

Richard Tell Associates, Inc.
1872 E. Hawthorne Avenue
Colville, WA 99114

Principal Investigator
R. Tell

This report describes research sponsored by EPRI and overseen by Gabor Mezei, MD, Ph.D, EPRI's Program Manager for the EMF and RF Health Assessment and Safety Program. Expertise, review and comment were provided by a cross-functional team at EPRI including Rob Kavet, D.Sc., Senior Technical Executive; Chris Melhorn, Program Manager; Kermit Phipps, Project Engineer/Scientist and Brian Seal, Senior Project Manager, EPRI.

Numerous individuals from Southern California Edison (SCE) Electric Company conducted and supported the measurement work reported here in both South Carolina and California: Glenn Sias, Manager, SCE EMF and Energy Group; Al Vazquez, Enterprise Network Architect, SmartGrid Engineering; Kevin Nesby, Project Manager in the Edison SmartConnect™ Deployment Program; Brian Thorson, EMF Specialist in the Operations Support Business Unit; Jack Sahl, Director of Operations Support in the SCE Operations Support Business Unit; and John Bubb, Manager of Product Management for SCE SmartConnect.

Background information on operational characteristics of smart meters was provided by Vijay Lakkasetty, System Engineering & Operations - Smart Meter Project, Jay Xu, Principal Engineer, and Jim Turman, Program Manager, Department & Employee Readiness, Safety and Emergency Services, all of San Diego Gas and Electric Company.

As further described within the report, testing support, facility access and cooperation was provided by Itron, which facilitated this work, particularly by Dan Lakich, Design & Development Manager, Electricity Metering; Mike Belanger, Product Line Manager, Itron OpenWay Network Communications; Sudhir Thumaty, R&D Manager; Suresh Kumar Yada, Design Engineer; Ben Smith, Engineer; Ken Prevatte, Project Director; and Matthew DeCubellis, Application Engineer.

This publication is a corporate document that should be cited in the literature in the following manner:

*An Investigation of Radiofrequency Fields
Associated with the Itron Smart Meter*
EPRI, Palo Alto, CA: 2010. 1021126

Product Description

Smart meters represent one component of the advanced metering infrastructure (AMI). Although data to and from smart meters may be transmitted through wired connections, many smart meters make use of miniature, low power radio transceivers to wirelessly communicate with the electric utility and with the Home Area Network (HAN) that provides home owners with the ability to interact with electrical appliances and systems within the home. Deployment of smart meters has raised concerns by members of the public about possible adverse health effects that could be related to exposure to the radiofrequency (RF) emissions of the meters. As part of on-going efforts to address public concerns on this issue, this report documents the collection of information on RF exposure related to the operation of two particular models of Smart Meter produced by Itron Inc.

Results & Findings

The smart meters studied in this report are currently being deployed by two electric utilities in California. The meters are part of wireless mesh networks in which one meter is configured as a collector point, referred to as a "cell relay" by Itron, for each of approximately 500 to 750 "end point meters." The cell relay collects data from the various end point meters and conveys these data onto the cellular wireless wide area network (WWAN) for communication back to the electric utility company's data management system. Mesh network communication among the many meters is provided by the 900 MHz band transceiver RF LAN (local area network). A HAN feature is supported by a 2.4 GHz transceiver.

Data collection was carried out in a laboratory setting and at residences and in neighborhoods in southern California and Colville, Washington, supplemented with theoretical modeling studies. The results indicate that RF field from the investigated smart meter are well below the maximum permitted exposure (MPE) established by the Federal Communications Commission (FCC). For instance, at one foot, the RF field from an end point meter would be expected to not exceed 0.8% of the MPE established by the Federal Communications Commission (FCC). For the cell relay, the RF field would not exceed 0.2% of the MPE. Even at very close distances, such as one foot directly in front of the meter, with an unrealistic assumption that the transmitters operate at 100% duty cycle, the resulting exposure is less than the FCC MPE. When viewed in the context of a typical, realistic exposure distance of 10 feet, the RF fields are much smaller, about 0.008% for the end point meter and about 0.002% of MPE for the cell relay. For occupants of a home equipped with a Smart Meter, interior RF fields would be expected to be at least ten times less intense simply due to the directional properties of the meter. When the attenuation afforded by a stucco home's construction is included, a realistic

value of the interior RF field would be about 0.023% of the MPE for an end point meter and about 0.065% for a cell relay. Regardless of duty cycle values for end point and cell relay meters, typical exposures that result from the operation of smart meters are very low and comply with scientifically based human exposure limits by a wide margin.

Challenges & Objective(s)

This report is focused on the RF aspects of smart meters and in particular, the strength of the transmitted RF fields that may be produced by the meters from a human exposure perspective. The greatest difficulty in arriving in determining realistic time-averaged exposure from smart meters is associated with determining transmitter duty cycles since the meters only emit RF radiation at intervals

Applications, Values & Use

This report documents an investigation of the characteristics of RF fields associated with Itron Smart Meter. The project was undertaken to improve understanding of public exposure to the RF emissions produced by smart meters and to respond to public concerns about potential health effects.

EPRI Perspective

Measuring electric energy consumption with so-called smart meters in residential and commercial environments is becoming more commonplace as part of the development of Advanced Metering Infrastructure (AMI) in the electric utility industry. With the deployment of smart meters public concern was raised about potential health effects associated with RF emissions from smart meters EPRI is responding to these concerns with research efforts to provide objective information on RF emissions related to smart meters.

Approach

The project team conducted laboratory and field measurements of the RF emissions of Itron smart meters. A key objective was to determine realistic estimates of the operational duty cycle of meter transmitters. The team also investigated the effectiveness of metal meshes and stucco walls in shielding smart meters.

Keywords

Smart meters
Radiofrequency emissions
EMF health assessment
Environmental issues

Table of Contents

Section 1: Summary	1-1
Section 2: Introduction and Background.....	2-1
Smart Meters as RF Sources.....	2-1
How Smart Meters are Deployed	2-2
Section 3: Objective of Investigation	3-1
Section 4: Technical Approach to Investigation	4-1
Measurements at Itron	4-1
Measurements in residential locations.....	4-1
Measurements in Colville, WA	4-2
Section 5: Transmitter Powers.....	5-1
Section 6: The Measurement Challenge Presented by Smart Meters.....	6-1
Section 7: Measurement Methods and Instrumentation.....	7-1
Section 8: Laboratory Pattern Measurements	8-1
Section 9: Smart Meter Field Measurements	9-1
Meter farm measurements	9-1
Individual meters	9-2
Groups of meters	9-8
Residential settings	9-15
Homes.....	9-15
Residential apartment setting.....	9-25
Neighborhoods with and without Smart Meters	9-29
Section 10: Shielding Effectiveness Measurements... 10-1	
Shielding effectiveness of different metal meshes.....	10-1
Shielding effectiveness of a simulated stucco wall	10-4
Section 11: Spatial Variation of RF Fields	11-1
Section 12: Operational Duty Cycle of Meter Transmitters	12-1
SRM-3006 measurements of peak and average values.....	12-1
Wi-Spy spectrum analyzer measurements	12-3
SCE Smart Meter Network Management System.....	12-7
SDG&E Smart Meter Network Management System.....	12-9

Section 13: Ancillary Measurements	13-1
Microwave Oven	13-1
Cordless telephone.....	13-2
Wireless router	13-3
Measurement comparison (Model B8742D probe and SRM-3006).....	13-4
Section 14: Theoretical Analysis of RF Fields.....	14-1
Section 15: RF Exposure Limits.....	15-1
FCC	15-1
IEEE.....	15-2
ICNIRP.....	15-3
Section 16: Discussion of Results and Insights	16-1
Section 17: Conclusions	17-1
Appendix A: Instrument Calibration Certificates	A-1
Appendix B: SRM-3006 900 MHz Spectrum Measurement Scans (meter farm)	B-1
Appendix C: SRM-3006 900 MHz Spectrum Measurements Scans (rear of meters)	C-1
Appendix D: SRM-3006 2.4 GHz Spectrum Measurement Scans (meter farm)	D-1
Appendix E: SRM-3006 2.4 GHz Spectrum Measurement Scans (rear of meters).....	E-1
Appendix F: Photos of Simulated Stucco Wall During Construction.....	F-1
Appendix G: Modeling of RF fields of a 915 MHz Dipole for Spatial Averaging	G-1
Appendix H: Glossary of Terms	H-1

List of Figures

Figure 1-1 Calculated RF fields near Itron end point and cell relay meters based on 99th percentile transmitter power values, main beam exposure (point of maximum RF field), inclusion of the possibility of ground reflected fields and an assumed 99th and 99.9th percentile duty cycles.	1-4
Figure 2-1 Photo of Itron Smart Meter.	2-2
Figure 2-2 Simplistic illustrative diagram of an RF mesh network. Each end point also provides a Home Area Network (HAN) feature. The cell relay acts as a collector point for multiple meters distributed in a neighborhood and transmits received data onto a cellular wireless wide area network (WWAN).	2-3
Figure 2-3 Cell relay meter with flexible, dual band (850 MHz and 1900 MHz) antenna affixed to interior surface of the meter cover.	2-4
Figure 5-1 Accumulative fraction of 900 MHz RF LAN transmitter output power vs. transmitter power for a sample of 200,000 units. The median transmitter power is approximately 24.1 dBm (257 mW).	5-1
Figure 5-2 Number of 900 MHz RF LAN transmitters with powers within selected ranges. The transmitter power mode is approximately 24.5 dBm (282 mW).	5-2
Figure 5-3 Accumulative fraction of 2.4 GHz Zigbee transmitter output power vs. transmitter power for a sample of 200,000 units. The median transmitter power is approximately 18.2 dBm (66.1 mW).	5-3
Figure 5-4 Number of 2.4 GHz Zigbee transmitters with powers within selected ranges. The transmitter power mode is approximately 18.5 dBm (70.8 mW mW).	5-4
Figure 7-1 Close up view of dual axis antenna positioner system used to obtain antenna patterns of Smart Meter transmitters.	7-1
Figure 7-2 Interior of anechoic chamber showing reception horn antenna with Smart Meter on antenna positioner in background. During pattern measurements, the spectrum analyzer shown below the Smart Meter is removed.	7-2
Figure 7-3 Instrumentation system for acquiring antenna pattern data.	7-3

Figure 7-4 Frequency shaped, isotropic, electric field probe and meter (Narda B8742D and Narda 8715 meter).	7-4
Figure 7-5 Selective radiation meter (Narda Model SRM-3006).	7-5
Figure 7-6 Wi-Spy USB spectrum analyzer connected to a notebook computer running software to operate the analyzer (Chanalyzer version 3.4) and an external yagi antenna.....	7-6
Figure 8-1 Azimuth plane pattern of the 900 MHz RF LAN transmitter configured in an end point meter showing the horizontal, vertical and total pattern as viewed from bottom of meter. The scale is in dB with the maximum field at the outer edge of the pattern circle.	8-2
Figure 8-2 Azimuth plane view of the total EIRP of the 900 MHz RF LAN transmitter configured in an end point meter.	8-3
Figure 8-3 Elevation plane pattern of the 900 MHz RF LAN transmitter in an end point meter showing the horizontal, vertical and total pattern. The scale is in dB with the maximum field at the outer edge of the pattern circle.	8-3
Figure 8-4 Elevation plane view of the total EIRP of the 900 MHz RF LAN transmitter in an end point meter.....	8-4
Figure 8-5 Azimuth plane pattern of the 900 MHz RF LAN transmitter in a cell relay showing the horizontal, vertical and total pattern as viewed from bottom of meter. The scale is in dB with the maximum field at the outer edge of the pattern circle.....	8-5
Figure 8-6 Azimuth plane view of the total EIRP of the 900 MHz RF LAN transmitter configured in a cell relay.	8-5
Figure 8-7 Elevation plane pattern of the 900 MHz RF LAN transmitter in a cell relay meter showing the horizontal, vertical and total pattern. The scale is in dB with the maximum field at the outer edge of the pattern circle.	8-6
Figure 8-8 Elevation plane view of the total EIRP of the 900 MHz RF LAN transmitter in a cell relay meter.	8-6
Figure 8-9 Azimuth plane pattern of the 2.4 GHz Zigbee transmitter configured in an end point meter showing the horizontal, vertical and total pattern as viewed from bottom of meter. The scale is in dB with the maximum field at the outer edge of the pattern circle.	8-7
Figure 8-10 Azimuth plane view of the total EIRP of the 2.4 GHz Zigbee transmitter configured in an end point meter.	8-7
Figure 8-11 Elevation plane pattern of the 2.4 GHz Zigbee radio in an end point meter showing the horizontal, vertical and total pattern. The scale is in dB with the maximum field at the outer edge of the pattern circle.	8-8

Figure 8-12 Elevation plane view of the total EIRP of the 2.4 GHz Zigbee radio in an end point meter.	8-8
Figure 8-13 Azimuth plane pattern of the 2.4 GHz Zigbee transmitter configured in a cell relay meter showing the horizontal, vertical and total pattern as viewed from bottom of meter. The scale is in dB with the maximum field at the outer edge of the pattern circle.	8-9
Figure 8-14 Azimuth plane view of the total EIRP of the 2.4 GHz Zigbee transmitter configured in a cell relay meter.....	8-9
Figure 8-15 Elevation plane pattern of the 2.4 GHz Zigbee radio in a cell relay meter showing the horizontal, vertical and total pattern. The scale is in dB with the maximum field at the outer edge of the pattern circle.	8-10
Figure 8-16 Elevation plane view of the total EIRP of the 2.4 GHz Zigbee radio in a cell relay meter.....	8-10
Figure 8-17 Azimuth plane pattern of the 836.6 MHz GSM cellular transmitter in a cell relay meter showing the horizontal, vertical and total pattern as viewed from bottom of meter. The scale is in dB with the maximum field at the outer edge of the pattern circle.	8-11
Figure 8-18 Azimuth plane view of the total EIRP of a GSM 836.6 MHz cellular radio in a cell relay meter.	8-11
Figure 8-19 Elevation plane pattern of the 836.6 MHz GSM cellular transmitter in a cell relay meter showing the horizontal, vertical and total pattern as viewed from bottom of meter. The scale is in dB with the maximum field at the outer edge of the pattern circle.	8-12
Figure 8-20 Elevation plane view of the total EIRP of a GSM 836.6 MHz cellular radio in a cell relay meter.	8-12
Figure 8-21 Azimuth plane pattern of the 1880 MHz GSM PCS transmitter in a cell relay meter showing the horizontal, vertical and total pattern as viewed from bottom of meter. The scale is in dB with the maximum field at the outer edge of the pattern circle.....	8-13
Figure 8-22 Azimuth plane view of the total EIRP of a GSM 1880 MHz PCS radio in a cell relay meter.	8-13
Figure 8-23 Elevation plane pattern of the 1880 MHz GSM PCS transmitter in a cell relay meter showing the horizontal, vertical and total pattern as viewed from bottom of meter. The scale is in dB with the maximum field at the outer edge of the pattern circle.....	8-14
Figure 8-24 Elevation plane view of the total EIRP of a GSM 1880 MHz PCS radio in a cell relay meter.	8-14

Figure 9-1 Aerial view of the Itron meter farm in West Union, SC. Yellow lines represent rows of Smart Meters grouped, generally, as racks of ten meters each. Photo courtesy of Itron. 9-1

Figure 9-2 Typical rack of ten meters shown in the western part of the Itron meter farm. 9-2

Figure 9-3 Layout of Smart Meter rack showing designated meter locations and frequency of various meters (L, M and H - see text) for the 900 MHz RF LAN and 2.4 GHz Zigbee transmitters. 9-3

Figure 9-4 Use of the broadband field probe with a cardboard spacer attached to the probe near meters in a rack of ten meters. 9-4

Figure 9-5 Corrected broadband probe RF field readings of the 900 MHz RF LAN transmitters from ten Smart Meters at the surface and at 20 cm and 30 cm from the meter. 9-5

Figure 9-6 Corrected broadband probe RF field readings of the 2.4 GHz Zigbee transmitters from ten Smart Meters at the surface and at 20 cm from the meter. 9-8

Figure 9-7 Using the Narda SRM-3006 to measure aggregate RF fields near a rack of ten meters programmed for fixed frequency, continuous transmission in the meter farm..... 9-9

Figure 9-8 900 MHz band composite RF field from rack of 10 SmartMeters at 1 foot. 9-10

Figure 9-9 Field measurements at successively greater distances behind the subject meter rack resulted in closer proximity to other meter racks with the probability of detecting stronger, but intermittent, signals due to the ambient background..... 9-11

Figure 9-10 Spectrum measurement of 2.4 GHz RF fields from ten simultaneously transmitting Smart Meters. 9-12

Figure 9-11 Integrated, total composite RF field obtained in meter farm for emissions from the 900 MHz RF LAN and 2.4 GHz Zigbee transmitters operating simultaneously in the vicinity of a meter rack (linear plot)..... 9-14

Figure 9-12 Integrated, total composite RF field obtained in meter farm for emissions from the 900 MHz RF LAN and 2.4 GHz Zigbee transmitters operating simultaneously in the vicinity of a meter rack (logarithmic plot)..... 9-14

Figure 9-13 SCE meter technician replacing existing Smart Meter with specially programmed meter for residential measurements. 9-16

Figure 9-14 Planar scans were performed at several distances in front of a residential Smart Meter by slowly moving the SRM-3006 within a plane at a fixed distance..... 9-17

Figure 9-15 Interior residential measurements included measurements on the opposite side of the wall where the Smart Meter was installed at the home..... 9-19

Figure 9-16 Residential measurements at residence A included both outdoors and indoors measurements of RF fields in both the 900 MHz and 2.4 GHz bands..... 9-20

Figure 9-17 Measurements at residence A included exterior locations in the backyard. 9-21

Figure 9-18 Residence B in Downey, CA where indoor and outdoor measurements were made with specially programmed Smart Meters installed to facilitate measurements. 9-22

Figure 9-19 Performing a planar scan of RF fields adjacent to a Smart Meter at residence B. 9-23

Figure 9-20 Measured RF fields inside residence B, similar to residence A, tended to be predominated by signals produced by wireless routers used for Internet connectivity throughout the home. 9-24

Figure 9-21 A nine-meter bank at an apartment house in Downey, CA..... 9-26

Figure 9-22 An eleven-meter bank at an apartment house in Downey, CA..... 9-27

Figure 9-23 Measured maximum (peak) and average RF fields in the 900 MHz band at one foot in front of a nine-meter bank of Smart Meters. 9-28

Figure 9-24 Measured maximum (peak) and average RF fields in the 900 MHz band at one foot in front of an eleven-meter bank of Smart Meters. 9-28

Figure 9-25 Route in Downey, CA neighborhood with SCE deployed Smart Meters over which a driving survey was conducted to test the ability to detect RF signals associated with residential meter installations. 9-29

Figure 9-26 Conducting a “driving survey” of a Smart Meter deployed neighborhood..... 9-30

Figure 9-27 Measured peak spectrum of RF fields detected with the SRM-3006 during traveling the route mapped in Figure 9-25. Fields were monitored for a total of approximately 34 minutes. 9-31

Figure 9-28 Route in Santa Monica, CA neighborhood where SCE Smart Meters have not been deployed over which a driving survey was conducted to test the ability to detect RF signals that might exist in the 900 MHz band. 9-32

Figure 9-29 Spectrum scan in residential neighborhood of Santa Monica, CA consisting of an approximately 20 minute drive. The single peak near 912 MHz is an apparent internal spurious signal due to the SRM-3006 electronics and not caused by external RF fields.....	9-32
Figure 9-30 Spectrum scan in residential neighborhood of Santa Monica, CA showing weak signals, apparently caused by 900 MHz cordless telephones.	9-33
Figure 9-31 Spectrum scan in a commercial district of Santa Monica, CA showing noticeable activity from devices other than Smart Meters.	9-33
Figure 9-32 Spectrum scan of the FM radio broadcast band in Santa Monica, CA with a band integrated RF field equivalent to 0.013% of the FCC MPE for the public.	9-34
Figure 9-33 Spectrum scan of the 800 MHz to 900 MHz band in Santa Monica, CA, with a band integrated RF field equivalent to 0.012% of the FCC MPE for the public.	9-35
Figure 9-34 Spectrum scan of the 1.9 GHz to 2.0 GHz band in Santa Monica, CA, with a band integrated RF field equivalent to 0.103% of the FCC MPE for the public.	9-35
Figure 9-35 Spectrum scan of the 50 MHz to 216 MHz band in Santa Monica, CA, with a band integrated RF field equivalent to 0.036% of the FCC MPE for the public.	9-36
Figure 9-36 Spectrum scan of the 2.4 GHz to 2.5 GHz band in Santa Monica, CA, with a band integrated RF field equivalent to 0.0026% of the FCC MPE for the public.	9-36
Figure 10-1 Measurement setup to determine the insertion loss presented by a conductive mesh (chicken wire in this case).....	10-2
Figure 10-2 Measurement setup to determine the insertion loss presented by a conductive mesh (chicken wire in this case).....	10-3
Figure 10-3 Insertion loss of three different metal mesh sizes. ...	10-3
Figure 10-4 Measurement setup for determining insertion loss of simulate stucco wall shown with the 900 MHz yagi antenna.....	10-5
Figure 10-5 Measurement setup for determining insertion loss of simulate stucco wall shown with the 2.4 GHz yagi antenna.....	10-6
Figure 10-6 Illustrative display of the Wi-Spy spectrum analyzer display showing the captured average signal measured over a period of 81 seconds from a 900 MHz RF LAN Smart Meter transmitter. In this measurement, the simulated wall was not present. Marker readout data are shown on the right side of the display.	10-7

Figure 11-1 Vertical spatial variation in Smart Meter 900 MHz RF LAN field from 0 to 6 feet above the floor at a lateral distance from the Smart Meter of approximately 1 foot.....	11-1
Figure 11-2 Vertical spatial variation in Smart Meter 2.4 GHz Zigbee transmitter field from 0 to 6 feet above the floor at a lateral distance from the Smart Meter of approximately 0.5 feet.....	11-2
Figure 12-1 Measurements of aggregate maximum and average RF fields found along two rows of Smart Meters in the Itron meter farm during normal operation of the meters.....	12-2
Figure 12-2 Spectrum analysis measurement of RF fields during walk through section of the Itron meter farm in which both the maximum (peak) field and the average field was measured.	12-3
Figure 12-3 Wi-Spy display of Smart Meter RF fields observed during 66 minute monitoring period beginning at 10:56 P.M. local time. The blue spectrum is the “max hold” spectrum showing the maximum received signal power detected during the entire monitoring period. The four peaks that stand out from all of the rest of the detected signals, because of close proximity of the Wi-Spy to the meter, represent the momentary emissions detected from the Smart Meter being studied. Lower level signal peaks (typically 20 to 30 dB lower) are from other smart meters in the neighborhood.	12-4
Figure 12-4 Wi-Spy display of Smart Meter RF fields observed during 115 minute monitoring period beginning at 9:25 P.M. local time.	12-5
Figure 12-5 Processed signal power values obtained with the Wi-Spy spectrum analyzer on November 4, 2010, in the Itron meter farm. The average values of the peak and average spectra were -51.8 dBm and the -88.1 dBm respectively.....	12-6
Figure 12-6 Analysis of SCE daily average duty cycle distribution for different percentiles based on 4,156,164 readings of transmitter activity from an average of 46,696 Itron Smart Meters over a period of 89 consecutive days. Analysis based on estimated transmitter activity during a day (see text).	12-8
Figure 12-7 Results of an analysis of duty cycles for a sample of 6865 Itron Smart Meters deployed by SDG&E based on transmit duration during a single day of observation.....	12-9
Figure 13-1 Measurement of microwave oven leakage at 1 foot from oven door seal.	13-1
Figure 13-2 Microwave oven leakage vs. distance.....	13-2

Figure 13-3 900 MHz cordless telephone RF fields from the base unit near the upper end of the spectrum and from the portable receiver unit near the lower end of the spectrum, measured at 1 foot from the base and receiver. 13-3

Figure 13-4 Measured RF emission spectrum of a wireless router at one foot from the router. The router was set to operate on Wi-Fi channel 10. 13-3

Figure 14-1 Relative EIRP of a 900 MHz RF LAN transmitter as observed along a six foot vertical line located one foot adjacent to the Smart Meter..... 14-3

Figure 14-2 Calculated RF fields up to 100 feet at point of maximum intensity in main beam expressed as percentage of FCC general public MPE as function of distance in maximum beam for Itron Smart Meter components investigated in this study. No ground reflections have been included in this analysis, the field values are relevant to the peak value of field during the time that the transmitter is actually transmitting (no duty cycle correction) and spatial averaging has not been applied to the values. Normal operation of the Smart Meter will significantly reduce the actual field found in practice near operating meters. 14-4

Figure 14-3 Calculated RF fields up to 1000 feet associated with Smart Meters included in this study with the assumption that the transmitters operate continuously (not possible in actual operation in a mesh network) and no ground reflections occur that might add constructively to enhance the field at the point of interest. 14-5

Figure 14-4 Calculated RF field produced by Smart Meter 900 MHz RF LAN transmitter using most likely transmitter power (solid curve) and 99th percentile transmitter power (bars above solid curve). Calculated maximum possible values are based on the 99th percentile transmitter power but assume the possibility of ground reflections ($\Gamma = 2.56$) that would enhance the RF field at the calculation point (point of maximum RF field emission near the meter). Such ground reflections are not realistic but follow guidance in FCC OET 65..... 14-7

Figure 14-5 Calculated RF field produced by Smart Meter 2.4 GHz Zigbee transmitter using most likely transmitter power (solid curve) and 99th percentile transmitter power (bars above solid curve). Calculated maximum possible values are based on the 99th percentile transmitter power but assume the possibility of ground reflections ($\Gamma = 2.56$) that would enhance the RF field at the calculation point (point of maximum RF field emission near the meter). Such ground reflections are not realistic but follow guidance in FCC OET 65..... 14-8

Figure 14-6 Relative calculated plane wave equivalent power density along a six-foot vertical path, one foot adjacent from a 900 MHz half-wave dipole positioned at five feet above the ground. Power density values are compared with and without ground reflections.....	14-10
Figure 14-7 Impact of ground reflections on six-foot spatial average of power density for different distances lateral to a 900 MHz dipole antenna mounted at five feet above ground. Vertical axis is represents the percentage that the spatially averaged power density that includes any ground reflected fields is greater than the spatially averaged power density in free space (without any ground reflected fields).	14-11
Figure 14-8 Ratio of magnitude of measured RF fields of group of ten meters to magnitude of calculated RF field of a single meter from 1 to 100 feet.	14-12
Figure 15-1 Chart of FCC MPEs applicable to members of the general public.	15-1
Figure 15-2 Summary of the IEEE C95.1-2005 action levels or MPEs for the lower tier (applicable to members of the general public if uninformed about RF exposure and not able to reduce their exposure if necessary).	15-3
Figure 15-3 Summary of ICNIRP guidelines on RF exposure limits for the general public.....	15-4
Figure 16-1 Estimated maximum likely time-averaged RF fields near Itron end point and cell relay Smart Meters included in this study. The plotted values are based on the 99th percentile values of transmitter powers, duty cycles given in Table 14-3 based on the conservative estimates from SCE data, main beam exposure and inclusion of realistic ground reflected fields ($\Gamma = 1.344$) that might add constructively to the resultant field. An assumption is made that the maximum RF field from all transmitters occurs at the same point in space. The graph pertains to a single end point meter and a single cell relay meter.	16-4
Figure A-1 Calibration certificate for the Narda Model 8715 digital meter for use with the Model B8742D probe.	A-1
Figure A-2 Calibration certificate for the Narda Model B8742D broadband probe.....	A-2
Figure A-3 Calibration certificate sheet 1 for the Narda Model SRM-3006 SN A-0077.	A-3
Figure A-4 Calibration certificate sheet 1 for the Narda Model SRM-3006 SN H-0100.	A-9
Figure A-5 Calibration certificate sheet 1 for the Narda Model SRM-3006 SN H-0100.	A-14
Figure A-6 Calibration certificate sheet 1 for the Narda Model SRM-3006 SN H-0100.	A-20

Figure B-1 900 MHz band composite RF field from rack of 10 SmartMeters at 1 foot.....	B-1
Figure B-2 900 MHz band composite RF field from rack of 10 SmartMeters at 2 feet.....	B-2
Figure B-3 900 MHz band composite RF field from rack of 10 SmartMeters at 3 feet.....	B-2
Figure B-4 900 MHz band composite RF field from rack of 10 SmartMeters at 4 feet.....	B-3
Figure B-5 900 MHz band composite RF field from rack of 10 SmartMeters at 5 feet.....	B-3
Figure B-6 900 MHz band composite RF field from rack of 10 SmartMeters at 6 feet.....	B-4
Figure B-7 900 MHz band composite RF field from rack of 10 SmartMeters at 7 feet.....	B-4
Figure B-8 900 MHz band composite RF field from rack of 10 SmartMeters at 8 feet.....	B-5
Figure B-9 900 MHz band composite RF field from rack of 10 SmartMeters at 9 feet.....	B-5
Figure B-10 900 MHz band composite RF field from rack of 10 SmartMeters at 10 feet.....	B-6
Figure B-11 900 MHz band composite RF field from rack of 10 SmartMeters at 15 feet.....	B-6
Figure B-12 900 MHz band composite RF field from rack of 10 SmartMeters at 20 feet.....	B-7
Figure B-13 900 MHz band composite RF field from rack of 10 SmartMeters at 25 feet.....	B-7
Figure B-14 900 MHz band composite RF field from rack of 10 SmartMeters at 30 feet.....	B-8
Figure B-15 900 MHz band composite RF field from rack of 10 SmartMeters at 40 feet.....	B-8
Figure B-16 900 MHz band composite RF field from rack of 10 SmartMeters at 50 feet.....	B-9
Figure B-17 900 MHz band composite RF field from rack of 10 SmartMeters at 75 feet.....	B-9
Figure B-18 900 MHz band composite RF field from rack of 10 SmartMeters at 100 feet.....	B-10
Figure C-1 900 MHz band composite RF field from rack of 10 SmartMeters at 20 cm behind meters.....	C-1
Figure C-2 900 MHz band composite RF field from rack of 10 SmartMeters at 5 feet behind meters.....	C-2
Figure C-3 900 MHz band composite RF field from rack of 10 SmartMeters at 10 feet behind meters.....	C-2

Figure D-1 2.4 GHz band composite RF field from rack of 10 SmartMeters at 1 foot.....	D-1
Figure D-2 2.4 GHz band composite RF field from rack of 10 SmartMeters at 2 feet.....	D-2
Figure D-3 2.4 GHz band composite RF field from rack of 10 SmartMeters at 3 feet.....	D-2
Figure D-4 2.4 GHz band composite RF field from rack of 10 SmartMeters at 4 feet.....	D-3
Figure D-5 2.4 GHz band composite RF field from rack of 10 SmartMeters at 5 feet.....	D-3
Figure D-6 2.4 GHz band composite RF field from rack of 10 SmartMeters at 6 feet.....	D-4
Figure D-7 2.4 GHz band composite RF field from rack of 10 SmartMeters at 7 feet.....	D-4
Figure D-8 2.4 GHz band composite RF field from rack of 10 SmartMeters at 8 feet.....	D-5
Figure D-9 2.4 GHz band composite RF field from rack of 10 SmartMeters at 9 feet.....	D-5
Figure D-10 2.4 GHz band composite RF field from rack of 10 SmartMeters at 10 feet.....	D-6
Figure D-11 2.4 GHz band composite RF field from rack of 10 SmartMeters at 15 feet.....	D-6
Figure D-12 2.4 GHz band composite RF field from rack of 10 SmartMeters at 20 feet.....	D-7
Figure D-13 2.4 GHz band composite RF field from rack of 10 SmartMeters at 25 feet.....	D-7
Figure D-14 2.4 GHz band composite RF field from rack of 10 SmartMeters at 30 feet.....	D-8
Figure D-15 2.4 GHz band composite RF field from rack of 10 SmartMeters at 40 feet.....	D-8
Figure D-16 2.4 GHz band composite RF field from rack of 10 SmartMeters at 50 feet.....	D-9
Figure D-17 2.4 GHz band composite RF field from rack of 10 SmartMeters at 75 feet.....	D-9
Figure D-18 2.4 GHz band composite RF field from rack of 10 SmartMeters at 100 feet.....	D-10
Figure E-1 2.4 GHz band composite RF field at 20 cm behind rack of 10 SmartMeters.....	E-1
Figure E-2 2.4 GHz band composite RF field at 5 feet behind rack of 10 SmartMeters.....	E-2
Figure E-3 2.4 GHz band composite RF field at 10 feet behind rack of 10 SmartMeters.....	E-2

Figure E-4 2.4 GHz band composite RF field obtained with lateral walk at 3 feet in front of rack of 10 SmartMeters from well beyond each side of rack. E-3

Figure F-1 Simulated wall section prior to installation of insulation, sheetrock and stucco lath (netting). F-1

Figure F-2 Simulated wall section showing initial installation of stucco scratch coat of stucco during construction with underlying 1.5 inch stucco netting. F-2

Figure G-1 Plane wave equivalent power density with and without ground reflections along a six-foot vertical line at 1 foot adjacent to a 900 MHz horizontally polarized dipole located at 5 feet above ground. Ratio of spatial average with reflections to spatial average without reflections is 1.032. G-1

Figure G-2 Plane wave equivalent power density with and without ground reflections along a six-foot vertical line at 3 feet adjacent to a 900 MHz horizontally polarized dipole located at 5 feet above ground. Ratio of spatial average with reflections to spatial average without reflections is 1.103. G-2

Figure G-3 Plane wave equivalent power density with and without ground reflections along a six-foot vertical line at 6 feet adjacent to a 900 MHz horizontally polarized dipole located at 5 feet above ground. Ratio of spatial average with reflections to spatial average without reflections is 1.190. G-2

Figure G-4 Plane wave equivalent power density with and without ground reflections along a six-foot vertical line at 10 feet adjacent to a 900 MHz horizontally polarized dipole located at 5 feet above ground. Ratio of spatial average with reflections to spatial average without reflections is 1.344. G-3

Figure G-5 Plane wave equivalent power density with and without ground reflections along a six-foot vertical line at 15 feet adjacent to a 900 MHz horizontally polarized dipole located at 5 feet above ground. Ratio of spatial average with reflections to spatial average without reflections is 1.432. G-3

Figure G-6 Plane wave equivalent power density with and without ground reflections along a six-foot vertical line at 20 feet adjacent to a 900 MHz horizontally polarized dipole located at 5 feet above ground. Ratio of spatial average with reflections to spatial average without reflections is 1.650. G-4

List of Tables

Table 5-1 Sierra Wireless Transceivers Operation Maximum Powers	5-4
Table 8-1 Summary of antenna measurement data	8-15
Table 9-1 Measurements of 900 MHz RF LAN emissions of individual Smart Meters installed in meter position A in the meter rack with the broadband field probe.....	9-4
Table 9-2 Summary of measurements of the 900 MHz composite RF field produced by an increasing number of closely spaced, collocated Smart Meters (meters A - J).	9-6
Table 9-3 Summary of corrected measurement data on RF fields of individual 2.4 GHz Zigbee transmitters installed in meter position A and of the collection of all ten meters.....	9-7
Table 9-4 Summary of composite RF field values (% general public MPE) determined with the SRM-3006 at various distances in front of a meter rack of 10 simultaneously operating Smart Meters.....	9-13
Table 9-5 Summary of planar area scans performed with the SRM-3006 in front of residential meter installation at residence A, Downey, CA.	9-15
Table 9-6 Spectrum scan measurements of Smart Meter fields in the 900 MHz and 2.4 GHz bands in residence A, Downey, CA. RF field is peak value obtained from a spatial scan of the room interior or area in percent of FCC general public MPE.	9-18
Table 9-7 Summary of planar area scans performed with the SRM-3006 in front of residential meter installation at residence B, Downey, CA.	9-24
Table 9-8 Spectrum scan measurements of Smart Meter fields in the 900 MHz and 2.4 GHz bands in residence B, Downey, CA. RF field is peak value obtained from a spatial scan of the room interior or area in percent of FCC general public MPE.	9-25
Table 10-1 Insertion loss measurement results for three different types of metal lath expressed as a reduction factor (F) and in decibels (dB).	10-3
Table 10-2 Insertion loss measurement data for simulated wall in 900 MHz and 2.4 GHz bands.....	10-8
Table 13-1 Comparison of RF field probe readings at 902.25 MHz and 2405 MHz	13-4

Table 14-1 Approximate RF field reductions (dB) caused by Smart Meter elevation plane patterns in the 60° to 90° range below a horizontal to the meter.	14-2
Table 14-2 Summary of nominal transmitter peak powers and 99 th percentile powers for Itron Smart Meters studied in this investigation.°	14-6
Table 14-3 Calculated worst case maximum possible RF fields associated with the 900 MHz RF LAN, 2.4 GHz Zigbee and cellular cell relay Smart Meter transmitters. The 99 th percentile powers for the RF LAN and Zigbee transmitters, main beam exposure, 100% duty cycle and presence of ground reflections (using a ground reflection factor of 2.56) to enhance fields was assumed. However, no spatial averaging was assumed.....	14-9
Table 16-1 Estimated maximum likely RF fields as a percentage of the FCC MPE for the public associated with Itron end point meters and cell relay meters including all RF components (900 MHz RF LAN, 2.4 GHz Zigbee and 850 MHz cellular transmitters). The 99 th percentile powers for the RF LAN and Zigbee transmitters, main beam exposure and possibility of ground reflections to enhance fields was assumed.....	16-3
Table 16-2 Summary of interior residential RF field measurements on two residences equipped with Smart Meters operating in continuous transmit mode.	16-5

Section 1: Summary

Measuring electric energy consumption with so-called Smart Meters in residential and commercial environments is becoming more commonplace. Smart Meters represent one component of what is referred to as Advanced Metering Infrastructure (AMI) in the electric utility industry. AMI systems comprise both wired and wireless technologies with each exhibiting their own advantages. Electric utility companies, thus, have options to implementing AMI systems. Even within the wireless category of AMI system, equipment can operate over a wide range of frequencies and powers and levels of activity. The Smart Meters, based on wireless technology, make use of miniature, low power radio transceivers, typically inside the meter, to wirelessly communicate with the electric utility. Two-way radio communication provided by Smart Meters allows for transmission of energy consumption data from a residence or business to the utility company and reception of data pertaining to time-of-day pricing of electric energy.

As wireless AMI technology is projected to become widely distributed, it becomes prudent to quantitatively assess the levels of RF emissions from meters to which the public may be exposed. Nearly two dozen communities have placed moratoria on further deployment of Smart Meters in northern California and more than 2000 health-related complaints have been received by the California Public Utilities Commission¹. This report documents the collection of information related to the operation of two particular models of Smart Meters² produced by Itron Inc. for purposes of supporting exposure assessment exercises that can address public concerns about exposure. The Itron products are currently being deployed by Southern California Edison Electric Company (SCE) and San Diego Gas and Electric Company (SDG&E) and both companies provided support to EPRI (the Electric Power Research

Institute) for this activity. A number of companies currently manufacture different forms of Smart Meters and, most commonly, these meters employ radio transmitters that operate in Federal Communications Commission (FCC) designated license free bands³. The Itron meters in this study use transmitters that operate in the license free bands of 902 MHz to 928 MHz (the “900 MHz band”) and 2400 MHz to 2500 MHz (the “2.4 GHz band”).

The Smart Meters studied here act as nodes in wireless mesh networks consisting of approximately 500 residences (for SCE) or 750 residences (for SDG&E); these are referred to as “end point meters.” Within each mesh network, one residence, designated as a “collection point,” is equipped with a Smart Meter having an additional internal transmitter (referred to as a “cell relay” for communicating data to the utility over a wireless wide area network (WWAN). The cell relay collects data from the various end point meters and conveys these data onto the cellular wireless wide area network (WWAN) for communication back to the electric utility company’s data management system. Mesh network communications among the many meters is provided by the 900 MHz band transceiver RF LAN (local area network). A HAN feature is supported by the 2.4 GHz transceiver. A data protocol used by the HAN called Zigbee is used to refer to the 2.4 GHz transceiver as in “the 2.4 GHz Zigbee radio”.

The data collection effort included gathering of information and working with the manufacturer at their facility in West Union, South Carolina, measurements at residences and in neighborhoods in southern California and some more limited measurements in Colville, Washington. Itron graciously provided technical support and access to its facilities and personnel to assist in this effort. Data included transmitter power levels, radiation patterns, RF field strengths or power densities of individual meters and groups of meters, spatial variations of RF fields in a vertical plane near Smart Meters, attenuation of Smart

¹See, for example, “Smart Meters - They’re Smart, But Are They Safe?”. <http://www.publicnewsservice.org/index.php?content/article/16846-1> (November 8, 2010).

² Itron model CL200 (end point meter) and model C2SORD (cell relay).

³ Some Smart Meters are designed to operate in FCC licensed bands and may operate with higher powers.

Meter RF fields by building materials, and information potentially useful for assessing transmitter duty cycles. To characterize the systems currently operating, parallel efforts included modeling of RF fields based on measured values of maximum equivalent isotropic radiated power (EIRP) of both end point and cell relay meters and analysis of end point meter transmission statistics for estimating duty cycles. Antenna patterns were determined for the 900 MHz RF LAN and 2.4 GHz Zigbee transmitter in both end point and cell relay meter configurations. Patterns were also measured for both the 850 MHz and 1900 MHz cellular bands from a cell relay.

Antenna pattern measurements revealed that RF fields are emitted preferentially toward the frontal region of the meters; the direction of maximum EIRP, however, might not be directly normal to the front of the meter. Apparent antenna gain values were modest, ranging between 0.88 dBi and 5.08 dBi, depending on the frequency band and the configuration (end point vs. cell relay). Patterns typically exhibited a reduced RF field behind the meter of approximately 10 dB down from the maximum frontal value of field with relatively narrow notches in the pattern directly behind the meter of as much as 20-30 dB less than in front.

Transmitter power data were obtained on 200,000 RF LAN 900 MHz transmitters with a most likely value of approximately 24.5 dBm (282 mW) with a 99th percentile power of 26.0 dBm (298 mW). Based on a sample size of 200,000 2.4 GHz radios, the most likely power was found to be 18.5 dBm (70.8 mW) with a 99th percentile power of 20.8 dBm (114.8 mW). Cellular transmitters were specified as 31.8 dBm in the 850 MHz band and 28.7 dBm in the 1900 MHz band.

Because of the very intermittent nature of transmissions from Smart Meters and their frequency hopping spread spectrum transmitters, accurate measurement of RF fields can be challenging. To facilitate the measurements, Smart Meters were programmed to transmit continuously on a single frequency. RF field measurements were performed on a single meter inside the Itron anechoic chamber and on ten individual meters installed in the Itron meter farm. These measurements were obtained with two different instruments including an isotropic, broadband, frequency conformal electric field probe (Narda Model B8742D) and a spectrum analyzer based selective radiation meter (Narda Model SRM-3006). Measurement data for the 900 MHz RF LAN

transmitters showed RF fields in the range of a few percent of the FCC MPE for the general public at 30 cm (approximately 1 foot) in front of the meters (0.7 to 5.5%) with the broadband probe depending on frequency. Similar measurements for the 2.4 GHz Zigbee radios at a distance of 20 cm showed 0.75% to 1.7% of the MPE, again depending on the frequency of the transmitter.

Using the SRM-3006 instrument, RF fields were measured as a function of distance from the rack of ten meters in both the 900 MHz and 2.4 GHz bands. These measurements produced readings ranging between approximately 8% at 1 foot to less than 0.1% at 75 feet from the meters in the 900 MHz band and approximately 4.5% at 1 foot to less than 0.01% at 75 feet in the 2.4 GHz band. 900 MHz field measurements showed that the emissions associated with the ten meters dropped into the background produced by other meters in the meter farm at a distance of approximately 50 feet.

By using the maximum hold and average measurement feature of the SRM-3006, a measurement in the meter farm obtained by walking along two rows of meter racks resulted in an integrated peak RF field equivalent to 0.114% of MPE and an average value of 0.00023% of MPE. The ratio of average to peak readings corresponds to an apparent duty cycle of about 0.2%. In measurements taken at two apartment houses in Downey, California, ratios of average to peak values of RF field obtained over five-minute monitoring periods resulted in estimated duty cycles of approximately 0.001%. Using a tiny USB spectrum analyzer designed specifically for just the 900 MHz band in the Itron meter farm, spectral measurements were captured for approximately one hour. This measurement resulted in an apparent duty cycle of approximately 0.02%.

Interior residential measurements were performed in two homes in Downey, California after temporarily replacing the existing Smart Meter with specially programmed units that would transmit continuously in the 900 MHz and 2.4 GHz bands. Inside measurements ranged from approximately 0.006% to 22% of MPE, the highest value associated with operation of a microwave oven in the kitchen at 2 feet from the oven. The greatest value immediately behind the Smart Meter, inside the home, was 0.009% of MPE. Wireless routers found in both homes resulted in RF fields in the range of 0.02 to 0.03% of MPE.

Residential neighborhood surveys were performed in areas with and without deployed Smart Meters while driving the streets of two communities, one in Downey, CA and one in Santa Monica, CA respectively. The exercise demonstrated that the emissions of randomly emitting Smart Meters could be detected in the Downey neighborhood but virtually no signals were detected in Santa Monica with the exception that when driving through a commercial district, the 900 MHz band came alive with noticeable activity, presumably caused by various 900 MHz sources, such as cordless telephones, etc. Spectrum measurements in several other band were also performed including the FM radio broadcast band, two cellular telephone bands and the 2.4 GHz Wi-Fi band.

The insertion loss of three different metal meshes was evaluated in California at one of the residences in which RF measurements were obtained. Three different sizes of mesh were used in the tests by inserting the mesh between a specially prepared, portable Smart Meter as a source, and the SRM-3006 meter. These measurements were performed at close range with the Smart Meter approximately six inches behind the mesh and the SRM-3006 probe approximately the same distance on the other side of the mesh. These measurements resulted in values for insertion loss ranging from 4.1 dB to 19.1 dB in the 900 MHz band and from 1.2 dB to 11.4 dB in the 2.4 GHz band, depending on mesh opening size. Additional insertion loss measurements were performed on a simulated stucco wall in Colville, WA resulting in values of 6.1 dB and 2.5 dB for the 900 MHz and 2.4 GHz bands respectively.

Since human RF exposure standards are based on spatial averages, spatially averaged values of RF fields were obtained along a vertical line at approximately one foot in front of a Smart Meter. It was found that over a six-foot vertical span, the spatially averaged RF field in the 900 MHz band corresponded to a value 23% of the measured peak value found near the height of the meter. In the 2.4 GHz band, the spatially averaged field was 18% of the spatial peak.

Using the detailed pattern measurement data described earlier, theoretical calculations of RF fields that could be associated with each of the transmitters in either end point meters or cell relays were made. A detailed analysis was developed to investigate the effect that ground reflected fields could have on the resultant field and what factors would be appropriate for including the

effect of ground reflections in theoretical RF field calculations.

Human exposure to RF fields is judged by comparison to applicable exposure limits or standards. For the United States, and in regard to Smart Meters, the most applicable limits are those promulgated by the FCC, a spatially averaged and time averaged value of 610 microwatts per square centimeter ($\mu\text{W}/\text{cm}^2$) in the 900 MHz band and 1000 $\mu\text{W}/\text{cm}^2$ in the 2.4 GHz band. A proper comparison of Smart Meter produced RF fields to these limits should involve a determination of the time-averaged value where the averaging time is specified as any 30-minute period. To arrive at time-averaged values, the measurements or calculated fields reported above must be corrected for the operational duty cycle of the transmitters. This is the most complex issue connected with Smart Meter RF evaluations since transmitter activity is semi-random in nature, with only brief transmissions occurring throughout a day. The maximum value of duty cycle for end point meters has been estimated by Itron to be in the range of 5%. Actual measurements, however, tend to result in substantially smaller values, typically less than 1%. Because of the variable nature of transmitter activity, even accurate measurements of a specific meter or meters need to be repeated for some days and, possibly, weeks to obtain reliable estimates of typical duty cycles. Rather than measurements, Itron developed special software implemented by the two companies to collect transmit data gathered and reported on in this report. Such an approach represents a practical way for bracketing realistic values of meter duty cycles since it can be implemented in software and extended to a very large sample size, something that would be impractical to do via physical measurements of RF fields at the meters. Using this approach, SCE generated data were examined to identify what fraction of meters in the sample exhibited transmit durations over a range of times which are related directly to the transmitter duty cycle. This exercise, for example, supported 99th and 99.9th percentile duty cycles of 0.11% and 4.7% for the RF LAN component of end point meters. A complimentary analysis conducted by SDG&E but using a more accurate determination of transmitter activity revealed smaller duty cycles. Similarly small duty cycle values are associated with the HAN and cellular transmitters. Figure 1-1 illustrates the estimated maximum likely time-averaged RF fields that would be produced by both end point and cell relay meters.

**Estimated Maximum Likely Time-Averaged RF Field
Near an Itron Smart Meter
(Not including spatial averaging)**

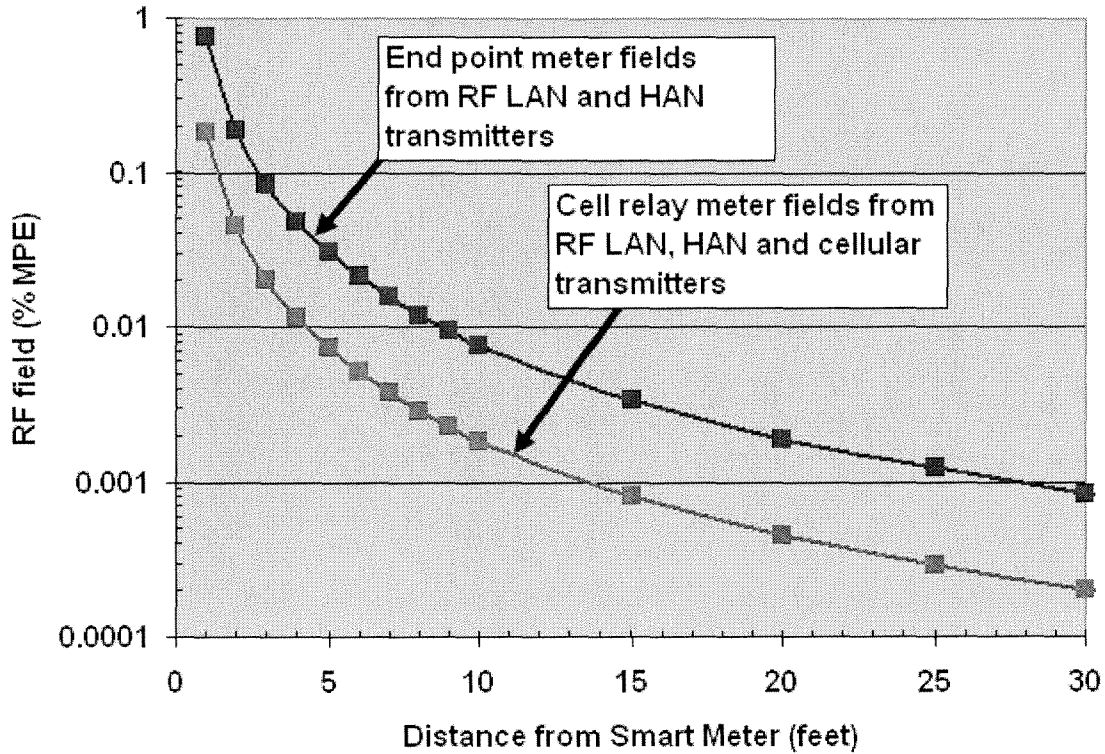


Figure 1-1
 Calculated RF fields near Itron end point and cell relay meters based on 99th percentile transmitter power values, main beam exposure (point of maximum RF field), inclusion of the possibility of ground reflected fields and assumed 99th percentile duty cycles.

These data, when taken collectively, indicate that the RF emissions produced by the Itron Smart Meters evaluated in this study result in RF fields <0.06 mW/cm² (at least 10-fold below the FCC limit at 900 MHz). For instance, at one foot, the RF field from an end point meter would be expected to not exceed 0.8% of the MPE. For the cell relay, the RF field would not exceed 0.2% of the MPE. Even at very close distances, such as one foot directly in front of the meter, with an unrealistic assumption that the transmitters operate at 100% duty cycle (at which point the mesh network would not function) the resulting exposure is less than the FCC MPE. When viewed in the context of a typical, realistic exposure distance of 10 feet, the RF fields are much smaller, about 0.008% for the end point meter and about 0.002% of MPE for the cell relay. Spatial averaging of these “spatial maximum” fields brings the estimated values down to approximately one-fourth of these magnitudes.

For potential exposure of occupants of a home equipped with a Smart Meter, interior RF fields would be expected to be at least ten times less intense simply due to the directional properties of the meter. When the attenuation afforded by a stucco home’s construction is included, a realistic value of the interior RF field would be about 0.023% of the MPE for an end point meter and about 0.065% for a cell relay meter. The WWAN operates at a far greater data throughput than the RF LAN within the mesh. Therefore, the duty cycle is correspondingly less for the cellular modem within the cell relay, despite the fact that it transmits all of the data collected from the relevant meters of its mesh network.

The most uncertainty in determining realistic time-averaged exposure from Smart Meters is associated with transmitter duty cycles. Hence, the most potentially useful avenue of future RF exposure assessment would include extensive statistical analyses of Smart Meter transmitter activity.

A detailed evaluation of possible RF fields produced by the Itron meters included in this study shows that regardless of duty cycle values for end point and cell relay meters, typical exposures that result from the operation of Smart Meters are very low and comply with scientifically based human exposure limits by a wide margin.

Section 2: Introduction and Background

As the electric utility industry in the United States moves toward implementing a “smart grid”, one of the key components consists of so-called Smart Meters. These new technology electric power meters represent a part of the advanced metering infrastructure (AMI) that provides for automatic meter reading (AMR) and sophisticated control over the use of electric energy by consumers in their homes and businesses. When AMI technology is fully implemented, an enhanced balancing of power distribution throughout the various electrical grids of the country will exist and utility customers will be able to, among other things, determine when certain electrically operated appliances may operate, based on time-of-day pricing of electricity. Such advanced capability requires close to real-time data acquisition on electric energy usage and such data requirements mean that the existing, traditional electric power meters that employ manual energy consumption readings, for example, once a month, can’t provide such timely data.

The modern technology of Smart Meters provides for an ability to almost instantly interrogate specific power meters as to electric energy usage. For the Smart Meters investigated in this study, this capability is accomplished via the use of data communications between the electric

utility company and individual power meters through the medium of radio signals. This report is focused on the radiofrequency (RF) aspects of Smart Meters and in particular, the strength of the transmitted RF fields that may be produced by the meters from a human exposure perspective.

Smart Meters as RF Sources

A wireless Smart Meter makes use of miniature, low power (typically less than one watt) radio transceivers inside the meter to wirelessly communicate with the electric utility company. The transceivers (transmitter and receiver) allow both transmission of data as well as reception of data and instructions from the utility. These transmitters are contained within the housing of the electric meter but are not necessarily visually obvious to an observer. Antennas used for the transmitters are commonly created as slots on the various printed circuit boards that constitute the electronic makeup of the meter. A common transmitter configuration of Smart Meters includes two or three transmitters in the meter. Figure 2-1 shows a Smart Meter with its digital display that is used to indicate electric energy usage.

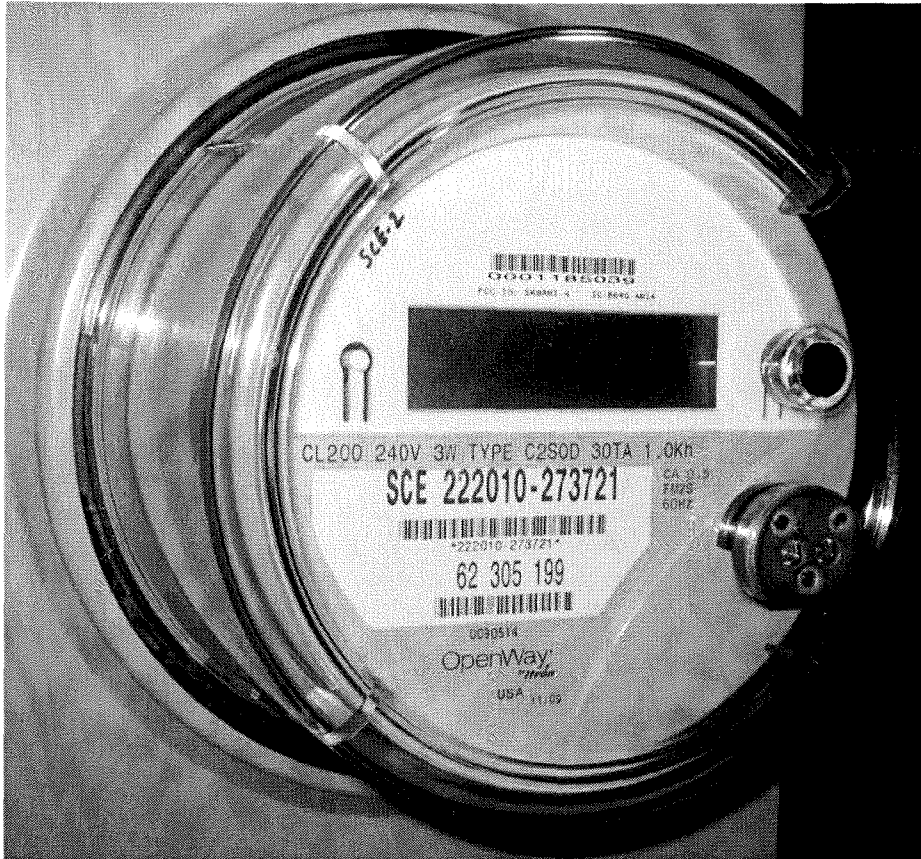


Figure 2-1
Photo of Itron Smart Meter.

How Smart Meters are Deployed

Radio communication by Smart Meters makes use of wireless networks whereby each Smart Meter can both transmit and receive data to and from the electric utility company. The wireless network is configured as a so-called mesh network. Mesh networks are characterized by providing a means for routing data and instructions between nodes. A mesh network allows for continuous connections and reconfiguration around broken or blocked data paths by “hopping” from node to node until the destination is reached. In the context of how Smart Meters are deployed, end-point meters are installed throughout neighborhoods, replacing existing electromechanical meters. The transceivers⁴ within the

Smart Meters act as wireless routers, identifying and, then, connecting with available transmission paths between themselves and a cell relay meter that collects data from the many, various meters in the region.⁵ If communication between a given end-point meter and the associated cell relay cannot be achieved due to inadequate signal strength, an alternative end-point meter is used to establish communications onward toward the cell relay meter. In this sense, the mesh network is said to be self-healing in that should a particular transmission path becomes blocked, the network finds another way to get its data through the system. A simple example of this process could be that at some particular moment, a moving van travels down a street and temporarily blocks the previously preferred path from an end-point meter to the cell relay meter. In

⁴ The RF devices inside the Smart Meter function as transceivers since they both transmit and receive radio signals. In this report, the term transmitter is often used in place of transceiver since the primary characteristic of the meters of interest in this study is the meter’s ability to transmit radio signals.

this case, the data is rerouted via other end-point meters that act as alternative paths for the meter to initiate the data communications. This very powerful networking approach provides for good data communication reliability and can even allow communications for end-point meters that are outside the line-of-sight range to their cell relay meter. Additional end-point meters,

therefore, have the ability to expand the geographical extent of a network. Figure 2-2 illustrates the concept behind a wireless mesh network implemented for a Smart Meter equipped neighborhood. Each meter communicates either directly with the cell relay meter or via multiple “hops” of the signals through other meters.

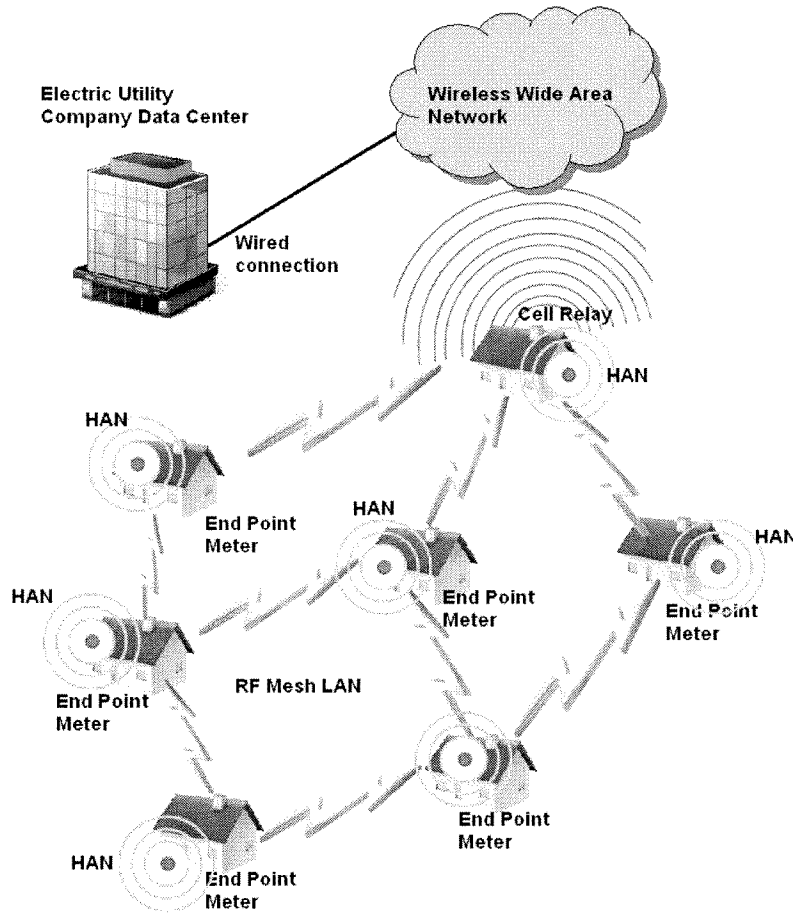


Figure 2-2
Simplistic illustrative diagram of an RF mesh network. Each end point also provides a Home Area Network (HAN) feature. The cell relay acts as a collector point for multiple meters distributed in a neighborhood and transmits received data onto a cellular wireless wide area network (WWAN).

⁵ Southern California Edison Electric Company is deploying Smart Meters as part of their SmartConnect™ program with one access point for approximately every 500 end-point meters on residences. In the case of San Diego Gas and Electric Company, each access point serves for data collection from approximately every 750 end-point meters.

For the Itron equipment that was the subject of this investigation, two separate transmitters are contained in the end-point meters. The wireless mesh network can be referred to as an RF LAN (radio frequency local area network). The Itron RF LAN operates in the 902-928 MHz license free band using spread spectrum transmitting technology. A second, separate transmitter that operates in the 2.4 GHz frequency range (2405 MHz to 2483 MHz) uses direct sequence spread spectrum technology that is referred to as a Zigbee radio⁶. This second transmitter is included for use with Home Area Networks (HANs) allowing customers, for example, to control certain electric appliances or systems within the home. When fully implemented, the customers will be able to connect wirelessly with the HAN radio and set times at which various appliances and/or electrical systems may operate, thereby taking

advantage of those times during which electricity rates are lowest.

The RF LAN provides data communications among the various end-point meters and an associated cell relay meter. Cell relays are end-point meters that contain yet a third transceiver that is designed for wireless connection to the cellular WWAN, i.e., relaying of the data received from the various end-point meters over a private connection to the electric utility company. The transceivers use the same frequency bands used by cell phones. Two different frequency bands are used by these cell-relay transceivers, either the 850 MHz band or the 1900 MHz band.⁷ Figure 2-3 shows a cell relay with the flexible dual band antenna located on the inside surface of the meter cover.

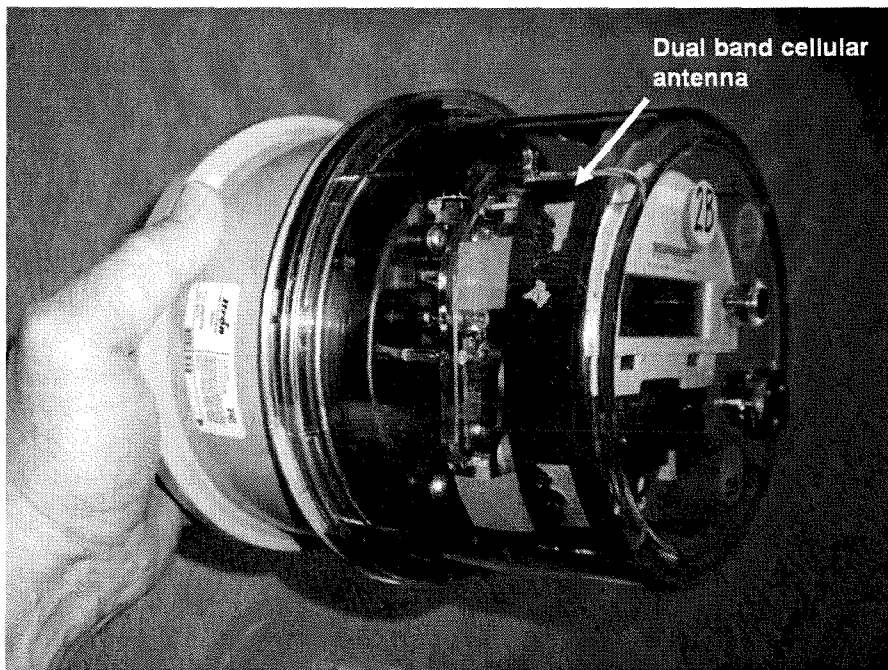


Figure 2-3
Cell relay meter with flexible, dual band (850 MHz and 1900 MHz) antenna affixed to interior surface of the meter cover.

⁶Zigbee is a name for a particular data communications protocol used in the HAN system.

⁷These frequency designations indicate the nominal frequencies used for the wireless WAN for Internet connectivity.

An important characteristic of this wireless mesh network technology is the fact that the RF emissions produced by Smart Meters, i.e., the signals that represent the data being transmitted, are not continuous but very intermittent in nature. For example, an electric utility company may interrogate the Smart Meters multiple number of times a day to acquire electric energy usage by the customer. While the Smart Meter may remain in stand-by in terms of transmissions at other times of the day, when an instruction is received to transmit energy consumption data, the meter transmits and proceeds to deliver the requested data to the cell relay meter. Hence, for the most part, Smart Meter transmissions are relatively infrequent during the day and may only consist of emissions for a few milliseconds during each of the interrogations throughout the day. This means that while the transceivers stand ready to transmit, there may be very little or no activity during most of the time. In addition to those periods during which data on electricity usage has been requested, however, Smart Meters must insure that they have a mesh network connection with at least one other Smart Meter so that, when necessary, it can deliver the data requested. Maintaining this connectivity within the mesh network requires periodic transmissions to alert the cell relay meter and other meters to its availability to be interrogated for data. So, Smart Meters spend part of their time in a so-called stand-by mode in which they issue beacon signals⁸ to signify their identity to other nodes of the network with the objective of establishing a connection with the network. These beacon signals last for very brief periods of, nominally, 7.5 milliseconds and occur at various intervals. Finally, there are other instances during which certain network maintenance activities are accomplished and during which, again, various, very short duration and intermittent emissions exist. The cumulative effect of these transmissions is that while the total time spent transmitting signals from a Smart Meter is generally very modest within a day, the signals are very intermittent. They are not continuous in the same sense as the signal received from an FM radio broadcast station but, rather, exist as very short duration signals scattered throughout the day. This intermittency contributes to the difficulty in accurately measuring the strength of the emissions.

In practice, homes in a Smart Meter equipped neighborhood will have end-point Smart Meters installed that communicate with a cell relay meter either directly or through the medium of multiple end-point meter radio signal hops. Approximately every 500th (in

the case of SCE) or 750th (in the case of SDG&E) residence may be equipped with a cell relay that not only handles the normal RF LAN communications but, also, relays these data onward, wirelessly, to the electric utility. All of these data communications proceed intermittently throughout each day.

The fact that the Itron Smart Meters studied here contain RF transmitters, albeit low power transmitters, means that relatively weak ambient RF fields exist in the vicinity of the meters. At the surface of the meter, the RF field strengths will be greatest with rapidly decreasing field strengths with increasing distance from the meter. While these low power transmitters cannot produce extremely intense RF fields, nonetheless, the issue of potential human exposure to these RF fields has, in some areas, become a question by the public.⁹ A concern expressed by some has been the potential for adverse health effects that might be caused by exposure to the weak RF fields produced by Smart Meters. This report documents an investigation of the characteristics of RF fields associated with the Itron wireless Smart Meter that can assist in a better understanding of possible public exposure to the RF emissions produced by Smart Meters. Throughout this report, the term Smart Meter is intended to refer to the wireless type represented by the Itron meters discussed in this report.

⁸ During the initial installation of an Itron Smart Meter, the meter enters a “discovery phase” in which it seeks to establish a link with the mesh network. During this discovery phase, beacon signals are emitted during approximately 3.5 second intervals until the meter becomes synchronized with the network or until a total time of about 6 minutes is reached after which beacons are emitted once about every 34 seconds until linked with the network or for up to 1½ hours. After this period, if a meter does not establish a link, it issues beacons once every hour during which it attempts to connect with the network. After 104 attempts, if still not linked with the network, the meter resets itself and begins the discovery sequence again. Once the meter becomes synchronized with the network, a beacon signal is emitted once every 94 seconds to 30 minutes depending on the level of other data traffic.

⁹ Newspaper accounts of public reaction to Smart Meters

Section 3: Objective of Investigation

The work described in this report was focused on understanding the physical characteristics of the RF fields that are produced by Smart Meters such that an informed conclusion can be made as to the magnitude of possible human RF exposure caused by the meters. In

this context, the objective of the work was to develop insight to the magnitude and spatial characteristics of Smart Meter RF fields including temporal aspects of the emissions that would allow a meaningful evaluation of possible exposures by reference to applicable RF human exposure limits.

Section 4: Technical Approach to Investigation

Characterizing RF fields produced by Smart Meters can be difficult. The intermittent nature of the emissions, addressed above, means that it is not a simple matter to simply bring instrumentation to an installed meter and be able to instantly detect the presence of the various emissions. The meter may or may not be in a transmit mode at the time when measurements are sought. Further, the spread spectrum characteristic of the emissions of the RF LAN and HAN transmitters leads to a further complication. For example, with the 900 MHz RF LAN transmitter, the emitted signal, at any particular instant in time, may be on any specific frequency within the 902 to 928 MHz band. When using narrow-band instrumentation, such as a frequency swept spectrum analyzer, the challenge is to have the analyzer on the specific frequency at the very instant in time that the emission is occurring to be able to measure its strength. Since the emissions are highly intermittent, this may take considerable time to insure that any such emissions have been captured by the instrumentation.

After careful consideration of the complexities associated with these kinds of measurements, it was decided that direct support of the testing by Itron, the manufacturer of the Smart Meter, could prove to be the most expedient approach to collecting the data useful to a complete exposure assessment study. As the manufacturer, Itron would have the knowledge and ability to control the Smart Meter to allow for meaningful measurements, avoiding the complications and uncertainties associated with working with already deployed meters.

Measurements at Itron

During the week of July 27, 2010, an extensive series of measurements was accomplished by the Principal Investigator at the Itron facility.

While at the Itron facility, detailed antenna pattern measurements were performed by the Principal Investigator on end point (Model CL200) and cell relay (Model C2SORD) meters. This included pattern measurements for the 900 MHz RF LAN transmitters in both the end point meter and as installed in a cell relay meter, pattern measurements of the 2.4 GHz

Zigbee transmitter in both an end point meter and a cell relay meter and pattern measurements of the cell relay cellular transceiver operating in both the 850 MHz and 1900 MHz bands.

In addition to pattern measurements, Itron provided access to their Smart Meter farm, an area of some 20 acres in which approximately 7000 Smart Meters are installed. The ability to access this field provided insight to the cumulative RF field environment of multiple Smart Meters in close proximity with one another, and whether aggregate exposure produced by a multiplicity of Smart Meters concentrated in one area raises exposure risks.

Measurements in residential locations

Beyond the on-site measurements performed at the Itron facility, additional Smart Meter measurements were performed in a variety of residential environments. Using two Smart Meters that had been specifically programmed by Itron to operate continuously, to facilitate the measurements of field strength, measurements were performed at two residences in Downey, CA. These specially programmed meters were temporarily installed in the electrical service panel at each home and RF measurements were accomplished in the near vicinity of the meter and throughout the interior of each home. This procedure allowed for characterizing the RF fields that might exist inside of residences equipped with a Smart Meter. As a part of the residential measurements, a brief evaluation of the insertion loss afforded by three different metallic meshes, similar to what might be used in the construction of residential stucco walls, was conducted.

In addition to residence specific measurements with pre-programmed meters, RF fields were also measured adjacent to two separate apartment buildings wherein groups of 9 and 11 Smart Meters were grouped tightly together. Finally, a general area survey was conducted by driving throughout an established route within Downey, CA representative of a Smart Meter deployed neighborhood to form general observations of the ability to detect the presence of Smart Meter emissions. The residential measurements aspect of the work reported

here was concluded with a driving survey through Santa Monica, CA within which, at the time, there had been no deployment of Smart Meters.

Measurements in Colville, WA

Separate from the measurements at the Itron facility and the residential measurements in Downey, California, some limited measurements were conducted at the author's location in Colville, WA. These measurements included an evaluation of the comparative readings of RF field obtained by both the broadband field probe and the spectrum analyzer (selective radiation meter) used in the project measurements as well as an evaluation of the attenuation effect on Smart Meter signal propagation through a simulated, residential stucco wall.

Section 5: Transmitter Powers

A crucial aspect of any RF source, relative to its ability to produce RF fields, is the power of the transmitter. At the beginning of interactions with Itron, measurement data were sought on transmitter power levels. Historically, Itron has determined the power level of every transmitter used for the 900 MHz RF LAN and the 2.4 GHz Zigbee radios. These are transmitter devices on Itron manufactured printed circuit boards. All of the transmitters used in the Itron Smart Meters

operate with low power, regardless of the frequency band used, nominally one watt or less. The 900 MHz RF LAN transmitter operates at a nominal power of 24 dBm (251 mW). Using Itron test data obtained from power measurements on a sample of 200,000 RF LAN transmitters, Figure 5-1 illustrates the accumulative fraction of transmitters having output powers across a range of power.

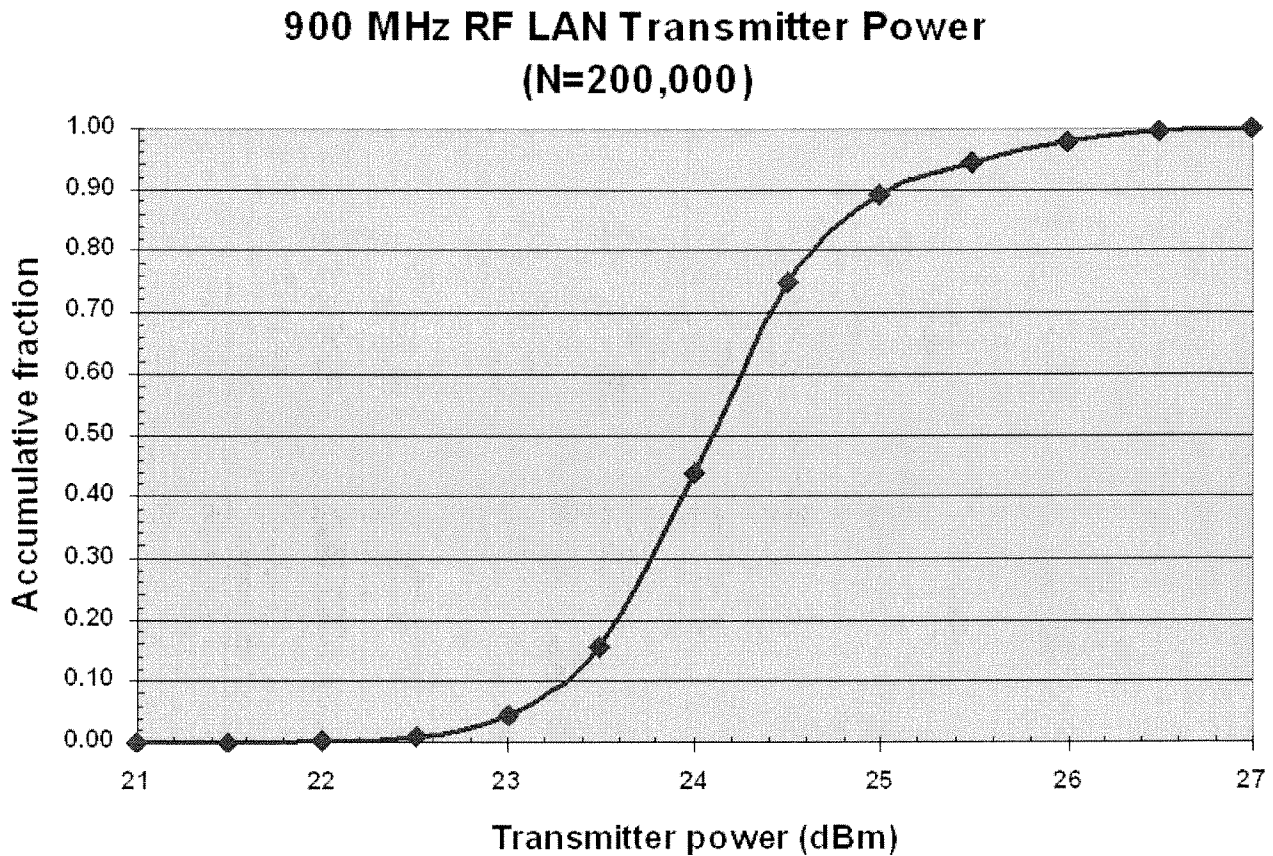


Figure 5-1
Accumulative fraction of 900 MHz RF LAN transmitter output power vs. transmitter power for a sample of 200,000 units. The median transmitter power is approximately 24.1 dBm (257 mW).

Based on a separate sample of 65,536 transmitters, used in end point meters, an average power output of 23.95 dBm (248 mW) was obtained with a standard deviation of 0.695 dBm. Using these data, the 95% confidence interval would correspond to a range of transmitter power from 22.6 dBm (182 mW) to 25.3 dBm (339 mW) and the 99% confidence interval would correspond to a power range from 22.2 dBm (166 mW) to 25.7 dBm (372 mW).

Using the 200,000 transmitter sample, the median power level corresponds to approximately 24.1 dBm (257). The number of transmitters with power values in selected ranges is shown in Figure 5-2. The mode of transmitter power is approximately 24.5 dBm (282 mW).

Number of 900 MHz RF LAN Transmitters with Powers in Selected Ranges (N=200,000)

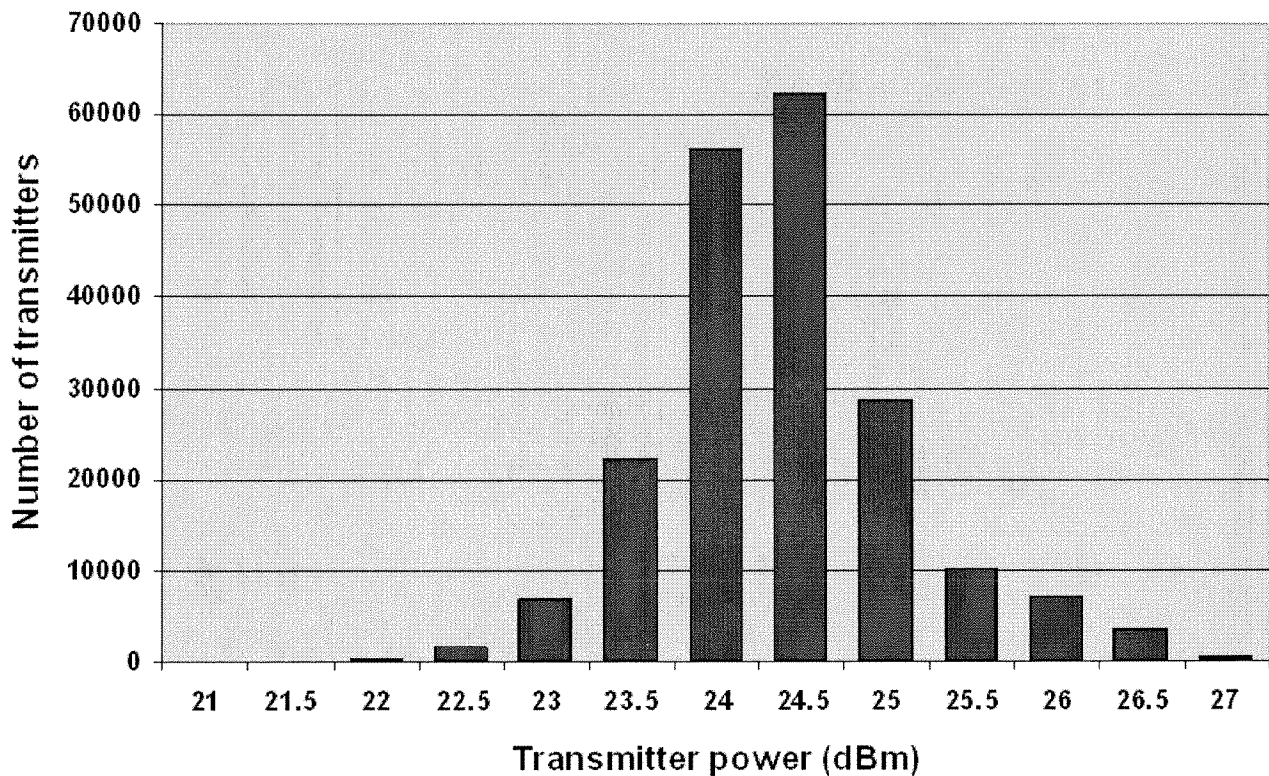


Figure 5-2
Number of 900 MHz RF LAN transmitters with powers within selected ranges. The transmitter power mode is approximately 24.5 dBm (282 mW).

These statistical data on the 900 MHz RF LAN transmitter powers indicate that the most likely power is 24.5 dBm (282 mW); an upper value of 26.0 dBm (398 mW), a value 41% greater than the most likely power, would include 99% of all transmitters.

mean value was found to be 18.31 dBm (67.6 mW) with a standard deviation of 0.76 dBm. This distribution would represent a 95% confidence interval of transmitter power from 16.8 dBm (47.9 mW) to 19.8 dBm (95.5 mW) and the 99% confidence interval would correspond to a power range from 16.4 dBm (43.7 mW) to 20.3 dBm (107.2 mW).

In the case of the 2.4 GHz Zigbee transmitters, in a sample of 65,535 units used in end point meters, the

Figure 5-3 shows the accumulative fraction of transmitters having output powers across a range of power. Figure 8 illustrates the number of 2.4 GHz

transmitters with powers within selected ranges. The transmitter power mode is approximately 18.5 dBm (70.8 mW).

2.4 GHz Zigbee Transmitter Power (N=200,000)

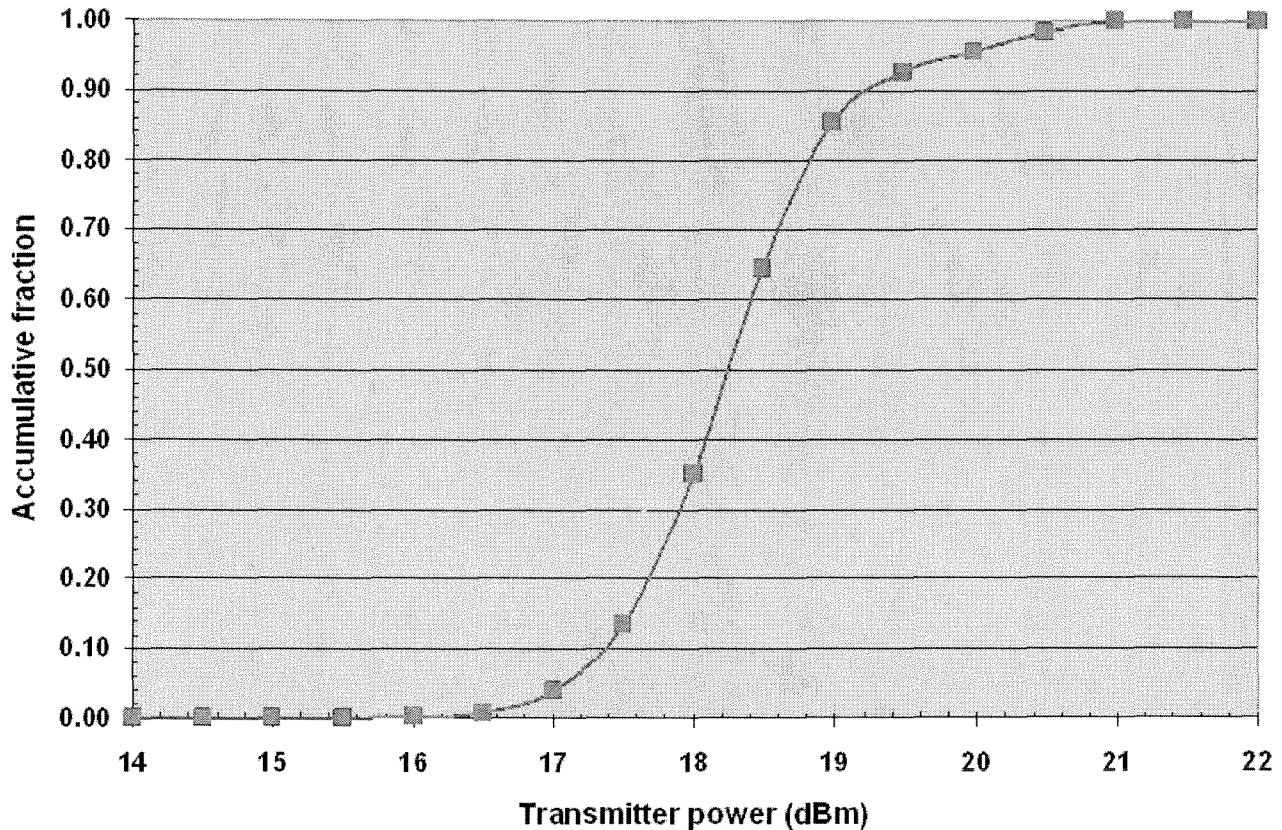


Figure 5-3
Accumulative fraction of 2.4 GHz Zigbee transmitter output power vs. transmitter power for a sample of 200,000 units. The median transmitter power is approximately 18.2 dBm (66.1 mW).

These statistical data on the 2.4 GHz Zigbee transmitter powers indicate that the most likely power is 18.5 dBm (70.8 mW); an upper value of 20.6 dBm (114.8 mW), a value 62% greater than the most likely power, would include 99% of all transmitters.

Cell relay meters contain the additional transceiver used for cellular WWAN connectivity in either the 850 MHz cellular band or 1900 MHz PCS band (personal

communications service). Because these transceiver boards are produced by a different company and the units are specified to operate with specific powers and the fact that these units are separately certified by independent test labs for compliance with those specifications, Itron does not carry out additional power measurements. The transceivers, produced by Sierra Wireless operate with the following maximum powers:

Table 5-1
Sierra Wireless Transceivers Operation Maximum Powers

	GSM Modem Model MC8790 FCC ID: N7NMC8790	CDMA Modem Model MC5725 FCC ID: N7N- MC5725
Frequency Band (MHz)	Maximum power output (dBm) (mW)	
850	31.8 (1,514)	25.13 (326)
1900	28.7 (741)	24.84 (305)

Cell relays operate at the highest power of any of the meters due to their cellular/PCS modems but, similar to cellular telephones, the output power of the cellular modem is dynamically controlled by the applicable WWAN base station. This means that the actual operating power of the cellular radio in a cell relay will, generally, be less than the maximum power but will be

determined by the signal strength it produces at whatever base station it is communicating with. Only one of the two modems would be active in a given deployment of Smart Meters in a neighborhood; the modem of choice is determined by the cellular wireless network service available and selected by the electric utility company.

Number of 2.4 GHz Zigbee Transmitters with Powers in Selected Ranges (N=200,000)

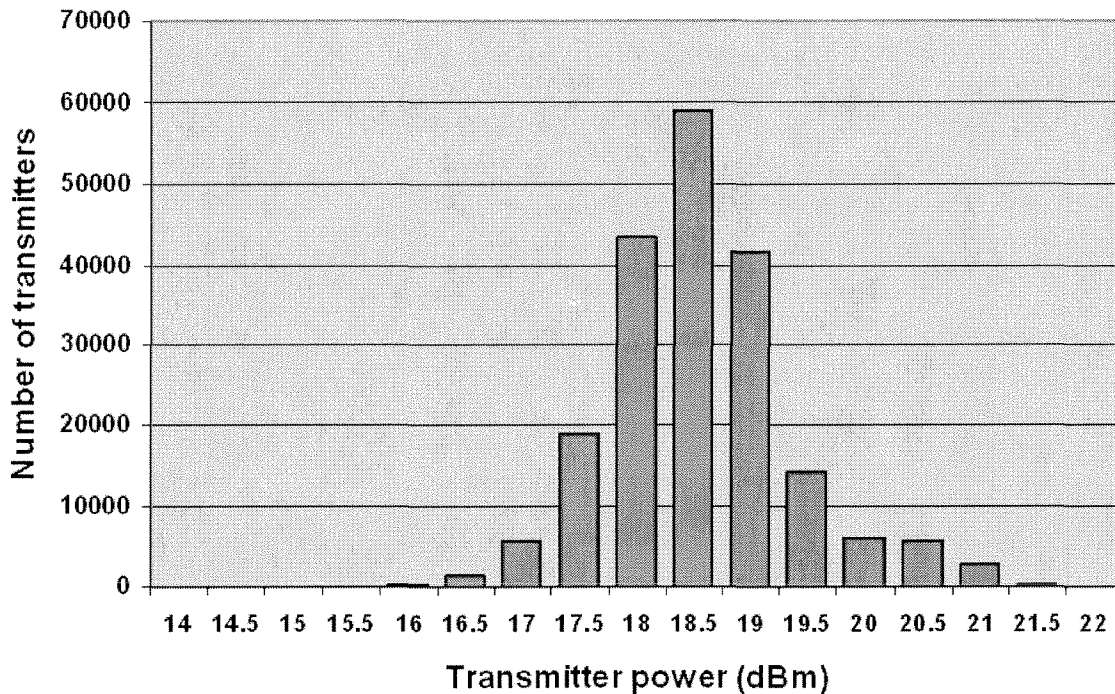


Figure 5-4
Number of 2.4 GHz Zigbee transmitters with powers within selected ranges. The transmitter power mode is approximately 18.5 dBm (70.8 mW).

Section 6: The Measurement Challenge Presented by Smart Meters

The difficulty of accurate RF field measurements near Smart Meters was discussed earlier. Low transmitted power levels in conjunction with intermittent emissions place considerable constraints on the measurement process. While a broadband measurement probe can eliminate the problem of the RF emissions occurring randomly on many different frequencies within the band, the relatively low sensitivity of broadband instruments places considerable restrictions on performing field strength measurements except within extremely close proximity of the meter. Intermittent emissions with very short duration, even if detectable, mean that it is difficult to observe when a transmission occurred. Generally, the desired measure of RF fields, from a human exposure perspective, is a measure of the average (root mean square - rms) value of the field strength or incident power density. The ratio of the average power density to the peak power density, for most Smart Meters is such that trying to measure the average field magnitude for a normally operating meter is very challenging. This can change if there exists a large aggregation of Smart Meters such that with their random on-off transmissions, much greater opportunity to “see” the emissions is possible.

Because of the rapid changes of frequency associated with the spread spectrum nature of the RF LAN and Zigbee radios in the Itron Smart Meters, an alternative

approach is used to facilitate any antenna pattern and field measurements. This approach involves programming the relevant radios to transmit continuously, rather than their normal intermittent operation, and to transmit on a specific frequency within the relevant band as opposed to hopping across more than 50 channels within the 900 MHz band. Through this programming of the radios, the average signal level is now at its maximum, making it much easier to detect the RF field, and the fact that the emitted signal is now fixed on a specific and known frequency allows for ready confirmation that the measurement is of the intended signal. Since measurements under this scenario will indicate the peak value of RF field, other information is required to translate the peak field into what the equivalent average field would be. This requires a knowledge of the duty cycle of the emissions from the Smart Meter. The duty cycle can be thought of as the ratio of the amount of time that the transmitter is transmitting its signal to the total observation period. For example, if the Smart Meter were to typically transmit as much as 10 seconds during an hour (3600 seconds), the duty cycle would be 0.28%. In other words, the time-averaged power density of the RF field would be just 0.28% of the peak power density measured. The issue of Smart Meter duty cycles will be addressed later in this report.

Section 7: Measurement Methods and Instrumentation

Several different methods were applied during the course of this investigation to measure Smart Meter RF fields. These included detailed antenna radiation pattern measurements of both end point and cell relay Smart Meters in the Itron anechoic chamber facility, survey type measurements used at close and far distances from single meters and groups of meters, such as in the Itron meter farm and at residences in California, drive-through type surveys in neighborhoods in which Smart Meters had been deployed, instrumentation comparison measurements using special Smart Meters programmed for the occasion and measurements of the attenuation provided by various forms of metal lath (commonly used in construction of stucco homes).

In the Itron facility, pattern measurements were

accomplished using a sophisticated system that permits orientation of a Smart Meter in 15 degree increments in all possible directions using a dual axis rotating system as shown in Figure 7-1. Associated instrumentation included a spectrum analyzer (Agilent Model E4405B (SN US40240612)) as the detector connected to a sense antenna (ETS Model 3115 double ridge guide horn (SN 0005-6166)) inside the anechoic chamber with instrumentation interfaced with a systems controller (Sunol Sciences Model SC104V). Data acquisition and analysis software provided for analysis and graphic display of measured antenna patterns (MI-Technologies Model MI-3000 workstation). Figure 7-2 shows the interior of the anechoic chamber with the reception horn antenna used to receive the signal emitted by the meter.

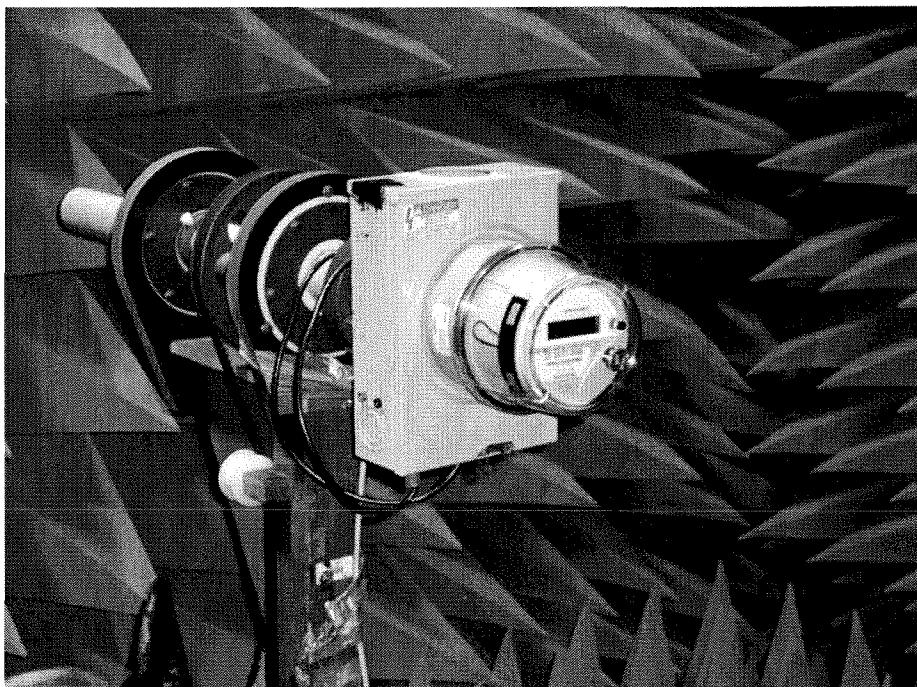


Figure 7-1
Close up view of dual axis antenna positioner system used to obtain antenna patterns of Smart Meter transmitters.

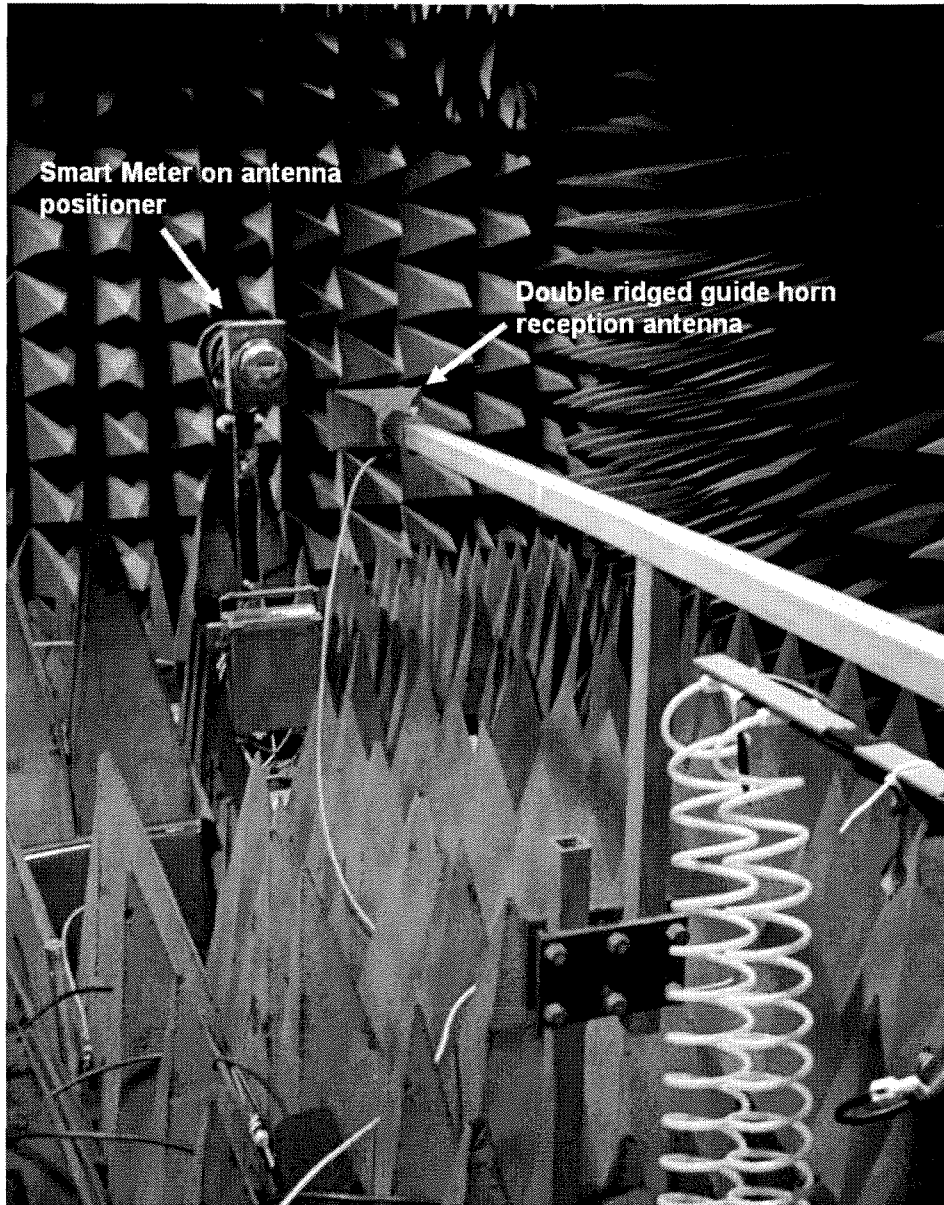


Figure 7-2
Interior of anechoic chamber showing reception horn antenna with Smart Meter on antenna positioner in background. During pattern measurements, the spectrum analyzer shown below the Smart Meter is removed.

Figure 7-3 shows the measurement instrumentation used for collecting and analyzing antenna pattern data. Smart Meters, when measured in the anechoic chamber, were installed in a metal meter box (Milbank Type 3R meter enclosure) supported on a dual axis rotator system

(see Figure 7-1 for a close-up photo of the dual axis rotator system and meter box). Calibration signals could be injected into the spectrum analyzer with a separate signal generator (Agilent Model E4432B).

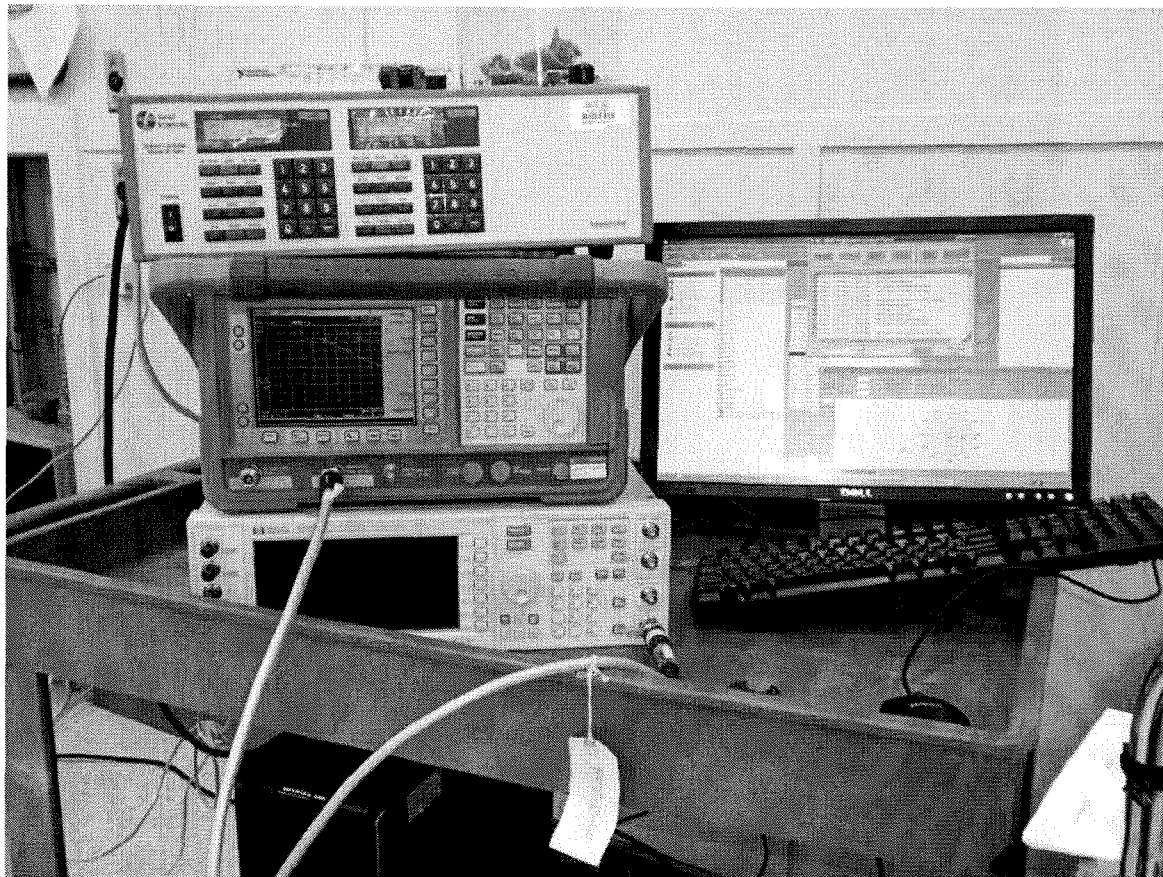


Figure 7-3
Instrumentation system for acquiring antenna pattern data.

All Smart Meter pattern measurements were performed in the Iron anechoic chamber. The interior of the shielded (0.2" metal) chamber measures 16 feet wide, 25 feet long and 12 feet high and is lined with anechoic material. The anechoic nature of the chamber provides for a very low level of reflection of RF fields from the floor, walls and ceiling, minimizing any perturbation that such reflections could have on the measured pattern of the Smart Meter transmitter.

Other instrumentation used in field measurements included use of a broadband, frequency conformal, isotropic, electric field probe (Narda Model B8742D, SN 03002) used with a readout meter (Narda Model 8715, SN 01028). This probe exhibits a frequency shaped response that follows the shape of the maximum permissible exposure (MPE) limit established by the Federal Communications Commission (FCC).¹⁰ Such a

shaped response allows the meter to read out directly in terms of a percentage of the MPE, regardless of the frequency or frequencies of the incident RF field(s). The B8742D is designed for response across the spectrum from 300 kHz to 3 GHz and is specified to yield reliable readings as low as 0.6% of the FCC general public MPE. Under optimum conditions (low ambient RF noise and a thermally stable environment), the meter can be used to read even lower RF field levels. The broadband probe consists of three, small mutually orthogonal elements combined electrically to yield an output on the meter that represents the resultant RF field magnitude. The isotropic nature of the probe

¹⁰ FCC rules

produces an output that is independent of the orientation of the probe within the field being measured, thereby accounting for all field components of any polarization. The meter and probe, shown in Figure 7-4, had been calibrated at the factory within the

previous twelve months of its application in this project as recommended by the manufacturer. Appendix A provides the calibration certificates for the meter and probe.



Figure 7-4
Frequency shaped, isotropic, electric field probe and meter (Narda B8742D and Narda 8715 meter).

Besides the use of the broadband meter, a special spectrum analyzer system was also used. This instrument (Narda Model SRM-3006 selective radiation meter, SN A-0077) combines a spectrum analyzer with an isotropic antenna (Narda three-axis-antenna, E-Field, SN H-0100) such that spectral scans may be performed with the resultant RF field value displayed on the analyzer's screen. The resultant field value is represented as the vector sum of the three orthogonal polarization components of the field, similar to how the broadband probe works. Built into the spectrum analyzer is a digital representation of the frequency dependence of the FCC MPE values. The

system automatically corrects the measured fields for this frequency dependence so that the indicated spectrum observed on its screen is expressed, again, as a percentage of the FCC MPE. Further, the instrument can be instructed to integrate across a desired frequency range so that the overall, equivalent RF field as a percentage of the MPE can be displayed. Since this instrument can also display both the peak and average value of the RF fields being measured, it can provide insight to the duty cycle of the Smart Meter emissions. The SRM-3006 is shown in Figure 7-5. Calibration certificates for the SRM-3006 are provided in Appendix A.



Figure 7-5
Selective radiation meter (Narda Model SRM-3006).

One other piece of equipment used in the project is a tiny band-specific spectrum analyzer designed for the 902-928 MHz band. This analyzer (Metageek Model Wi-Spy 900X) is a USB based instrument that is connected to a portable computer such as a laptop or notebook computer.¹¹ The instrument, shown in Figure 7-6, is designed for investigating RF signals in the 900 MHz range from an interference perspective. A similar instrument is available for measurements in the 2.4 GHz wireless network band. The use of this device was aimed at exploring its potential utility in measurement of Smart Meter emissions in view of its low cost. An associated software program (Chanalyzer version 3.4) creates displays of the measured spectrum and provides for analysis of the measured RF signals. Using the

¹¹ Metageek, LLC, 423 N. Ancestor Place, Suite 180, Boise, ID 83704 www.metageek.net.

software, for example, allows for retention of the maximum detected field at any given moment as well as the average value over whatever observation period is desired. A unique aspect of this spectrum analyzer is that, in conjunction with the connected computer, it records the result of each individual spectrum scan on the computer's hard disc drive. These recorded spectra can then be "replayed" at a later time to observe what the spectrum looked like at any previous point in time. Further, the stored, accumulated scans can be converted to a spreadsheet format for subsequent, custom analysis of the measurement data. Figure 7-6 shows a yagi antenna that was used with the Wi-Spy analyzer to achieve a higher level of system sensitivity and provide directionality for identifying the location of specific RF sources. The spectrum displayed on the notebook computer in Figure 7-6 is that acquired in the Itron laboratory with a Smart Meter operating on a fixed

frequency with lower level 900 MHz signals in the background from other meters in the vicinity.

The Wi-Spy unit was used for measurements of the insertion loss of a simulated wall in the Colville measurements. It was also employed in measurements

of Smart Meter transmission activity in California. The Wi-Spy 900X has a detection sensitivity of approximately -105 dBm in the 900 MHz band, an amazing achievement for a device costing less than \$200US.

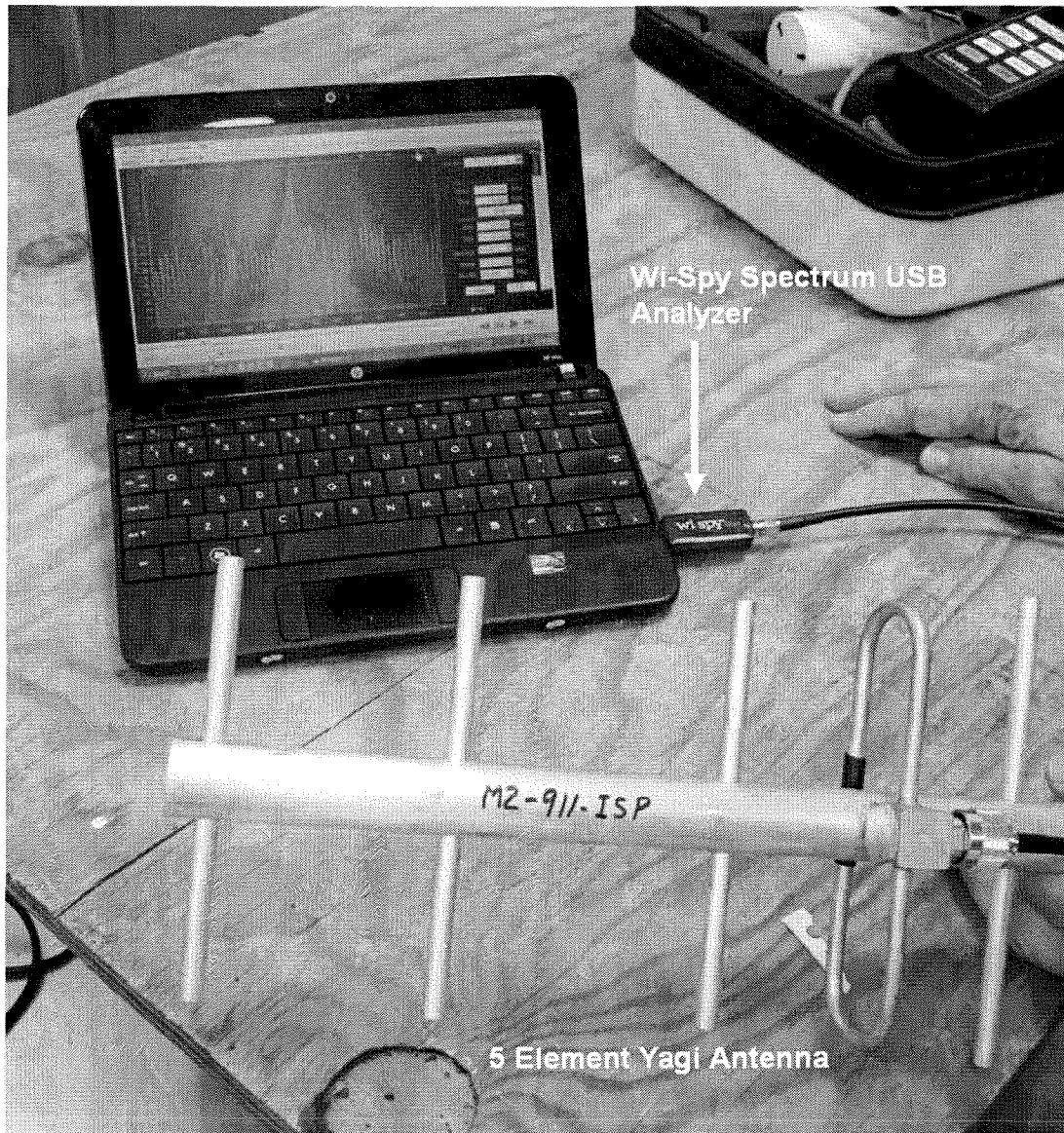


Figure 7-6
Wi-Spy USB spectrum analyzer connected to a notebook computer running software to operate the analyzer (Chanalyzer version 3.4) and an external yagi antenna.

Section 8: Laboratory Pattern Measurements

The radiation patterns for each antenna contained in the end point and access point Smart Meters were measured in the Itron anechoic chamber. This represented a total of six sets of patterns including: 900 MHz RF LAN in an end point meter and in a cell relay meter (access point), 2.4 GHz Zigbee radio in an end point meter and in a cell relay meter and the pattern of a cell relay meter using the GSM band (850 MHz) or the PCS band (1900 MHz). The 900 MHz RF LAN and 2.4 GHz Zigbee radios each have their own quarter-wave slot antennas that are etched on printed circuit boards inside the meter. The 900 MHz antenna is horizontal and located approximately 2.1 cm behind the front surface of the meter enclosure. When contained in a cell relay, the 900 MHz antenna is located approximately 15.1 cm from the front surface of the metal meter box in which it may be installed. The 2.4 GHz antenna is vertically oriented on its circuit board and is located approximately 2.5 cm behind the front surface of the meter enclosure; when installed in a cell relay, the antenna is approximately 14.7 cm in front of the metal meter box. A flexible dual band antenna is used for the cell relay function and it is adhered to the interior surface of the clear meter enclosure at a nominal nine o'clock position. The dual band antenna (AMR Under Glass Mount Antenna produced by WP Wireless)¹², shown in Figure 2-3, is approximately 2.5 cm wide with the front edge located approximately 0.4 cm from the front surface of the meter enclosure.

A feature of the Itron antenna pattern analysis system is the determination of the maximum isotropic effective radiated power (EIRP) for a particular amount of power being delivered to the antenna by the relevant transmitter. Because the Itron 900 MHz and 2.4 GHz transmitters are not designed for continuous operation (normal application in the Itron Smart Meters corresponds to a rather low duty cycle), all pattern measurements were obtained with the transmitters programmed to operate at a power level lower than their normal, maximum average power. This methodology

helped avoid a slight decrease in transmitter output power after prolonged periods of transmitter activity during which the transmitters can heat up, insuring that the measured data was representative of the peak power that is achieved under normal operating conditions. Knowing the EIRP of each transmitter system in a meter, relative to the particular transmitter output power during the test, allowed subsequent RF field calculations to be scaled to actual maximum transmitter power levels. Acquiring a complete three dimensional antenna pattern requires almost two hours of measurement. The meter is repositioned every 15 degrees in both azimuth and elevation and measurements are made of both the horizontal and vertical polarization components of the emitted field. Through examination of the entire data set after the pattern has been measured, the single maximum value of field is converted to EIRP. This single value was used in most of the subsequent analyses in this report since it represents the EIRP that is associated with the strongest RF fields in the vicinity of the Smart Meter.

Measured radiation patterns for the 900 MHz RF LAN transmitter configured in an end point meter, Model CL200 (Itron #62_305_199, SCE #222010-273721) are shown in Figures 8-1 – 8-4. In these figures, a drawing representing the Smart Meter as mounted in a meter box is shown for reference to the meter orientation. These patterns were determined at near-mid-band frequency of 914.8 MHz. Figure 8-1 represents the azimuth plane pattern of the 900 MHz emissions. This particular pattern is for a horizontal plane running through the meter and as viewed from the bottom of the meter. The pattern data are referenced to 0 dB at the point of maximum field, close to 0°, with each dotted line, in this particular pattern, representing a 20 dB variation in signal level. Three curves are shown in the figure; one representing the pattern for the horizontally polarized component of the field (the black curve), one representing the vertical polarization component of the field (the blue curve) and one representing the total field produced by the composite sum of both the horizontal and vertical components (the red curve). From an exposure

¹² WP Wireless - A Division of World Products Inc., 19654 Eight Street East, Sonoma, CA 95476 www.wp-wireless.com.

assessment perspective, the total pattern is of more relevance for evaluating RF fields relative to human exposure limits. The pattern shows a reduction of radiated field, generally, to the rear of the meter being between 10 and 20 dB less than the values to the front of the meter. A colorized picture in Figure 8-4 illustrates the azimuth plane representation of total EIRP of the 900 MHz RF LAN transmitter.

Elevation plane patterns for the 900 MHz RF LAN transmitter are shown in Figures 8-3 and 8-4 with

Figure 8-3 representing the patterns of the horizontal and vertical polarization components and the composite field (total), similar to the figure for the azimuth plane. Figure 8-4 illustrates the elevation plane representation of total EIRP of the 900 MHz RF LAN transmitter in an end point meter. In the elevation plane pattern, it can be seen that the maximum field is directed slightly upwards at about 30° rather than perfectly straight out toward the front of the meter.

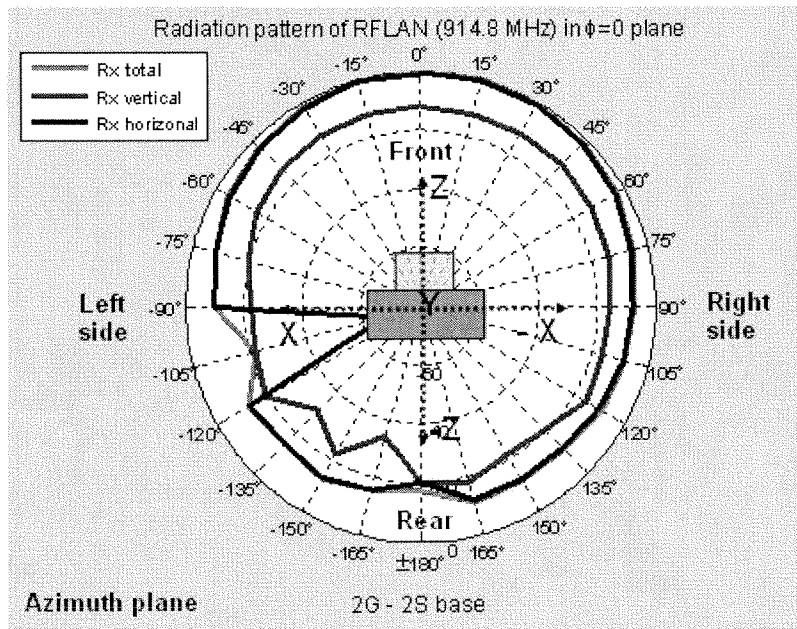


Figure 8-1
Azimuth plane pattern of the 900 MHz RF LAN transmitter configured in an end point meter showing the horizontal, vertical and total pattern as viewed from bottom of meter. The scale is in dB with the maximum field at the outer edge of the pattern circle.

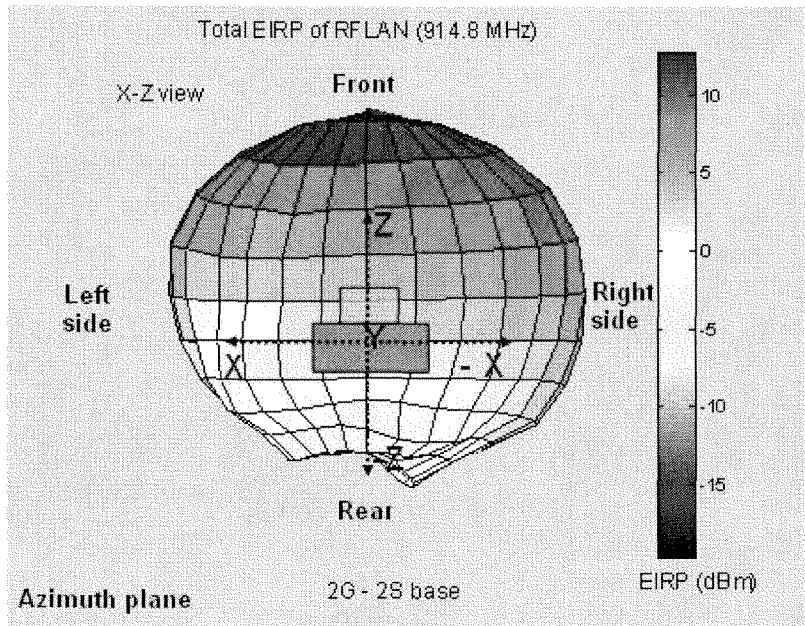


Figure 8-2
Azimuth plane view of the total EIRP of the 900 MHz RF LAN transmitter configured in an end point meter.

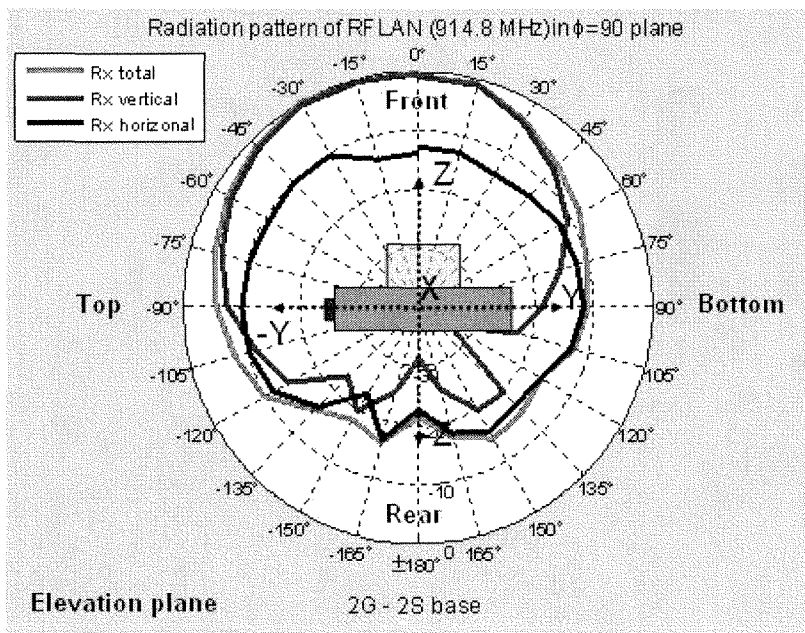


Figure 8-3
Elevation plane pattern of the 900 MHz RF LAN transmitter in an end point meter showing the horizontal, vertical and total pattern. The scale is in dB with the maximum field at the outer edge of the pattern circle.

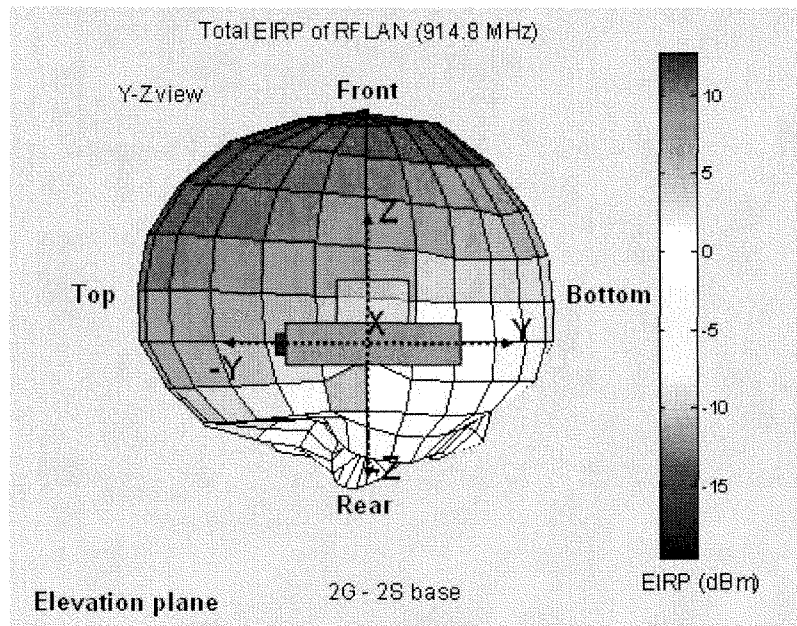


Figure 8-4
Elevation plane view of the total EIRP of the 900 MHz RF LAN transmitter in an end point meter.

Similar to the pattern measurements for the 900 MHz RF LAN transmitter in an end point meter, measured radiation patterns for the 900 MHz RF LAN transmitter configured in a cell relay meter, Model C2SORD, (Itron #661_912_646, SCE #222070-000082) are shown in Figures 8-5 – 8-8. The rationale behind documenting the pattern of the same transmitter and antenna type, but when installed in a cell relay, was to examine any differences that might be apparent that could be caused by the slightly different distance that the antenna would be relative to the front of the metal meter box.

Figures 8-5 and 8-6 represent the azimuth plane patterns of the 900 MHz cell relay emissions and total EIRP respectively. The pattern in Figure 8-5 shows a reduction of radiated field, generally, to the rear of the meter being between 10 and 20 dB less than the values to the front of the meter, similar to the 900 MHz RF LAN transmitter in an end point meter. A colorized

picture in Figure 8-6 illustrates the azimuth plane representation of total EIRP of the 900 MHz RF LAN transmitter.

Elevation plane patterns for the 900 MHz RF LAN transmitter in a cell relay are shown in Figures 8-7 and 8-8 with Figure 8-7 representing the patterns of the horizontal and vertical polarization components and the composite field (total), similar to the figure for the azimuth plane. Figure 8-8 illustrates the elevation plane representation of total EIRP of the 900 MHz RF LAN transmitter in a cell relay. Similar to the upward maximum radiation direction for the end point 900 MHz RF LAN transmitter, it can be seen that the maximum field is directed slightly upwards at about 30° rather than perfectly straight out toward the front of the meter.

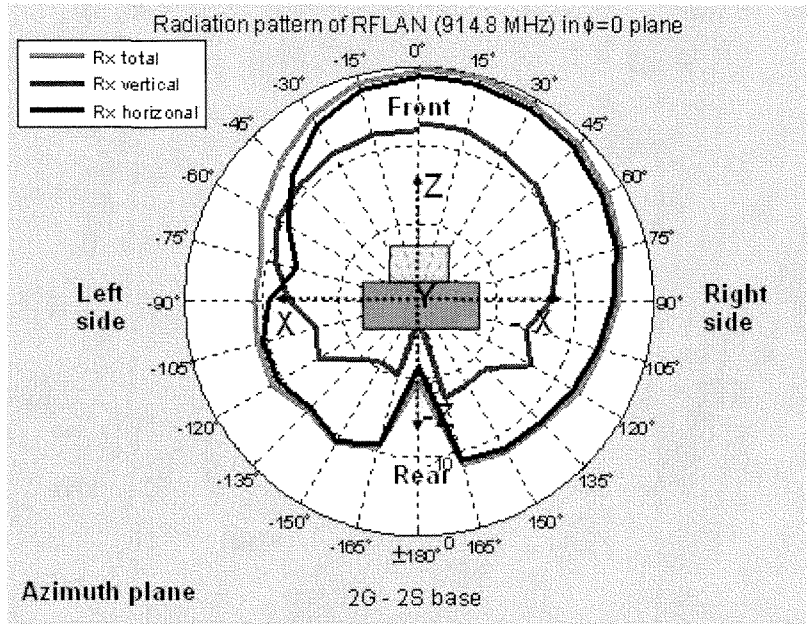


Figure 8-5
Azimuth plane pattern of the 900 MHz RF LAN transmitter in a cell relay showing the horizontal, vertical and total pattern as viewed from bottom of meter. The scale is in dB with the maximum field at the outer edge of the pattern circle.

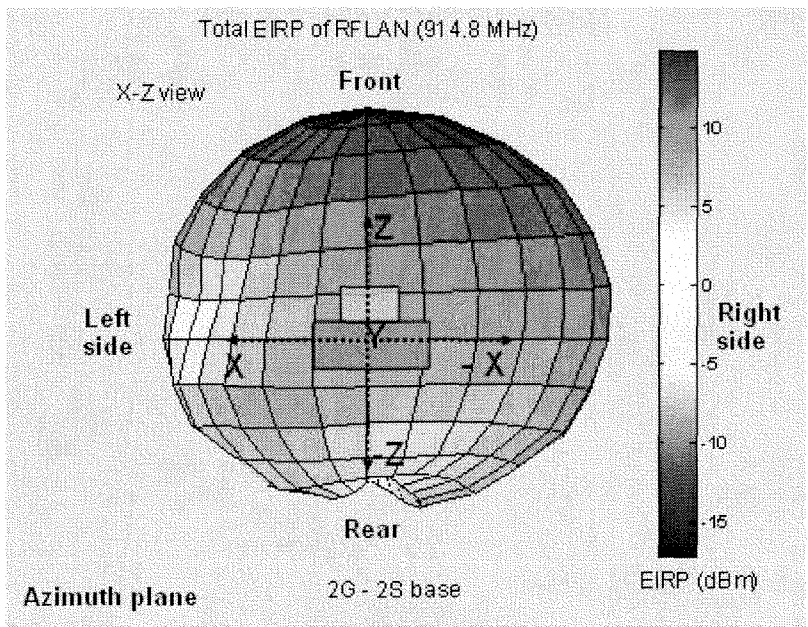


Figure 8-6
Azimuth plane view of the total EIRP of the 900 MHz RF LAN transmitter configured in a cell relay.

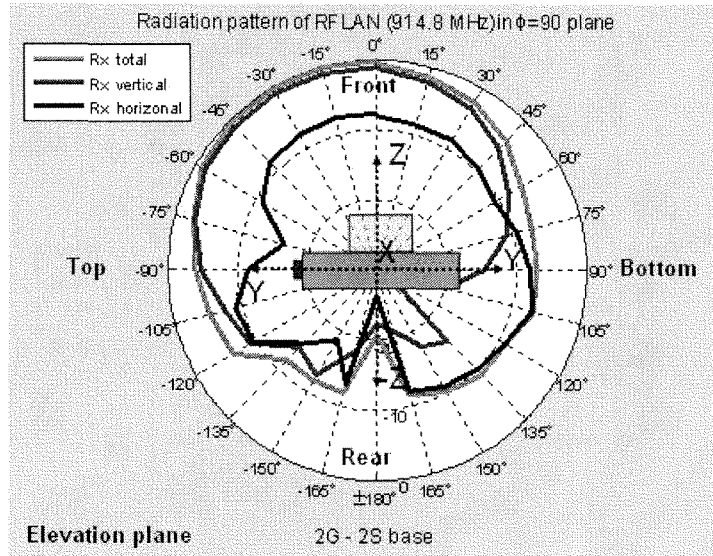


Figure 8-7
Elevation plane pattern of the 900 MHz RF LAN transmitter in a cell relay meter showing the horizontal, vertical and total pattern. The scale is in dB with the maximum field at the outer edge of the pattern circle.

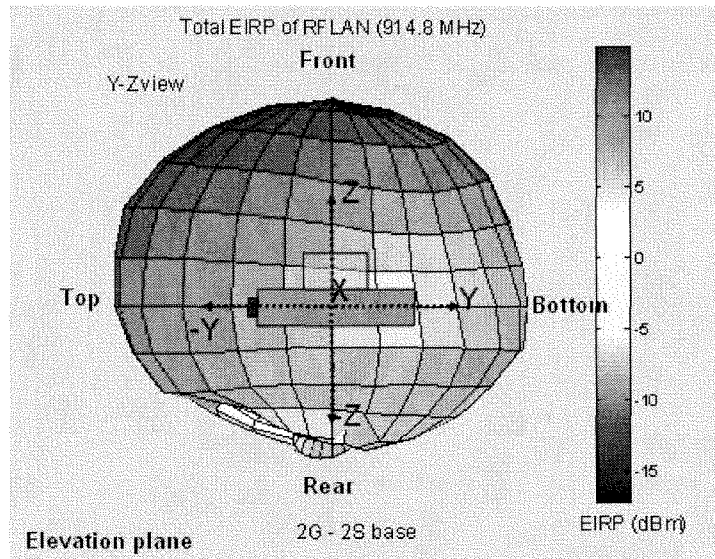


Figure 8-8
Elevation plane view of the total EIRP of the 900 MHz RF LAN transmitter in a cell relay meter.

A series of similar pattern measurements of the 2.4 GHz Zigbee radio configured in an end point meter, Model CL200 (Itron #62_305_199, SCE #222010-273721) are shown in Figures 8-9 – 8-12. Figure 8-9 shows the azimuth plane pattern; the azimuth plane

pattern total EIRP is shown in Figure 8-10. Figure 8-9 shows that the direction of the maximum radiated field is very slightly canted to the right side of the meter, as viewed from the front, at about 15°.

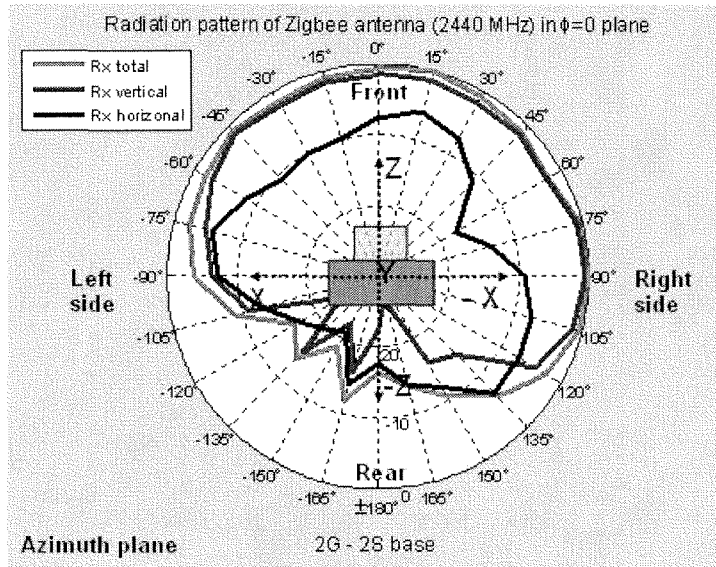


Figure 8-9
Azimuth plane pattern of the 2.4 GHz Zigbee transmitter configured in an end point meter showing the horizontal, vertical and total pattern as viewed from bottom of meter. The scale is in dB with the maximum field at the outer edge of the pattern circle.

The elevation plane pattern seen in Figure 8-11 reveals a tendency for the 2.4 GHz emission in the end point meter to be directed upwards, above the midline of the meter with a maximum field at approximately 45 to 60°.

61_912_646, SEC # 222070-000082). These patterns are shown in Figures 8-13 – 8-16 for the azimuth and elevation planes for relative field and total EIRP respectively. Figure 8-15 shows the tendency for an upward direction for emitted fields at approximately 45°.

Similar patterns were measured for the 2.4 GHz Zigbee radio in a cell relay meter (Model C2SORD, Itron #

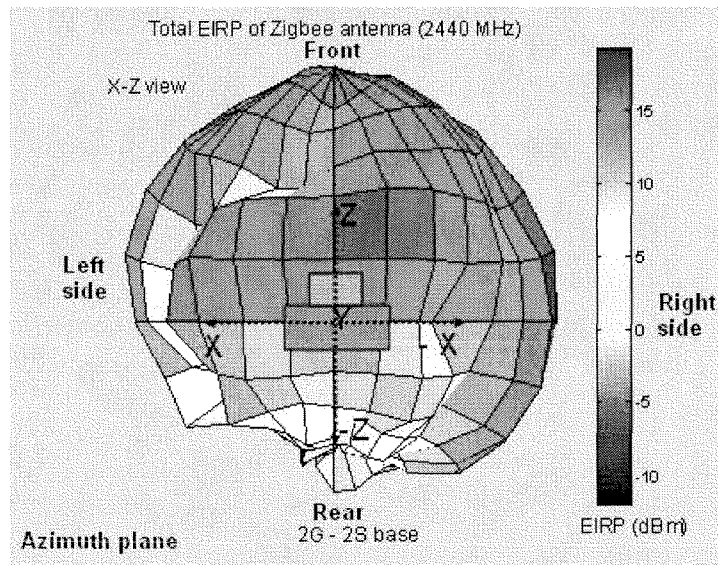


Figure 8-10
Azimuth plane view of the total EIRP of the 2.4 GHz Zigbee transmitter configured in an end point meter.

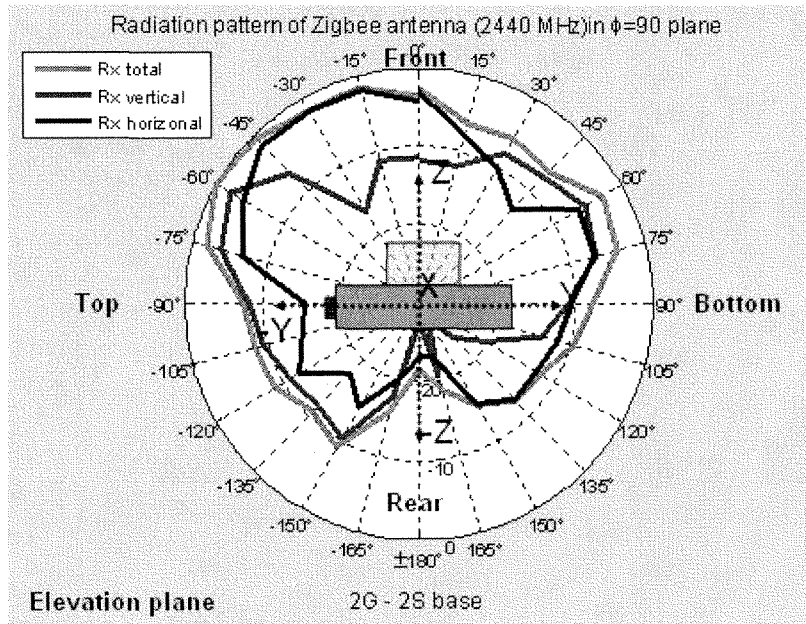


Figure 8-11
 Elevation plane pattern of the 2.4 GHz Zigbee radio in an end point meter showing the horizontal, vertical and total pattern. The scale is in dB with the maximum field at the outer edge of the pattern circle.

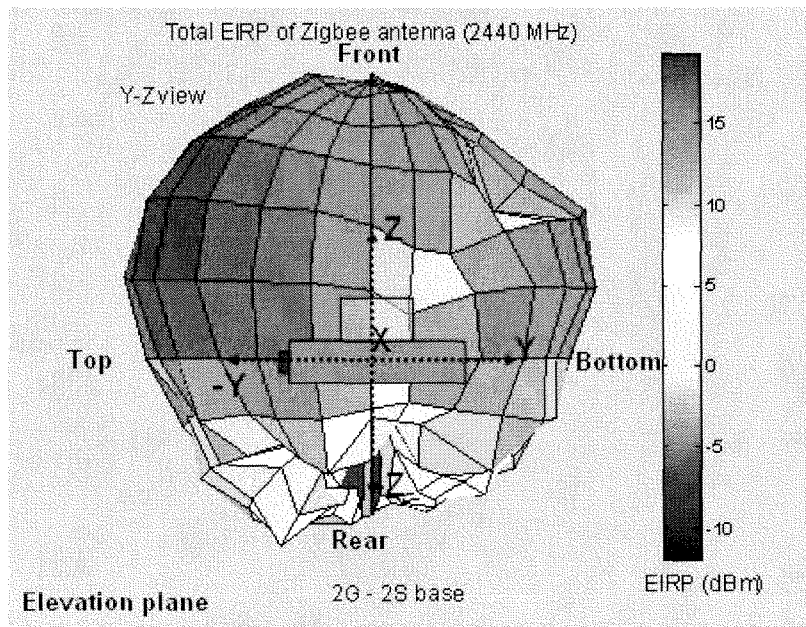


Figure 8-12
 Elevation plane view of the total EIRP of the 2.4 GHz Zigbee radio in an end point meter.

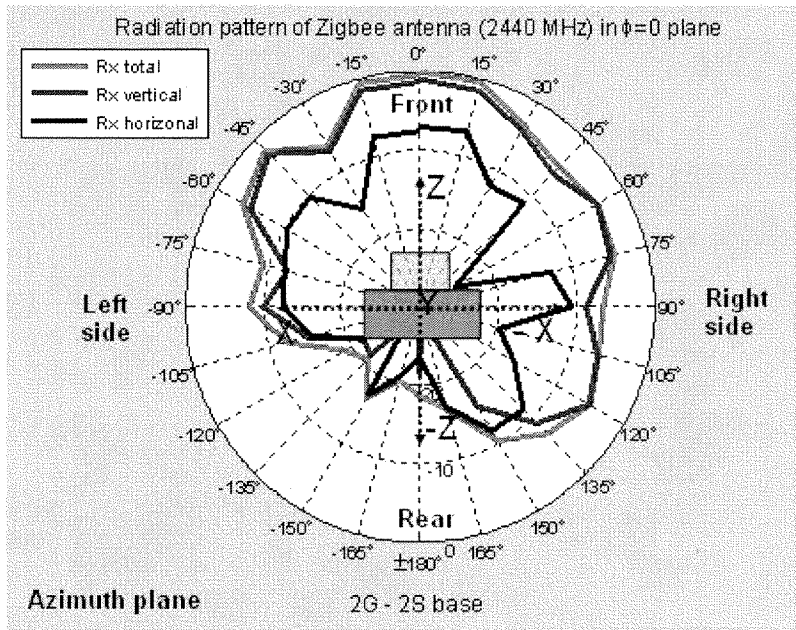


Figure 8-13
 Azimuth plane pattern of the 2.4 GHz Zigbee transmitter configured in a cell relay meter showing the horizontal, vertical and total pattern as viewed from bottom of meter. The scale is in dB with the maximum field at the outer edge of the pattern circle.

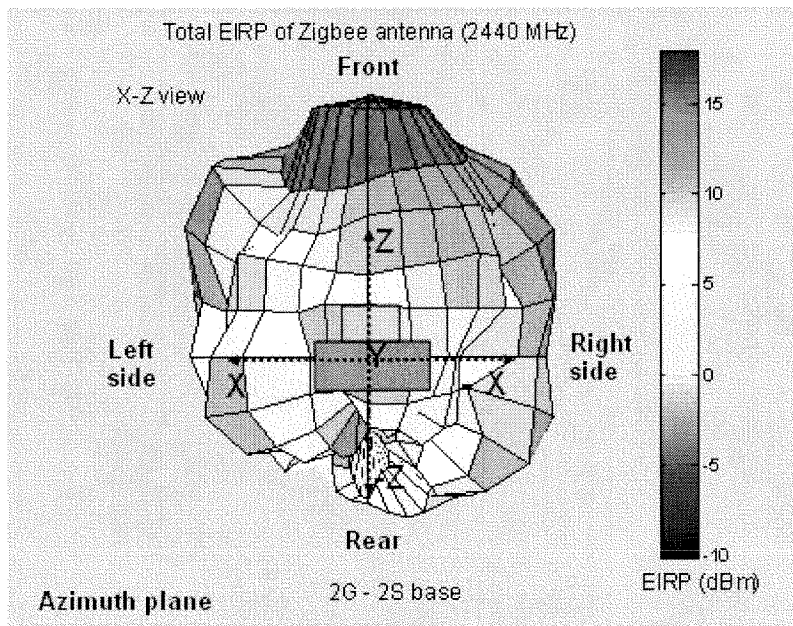


Figure 8-14
 Azimuth plane view of the total EIRP of the 2.4 GHz Zigbee transmitter configured in a cell relay meter.

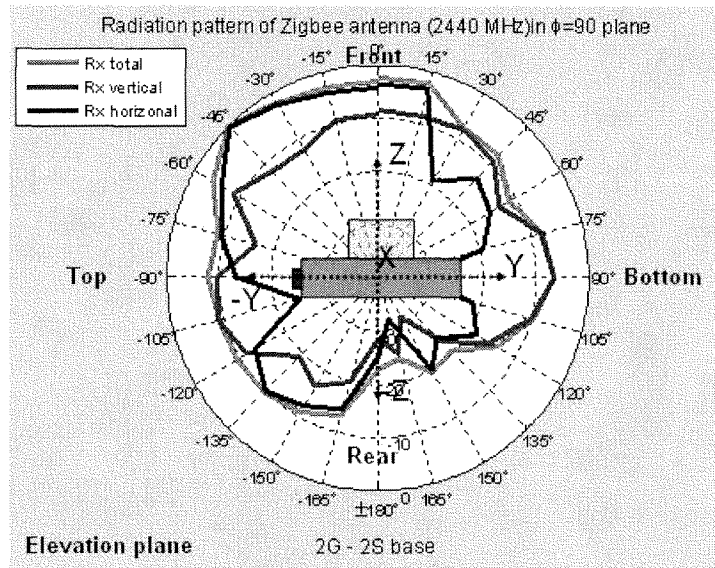


Figure 8-15
Elevation plane pattern of the 2.4 GHz Zigbee radio in a cell relay meter showing the horizontal, vertical and total pattern. The scale is in dB with the maximum field at the outer edge of the pattern circle.

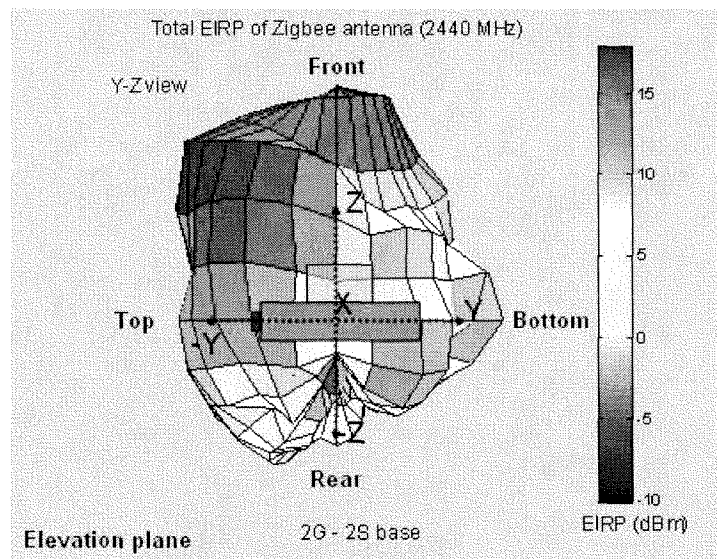


Figure 8-16
Elevation plane view of the total EIRP of the 2.4 GHz Zigbee radio in a cell relay meter.

For completeness, patterns of the cell relay cellular and PCS band antennas were also determined during this documentation. Figures 8-17 and 8-18, based on measurements at a frequency of 836.6 MHz for the cell relay Model C2SORD (Itron # 61_912_646, SCE # 222070-00082, GSM # 12460), show azimuth patterns for the relative field and total EIRP. Elevation patterns

for the 836.6 MHz GSM transmitter are shown in Figure 8-19 and 8-20.

Antenna patterns were measured for the GSM radio operated in the 1900 MHz band as well. Figures 8-21 and 8-22 represent the azimuth patterns and Figures 8-23 and 8-24, the elevation patterns. The patterns were measured with the transmitter operating on a frequency of 1880 MHz.

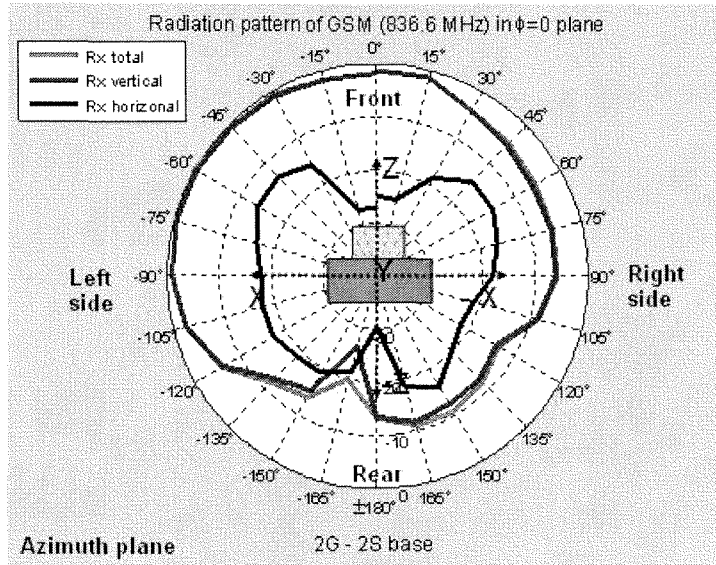


Figure 8-17
 Azimuth plane pattern of the 836.6 MHz GSM cellular transmitter in a cell relay meter showing the horizontal, vertical and total pattern as viewed from bottom of meter. The scale is in dB with the maximum field at the outer edge of the pattern circle.

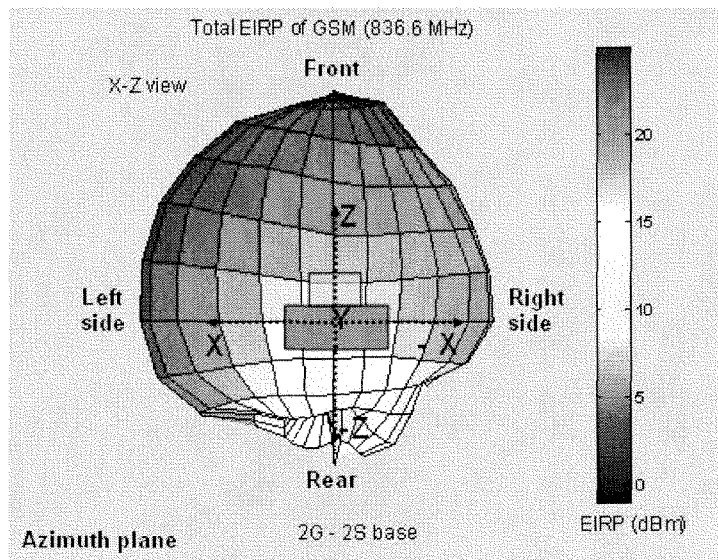


Figure 8-18
 Azimuth plane view of the total EIRP of a GSM 836.6 MHz cellular radio in a cell relay meter.

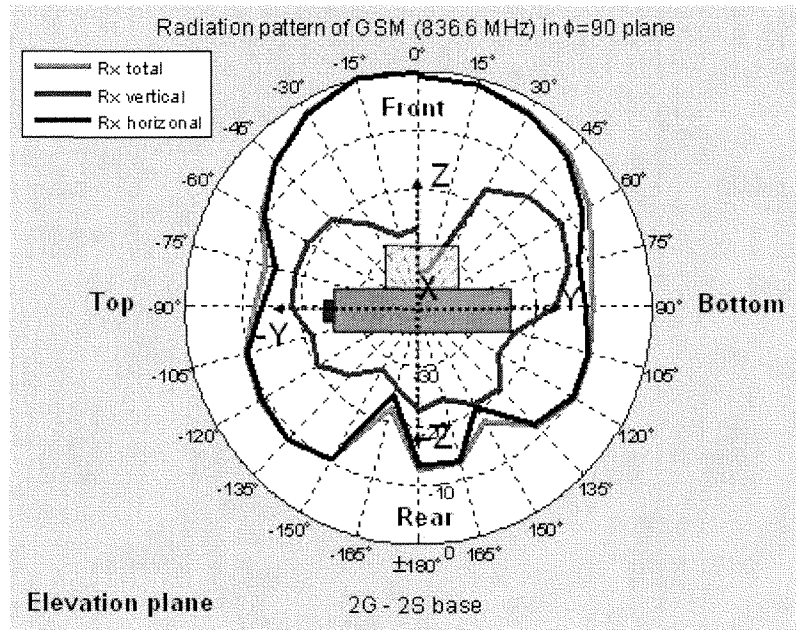


Figure 8-19
 Elevation plane pattern of the 836.6 MHz GSM cellular transmitter in a cell relay meter showing the horizontal, vertical and total pattern as viewed from bottom of meter. The scale is in dB with the maximum field at the outer edge of the pattern circle.

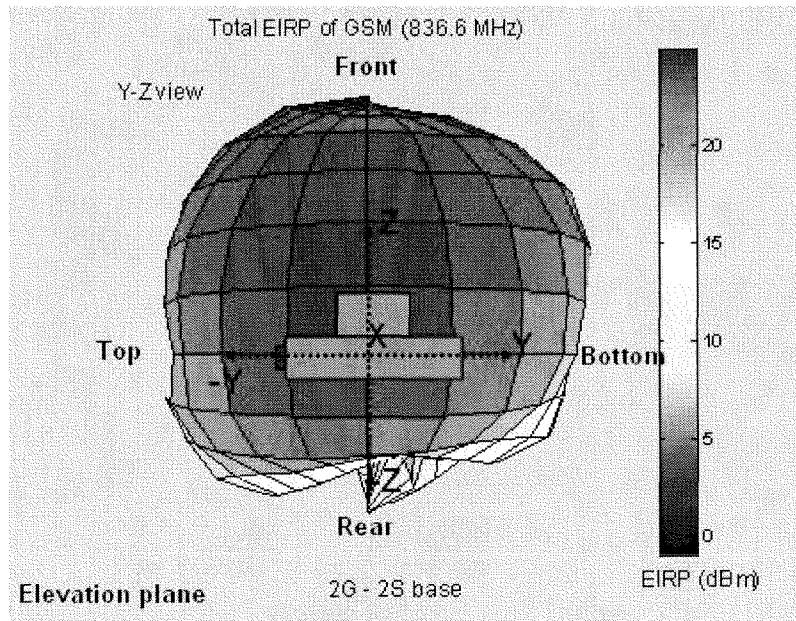


Figure 8-20
 Elevation plane view of the total EIRP of a GSM 836.6 MHz cellular radio in a cell relay meter.

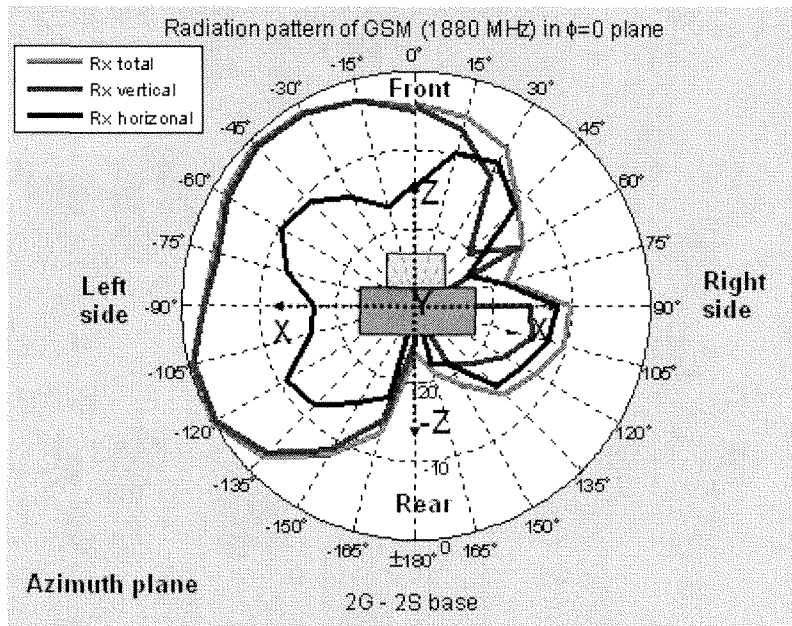


Figure 8-21
Azimuth plane pattern of the 1880 MHz GSM PCS transmitter in a cell relay meter showing the horizontal, vertical and total pattern as viewed from bottom of meter. The scale is in dB with the maximum field at the outer edge of the pattern circle.

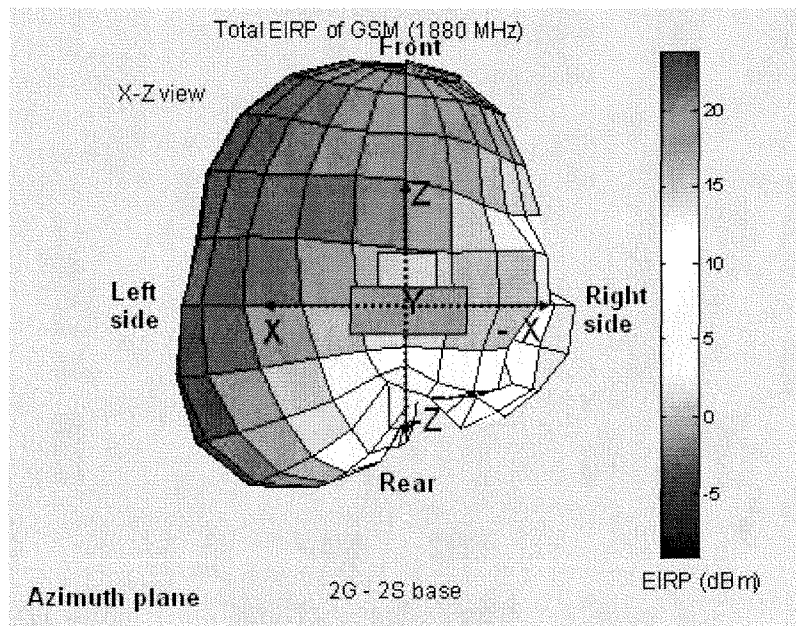


Figure 8-22
Azimuth plane view of the total EIRP of a GSM 1880 MHz PCS radio in a cell relay meter.

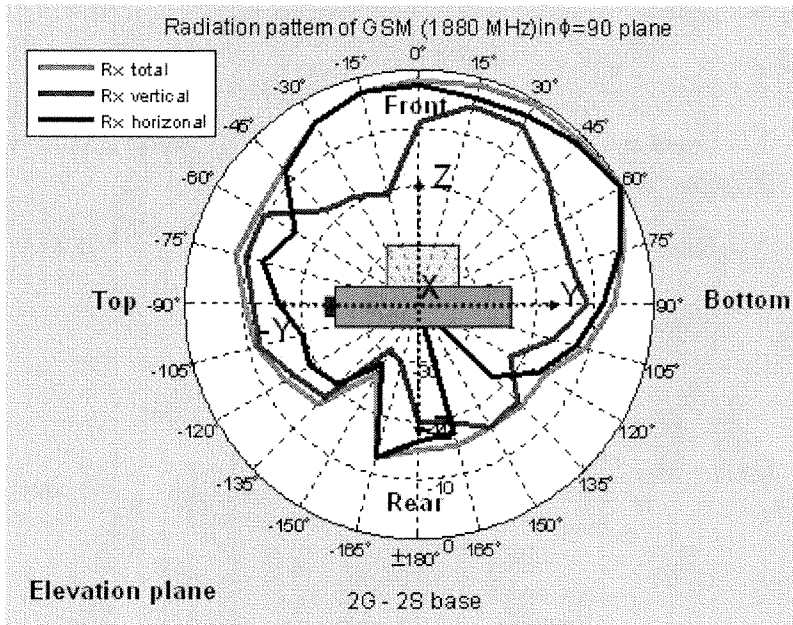


Figure 8-23
 Elevation plane pattern of the 1880 MHz GSM PCS transmitter in a cell relay meter showing the horizontal, vertical and total pattern as viewed from bottom of meter. The scale is in dB with the maximum field at the outer edge of the pattern circle.

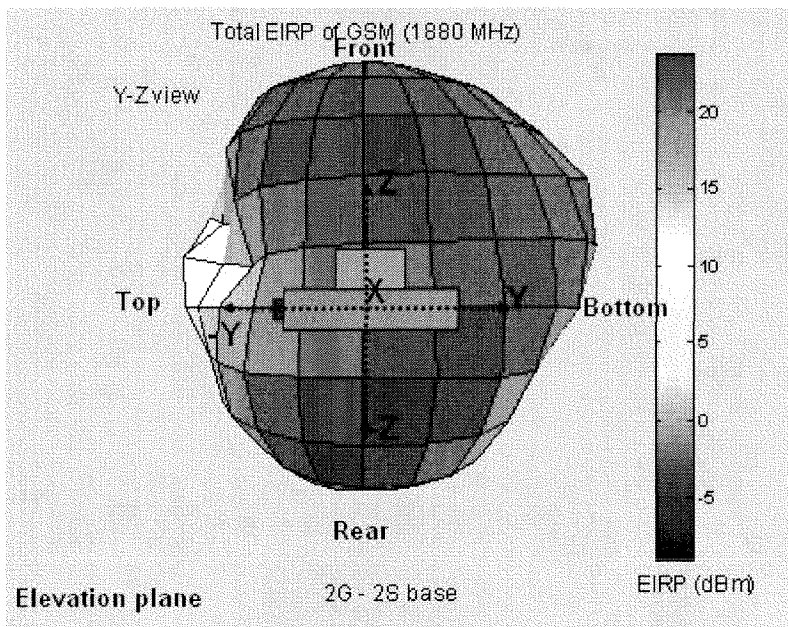


Figure 8-24
 Elevation plane view of the total EIRP of a GSM 1880 MHz PCS radio in a cell relay meter.

From analysis of each set of pattern measurement data, the EIRP was determined for a given transmitter output power delivered to the antenna. Table 8-1 summarizes the maximum EIRP found for each of the different measurement conditions described above. Maximum EIRP is the absolute greatest value of EIRP found from all of the pattern measurements at any angle. As observed from the pattern data shown above, the maximum EIRP may not be aligned with a line directly normal to the face of the Smart Meter. In each case, the

maximum EIRP has been referenced to one milliwatt. Hence, subsequent analyses making use of the maximum EIRP simply require adjusting the EIRP value for the actual transmitter power expected under normal operating conditions. In Table 8-1, the nominal specified transmitter power values are given in the next to last column and the maximum transmitter EIRP, referencing the nominal specified transmitter power, is given in the last column.

*Table 8-1
Summary of antenna measurement data*

Transmitter description	Max test EIRP (dBm)	Test power (dBm)	Gain (dBi)	Max TX P^a (dBm)	Max TX EIRP^b (dBm)
End point RF LAN, 914.8 MHz	12.8	9.9	2.9	24.0	26.9
Cell Relay RF LAN, 914.8 MHz	15.0	14.1	0.9	24.0	24.9
End point Zigbee, 2440 MHz	19.4	15.2	4.2	18.3	22.5
Cell Relay Zigbee, 2440 MHz	17.9	12.8	5.1	18.3	23.4
Cell Relay GSM, 836.6 MHz	24.9	23.1	1.8	31.8	33.6
Cell Relay GSM, 1880 MHz	23.9	22.3	1.6	28.7	30.3

^aNominal specified transmitter power

^bThe maximum transmitter EIRP assumes the nominal specified transmitter power.

Section 9: Smart Meter Field Measurements

The following narrative describes measurements of RF fields produced by Smart Meters that were obtained at the Itron meter farm in West Union, South Carolina, at residential settings in California and instrumentation comparisons and attenuation measurements for some selected materials including a simulated residential wall.

Meter farm measurements

A major feature of the Itron facility is a large “Smart Meter farm”. An aerial view of the geographic layout of the meter farm is seen in Figure 9-1. Approximately 20 acres comprise the installation of some 7000 Smart Meters for evaluating the performance of Itron’s meters in mesh networks. For the most part, Smart Meters are

organized in groups of ten meters on wooden racks as shown in Figure 9-2. The meters are arranged in two rows of five meters each, one above the other. The rack is 48 inches wide with the meters mounted so that there is a 16 inch vertical spacing of the two rows of meters, center to center. The bottom row of meters is nominally 48 inches above the ground. In one area in which area survey measurements were performed, the meter racks were found to be 16 feet apart, side to side, with the rows of racks 20.5 feet apart. Broadband probe and spectrum analyzer field measurements were performed on both individual Smart Meters and groups of ten meters comprising a rack.

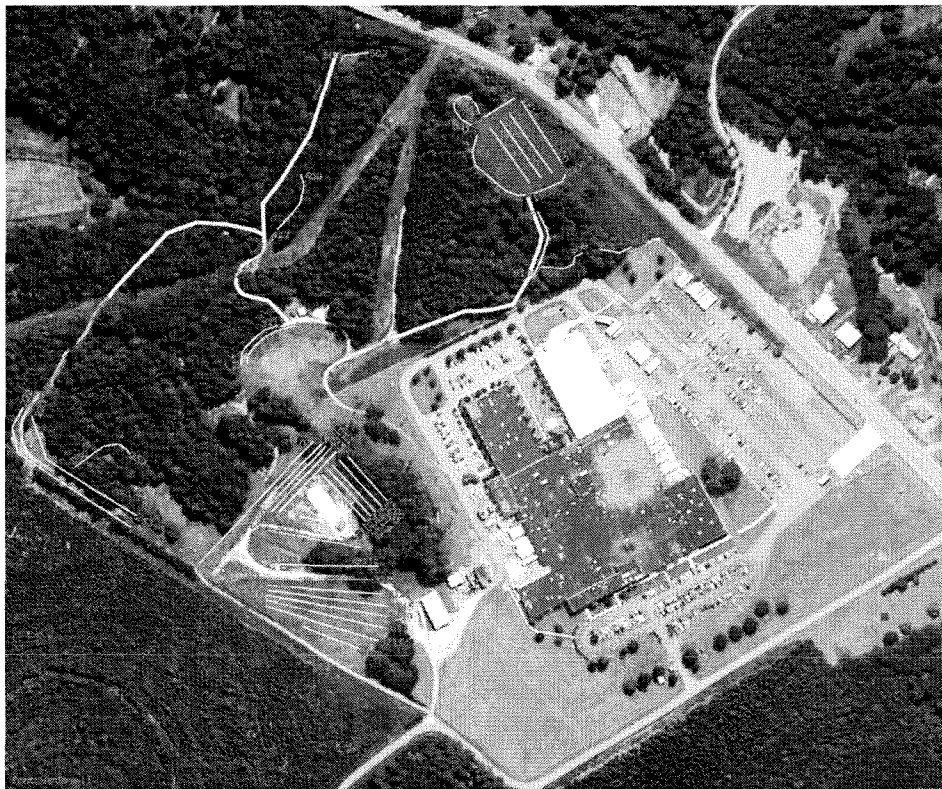


Figure 9-1
Aerial view of the Itron meter farm in West Union, SC. Yellow lines represent rows of Smart Meters grouped, generally, as racks of ten meters each. Photo courtesy of Itron.



Figure 9-2
Typical rack of ten meters shown in the western part of the Itron meter farm.

Individual meters

Initial field measurements in the meter farm were made using the broadband field probe (Narda Model B8742D). An objective of the broadband measurements was to assess what effect multiple Smart Meters might have on the measured RF field magnitude. The measurement approach sought to, first, examine the uniformity of measured field strengths among ten end point meters. To accomplish this, Itron programmed each of the ten meters to enter the continuous transmit mode of operation with three of the ten meters programmed to operate on the lowest frequency (L) in the 900 MHz RF LAN band (902.25 MHz), three meters to operate at the mid-band (M) frequency (914.75 MHz) and the remaining four meters to operate at the upper most channel (H) in the band (927.75 MHz). Measurements were performed over a

period of time during which the transmitter power was not expected to diminish due to transmitter heating. RF sources on precisely the same frequency and physically coincident with one another could lead to the possibility of phase addition or phase cancellation of the resultant RF field at specific points. In the measurement method used, the ten meters were physically distributed over a distance of up to 48 inches (this being equivalent to approximately four wavelengths in the 900 MHz band and approximately ten wavelengths in the 2.4 GHz band). Further, while individual meter frequencies on specific channels are very close to one another, they are not exactly the same due to crystal drift in the oscillator circuitry. Hence, the likelihood of RF fields from various meters actually being perfectly coherent is extremely small. Further, because of the measurement technique of scanning a planar area for the maximum,

peak RF field at each distance from the rack of meters, whether constructive or destructive phase addition may have existed, become irrelevant.

Each of the ten Smart Meter locations within a rack were identified with a letter from A to J and a location for each of these meters was determined as shown in Figure 9-3. The rationale behind this arrangement was to try to group meters in such a way as to enhance the potential for RF field contribution from adjacent meters

to the extent feasible when all ten meters were installed in the rack and actively transmitting. Initially, however, measurements were started with one meter only in the A position and successively replacing it with each of the other meters so that, ultimately, each of the ten meters had been installed in the A meter socket and the RF field was measured with the broadband probe. Each of the meter positions is also labeled as to the frequency of the associated meter as L, M or H, designating its frequency.

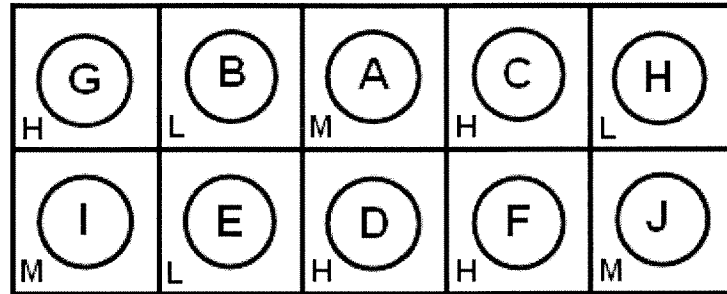


*Figure 9-3
Layout of Smart Meter rack showing designated meter locations and frequency of various meters (L, M and H - see text) for the 900 MHz RF LAN and 2.4 GHz Zigbee transmitters.*

Broadband field probe measurements were taken with the probe touching the surface of the meter face, with the probe at 20 cm from the meter face, with the probe at 30 cm from the meter face and, finally, with the probe behind the meter rack with the probe in contact with the rear of the rack, immediately behind meter position A. Use of the broadband field probe with a cardboard spacer affixed to the probe at the rack of ten meters is illustrated in Figure 9-4. These measurement results are given in Table 9-1. Each of the indicated

values was obtained by multiplying the meter reading by the manufacturer's calibration correction factor applicable at 915 MHz of 0.67. Surface field measurements with an isotropic probe must be interpreted with care due to the potential for erroneous readings. Nonetheless, because others may apply such probes in this fashion, it was deemed relevant to examine what kind of response would be exhibited when contacting the probe to the Smart Meter.



Figure 9-4
Use of the broadband field probe with a cardboard spacer attached to the probe near meters in a rack of ten meters.

Table 9-1
Measurements of 900 MHz RF LAN emissions of individual Smart Meters installed in meter position A in the meter rack with the broadband field probe.

Meter	Frequency	RF field measured (% of FCC public MPE)			
		Surface	20 cm	30 cm	Rear surface
A	M	45.9	4.2	2.2	0.0
B	L	65.3	6.9	5.5	0.0
C	H	18.5	1.6	1.1	0.0
D	H	16.8	2.3	1.6	0.0
E	L	53.7	5.6	4.2	0.0
F	H	19.1	2.1	0.7	0.0
G	H	20.5	1.9	0.7	0.0
H	L	48.6	4.9	3.5	0.0
I	M	45.7	4.6	2.8	0.0
J	M	29.6	3.1	1.9	0.0

In examining the results, two issues are immediately apparent. First the instrument readings appear to be related to the channel to which the 900 MHz RF LAN transmitter was programmed. This can be more easily seen in Figure 9-5. Clearly, the indicated field magnitude is related to the frequency of the 900 MHz RF LAN transmitter; the highest readings are correlated with the lowest frequency and the lowest

readings are correlated with the highest transmitter frequency. From data in Table 9-1 at 20 cm, the mean value of readings of the L meters is 5.8% while the mean value of the readings of the H meters is 2.0%; this corresponds to a ratio of 2.9 or a total range of about 4.6 dB from the lowest to the highest readings, i.e., a variation of ± 2.3 dB relative to the band center frequency.

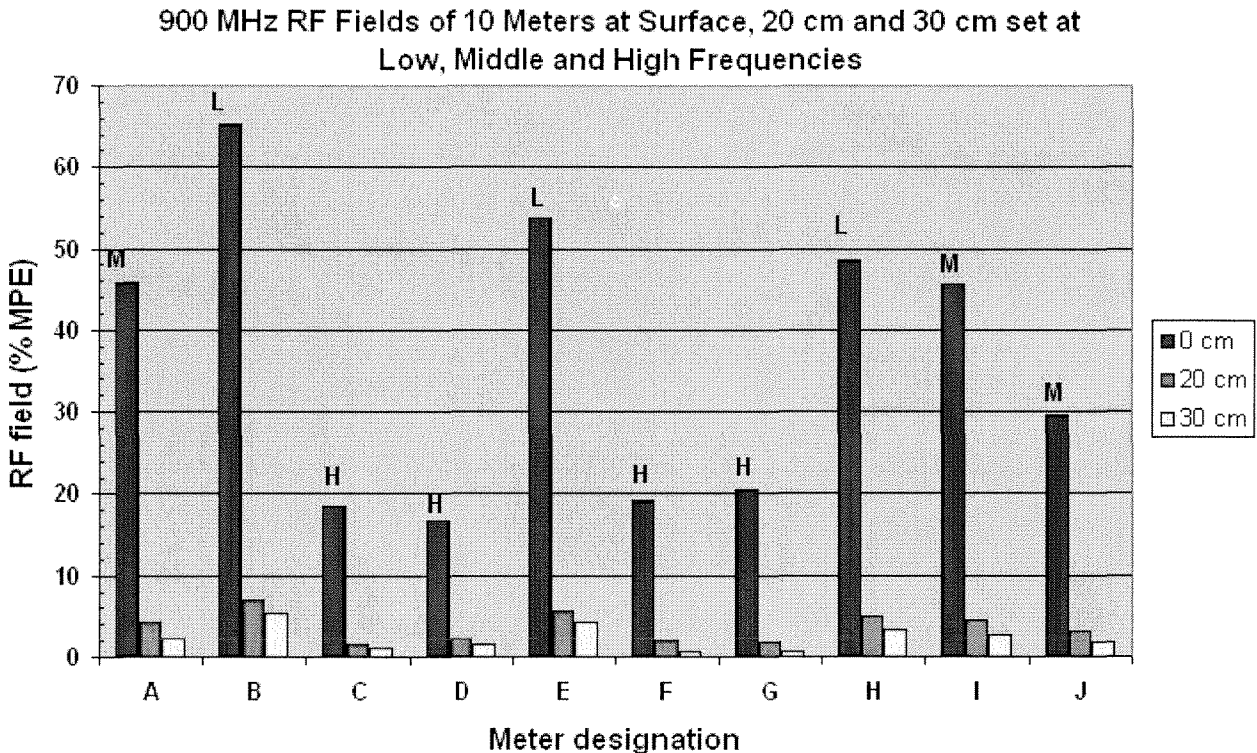


Figure 9-5
Corrected broadband probe RF field readings of the 900 MHz RF LAN transmitters from ten Smart Meters at the surface and at 20 cm and 30 cm from the meter.

A second observation is that the surface field strength readings are significantly greater than those at 20 cm. Why might this be the case? The probe protective shell surface is being placed in contact with the face of the Smart Meter, bringing the probe elements very significantly closer such that the probe is within the reactive near field region of the source antenna. The 900 MHz RF LAN antenna is only about 2.1 cm behind the meter envelope face; this is comparable to about only

0.06 wavelengths. Under these conditions, the probe may couple to the field source leading to erroneously high readings. Generally, field probes should not be used in such close proximity to the source because of this very issue. For example, IEEE Standard C95.3-2002¹³ recommends a minimum measurement distance

¹³ IEEE Standard C95.3-2002. IEEE Recommended Practice for Measurements and Computations of Radio Frequency

of 20 cm to minimize nearfield coupling and field gradient effects when using common broadband field probes. Measurement data can also be distorted when using an isotropic probe to measure steep spatial gradients close to a radiating element of the Smart Meter. These gradients can lead to considerable variation of the indicated amplitude of the field being measured over the volume of space occupied by the measurement probe elements. This is particularly true when employing field probes in the reactive near field that are comparable to the size of the source antenna. It should be noted that the elements inside the Narda B8742D probe are approximately 8 cm long; this is approximately the same length as the slot antenna of the 900 MHz RF LAN antenna that is approximately 6.3 cm long. Based on the potential for significant probe coupling with the Smart Meter internal transmitting antenna, the measured values indicated for surface contact of the probe with the Smart Meter should be considered suspect and, likely, substantial over estimates of the true field. Measurements at 20 cm and 30 cm,

however, are deemed to be reliable since they are substantial fractions of the 900 MHz wavelength (20 cm is equivalent to 0.6 wavelengths and 30 cm is equivalent to 0.9 wavelengths).

Following measurement of the fields produced by the ten individual meters, measurements of the maximum indicated RF field were conducted in front of and behind the rack as individual meters were successively installed into their respective meter sockets. The objective was to observe for any increase in cumulative RF field caused by the contribution of an increasing aggregate of actively transmitting Smart Meters. These measurement results are summarized in Table 9-2. Due to technical problems associated with programming of two of the meters at the time (meters D and F), not all meters were included in each collection of active meters. However, at the end of the process, all meters were included when all ten meters were active.

Table 9-2

Summary of measurements of the 900 MHz composite RF field produced by an increasing number of closely spaced, collocated Smart Meters (meters A - J).¹⁴

Meters active	RF field at 20 cm	RF field at 30 cm	RF field behind rack
A	4.2	3.3	0.0
AB	7.9	5.0	0.0
ABC	7.4	5.3	0.1
ABCE	7.9	5.9	0.1
ABCEG	8.6	6.1	0.1
ABCEGH	9.0	6.2	0.3
ABCEGHI	8.7	6.8	0.7
ABCEGHIJ	9.2	6.7	0.9
ABCDEGHIJ	9.1	7.2	0.7
ABCDEFGHJIJ	8.1	7.5	0.8

¹⁴ During the testing, meter D exhibited a problem that was subsequently fixed but was left out of some of the test rows in Table 3.

In each case of added meters, the entire surface of the meter rack was scanned with the broadband probe with 20 and 30 cm spacers attached to the probe to search for the greatest meter reading. The location of maximum reading was not necessarily the same in each case and the data strongly suggest that for a given distance from the front of the meter rack, a finite maximum value of field is developed that will not be exceeded with the addition of more meters. Beyond three or four meters, the aggregate field does not materially increase with additional meters. The data indicate a maximum observed, composite field of 9.2% of the general public MPE at 20 cm and a maximum of 7.5% of the MPE at 30 cm (almost one foot). Immediately behind the meter rack, a maximum composite field equivalent to 0.9% of the MPE was measured.

A somewhat similar approach was used to measure the collective composite RF field produced by multiple

Smart Meters with the 2.4 GHz Zigbee transmitters activated for transmission. Itron programmed each of the ten meters to enter the continuous transmit mode of operation with three of the ten meters programmed to operate on the lowest frequency (L) in the 2.4 GHz band (2405 MHz), three meters to operate at the mid-band (M) frequency (2440 MHz) and the remaining four meters to operate at the upper most channel (H) in the band (2475 MHz). In this case, the individual meters were measured with each meter being placed in position A but the overall composite field, with all meters active, was performed by inserting all meters into their designated positions without sequentially adding active meters as was done with the 900 MHz RF LAN tests. Table 9-3 summarizes the results of these measurements. All readings of the 2.4 GHz emissions were corrected by applying the manufacturer's determined correction factor for 2.45 GHz of 0.97.

Table 9-3

Summary of corrected measurement data on RF fields of individual 2.4 GHz Zigbee transmitters installed in meter position A and of the collection of all ten meters.

A	M		10.2	
B	L	11.8	1.7	0.0
C	H	5.1	1.4	0.0
D	H	5.5	1.0	0.0
E	L	11.8	0.9	0.0
F	H	6.3	1.5	0.0
G	H	5.4	0.9	0.0
H	L	8.8	1.0	0.0
I	M	7.0	1.0	0.0
J	M	5.1	0.7	0.0
All on		14.3	1.0	0.0
A	M	10.2	2.5	0.0

These data support the contention that the Zigbee transmitters operating at the lowest frequency within the 2.4 GHz band tended to produced the greatest

measured field strength, similar to the finding for the 900 MHz RF LAN transmitters. Figure 9-6 illustrates the data in Table 9-3 graphically.

2.4 GHz RF Fields of 10 Meters at Surface and 20 cm set at Low, Middle and High Frequencies

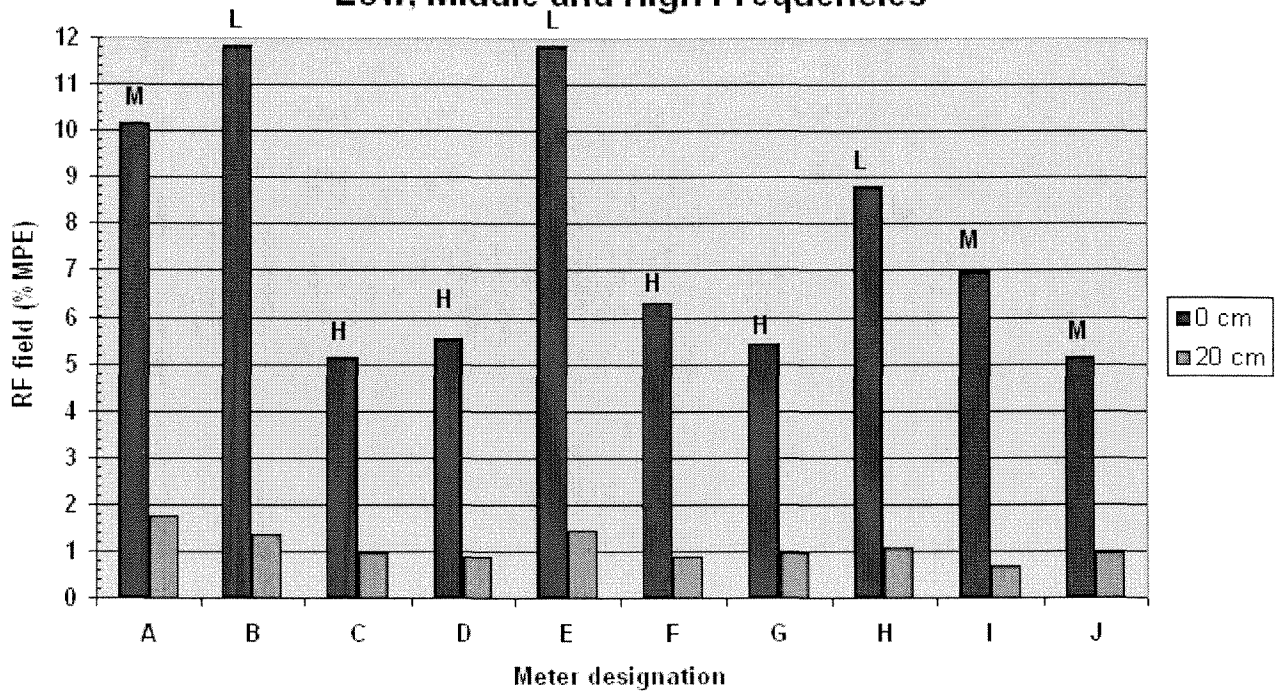


Figure 9-6

Corrected broadband probe RF field readings of the 2.4 GHz Zigbee transmitters from ten Smart Meters at the surface and at 20 cm from the meter.

Table 9-3 also indicates that the composite RF field associated with simultaneous operation of all ten Smart Meters with their Zigbee radios active provided a maximum reading of 14.3% of the FCC general public MPE with the probe in surface contact with the meters and a maximum of 2.5% of the MPE at 20 cm from the surface. The surface readings must also be considered suspect as is the case with the 900 MHz band measurements. The RF field behind the rack of ten active meters was not detectable with the broadband field probe.

Groups of meters

Through use of the Narda SRM-3006 instrument, measurements of RF fields could be made at much

greater distances from the meter rack due to the significantly greater sensitivity of the narrowband device when compared to the broadband field probe. The aggregate RF field produced by a meter rack of ten Smart Meters was examined with the SRM-3006 by making measurements at successively greater distances from the front of the rack and observing the spectral display of the measurement result. The measurement process consisted of holding the SRM-3006 at the approximate mid-height of the rack at different distances from the frontal plane of the meters in the rack as shown in Figure 9-7



*Figure 9-7
Using the Narda SRM-3006 to measure aggregate RF fields near a rack of ten meters programmed for fixed frequency, continuous transmission in the meter farm.*

The instrument was used to acquire a “max hold” spectrum over a period of approximately one minute while slowly moving the probe in a planar area measuring approximately 2 feet by 2 feet. Figure 9-8 shows the result of the measurement with the SRM-3006 probe/antenna positioned at 1 foot from the front of the meter rack. In this display, the continuously operating 900 MHz RF LAN transmitters are clearly

seen on their respective frequencies (902.25 MHz, 914.75 MHz and 927.95 MHz). A resolution bandwidth of 100 kHz was used in these spectral measurements within the frequency band of 902 MHz to 928 MHz. The SRM-3006 was set to display the maximum measured field at each distance directly as a percentage of the FCC general public MPE as seen on the vertical axis of the display.

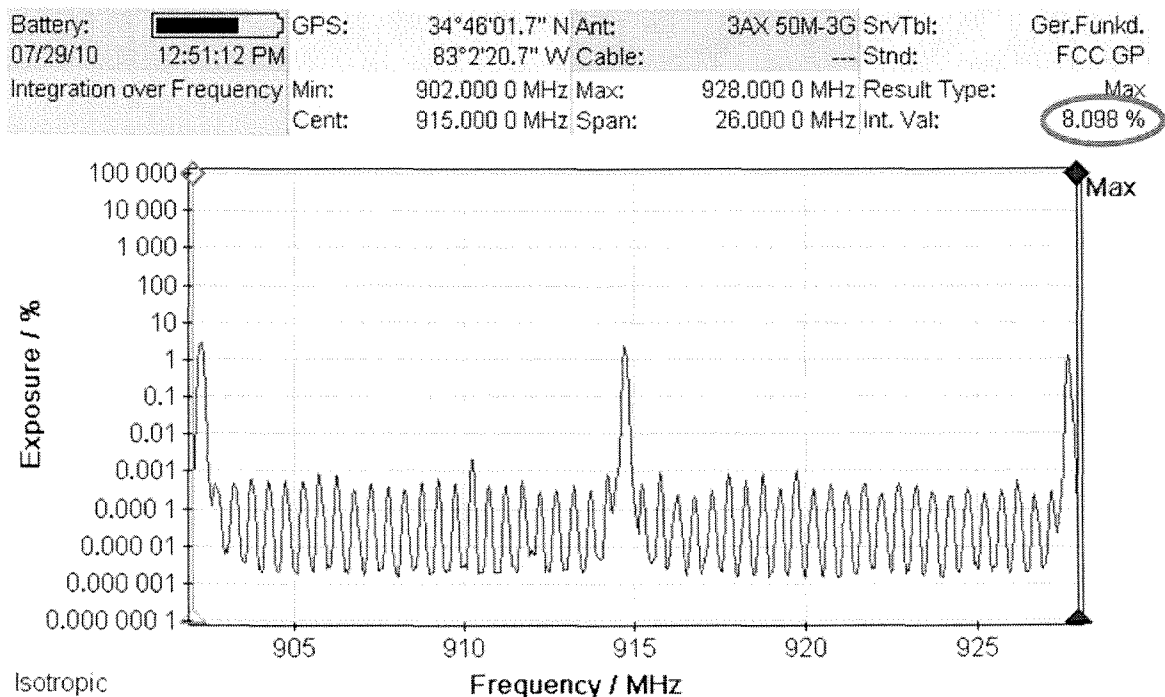


Figure 9-8
900 MHz band composite RF field from rack of 10 SmartMeters at 1 foot.

The many lower level spectral peaks were caused by the multiplicity of Smart Meters within the meter farm; in practice, it was not possible to completely remove oneself from the ambient background of RF fields present in the meter farm since moving away from one rack of meters meant that one was getting closer to another rack in some location. While the signals from the other thousands of Smart Meters were randomly occurring across the band, because of the number of meters simultaneously operating, the presence of signals on each frequency was evident. Had only one Smart Meter been operating, this would not have been the case, as discussed earlier. Using the internal integration feature of the SRM-3006, the total equivalent RF field power density was reported by the instrument as a percentage of the general public MPE in the upper right region of the spectral plot (see circled area). For the measurement at 1 foot in front of the meter rack, a total integrated RF field equivalent to 8.1% of the MPE was determined.

Using the spectrum analysis method describe above, measurements were made at successively greater distances from 1 foot to 100 feet from the Smart Meter

rack. These spectrum scans obtained from the SRM-3006 are shown in Appendix B. Referring to Appendix B, it can be seen that as the distance between the rack and the measuring instrument was increased, the signal level of the programmed meters decreased until, at approximately 50 feet from the rack, the signal levels of the meter rack being investigated blended into the background of all of the other ambient RF fields from other meters within that area of the meter farm. In other words, the emitted signals became indistinguishable from the ambient environment of RF fields and could not be identified as being contributed by a specific meter rack or collection of Smart Meters. Field measurements taken to the rear of the meter rack are provided in Appendix C. Figure 9-9 shows measurements being performed behind the rack of specially programmed Smart Meters. The presence of other racks of active meters are evident in the background. As distance from the back side of the subject rack was increased, the distance to the other meter racks located behind the subject rack decreased meaning that the ambient, but intermittent, RF fields of other meters in the farm could be detected.



Figure 9-9

Field measurements at successively greater distances behind the subject meter rack resulted in closer proximity to other meter racks with the probability of detecting stronger, but intermittent, signals due to the ambient background.

Another set of field measurements in front of the meter rack was performed with the Zigbee radios in the meters programmed for continuous transmit operation on 2405 MHz, 2440 MHz and 2475 MHz. The SRM-3006 was set for a resolution bandwidth of 200 kHz over the band of 2400 to 2483 MHz for these measurements. A similar pattern of decreasing field magnitude with increasing distance was observed for the Zigbee radio emissions. Figure 9-10 shows the spectrum plot obtained at 1 foot from the front of the meter rack with all ten radios operating with an

integrated RF field equivalent to 4.5% of the general public MPE. Appendix D provides each of the spectrum measurements of the ten Zigbee transmitters at distances from 1 foot to 100 feet from the front of the meter rack. Appendix E provides similar spectrum plots taken behind the meter rack as well as the result of a lateral walk at three feet in front of and across the face of the meter rack extending from a few feet beyond the edge of the rack to an equivalent distance beyond the opposite edge.

Battery: 07/29/10 02:29:42 PM	GPS: 34°46'01.2" N 83°2'20.3" W	Ant: 3AX 50M-3G	SrvTbl: ---	Ger.Funkd.: FCC GP
Integration over Frequency	Min: 2 400.000 MHz Cent: 2 441.500 MHz	Max: 2 483.000 MHz Span: 83.000 MHz	Result Type: Max	Int. Val: 4.499 %

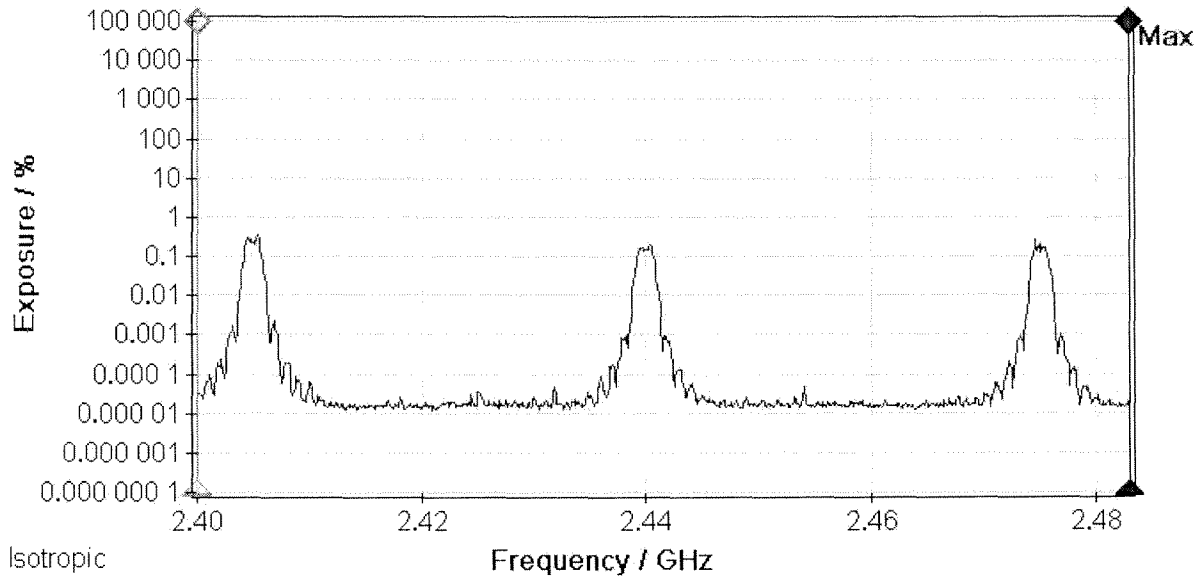


Figure 9-10
Spectrum measurement of 2.4 GHz RF fields from ten simultaneously transmitting Smart Meters.

Table 9-4 lists the integrated RF fields determined for both the 900 MHz RF LAN and 2.4 GHz Zigbee transmitters over the range of distances used. The data in Table 9-4 are plotted in both linear (Figure 9-11)

and logarithmic (Figure 9-12) formats to illustrate graphically the decrease in RF field with distance from the meter farm rack of ten meters.

Table 9-4

Summary of composite RF field values (% general public MPE) determined with the SRM-3006 at various distances in front of a meter rack of 10 simultaneously operating Smart Meters.

Distance (ft)	900 MHz	2.4 GHz
1	8.098	4.499
2	3.898	2.459
3	2.471	1.021
4	1.827	0.587
5	1.382	0.457
6	1.157	0.348
7	0.722	0.258
8	0.655	0.187
9	0.681	0.163
10	0.536	0.134
15	0.356	0.076
20	0.177	0.044
25	0.152	0.033
30	0.144	0.02
40	0.113	0.014
50	0.107	0.013
75	0.073	0.0091
100	0.092	0.00852
Distance (ft)	900 MHz	2.4 GHz

From Table 9-4 and Figures 9-11 and 9-12, it is evident that the peak RF field measured for the group of ten active Smart Meters drops to less than 1% of the FCC general public MPE at a distance of approximately seven feet where the combined RF field from both frequency bands are summed. This peak value is not

representative of the time averaged field that would be present during normal operation of the Smart Meter since the typical duty cycle of the meters would cause the composite time-averaged field to be substantially less.

**RF Fields vs Distance in Meter Farm
with 10 Meters Operating Continuously**

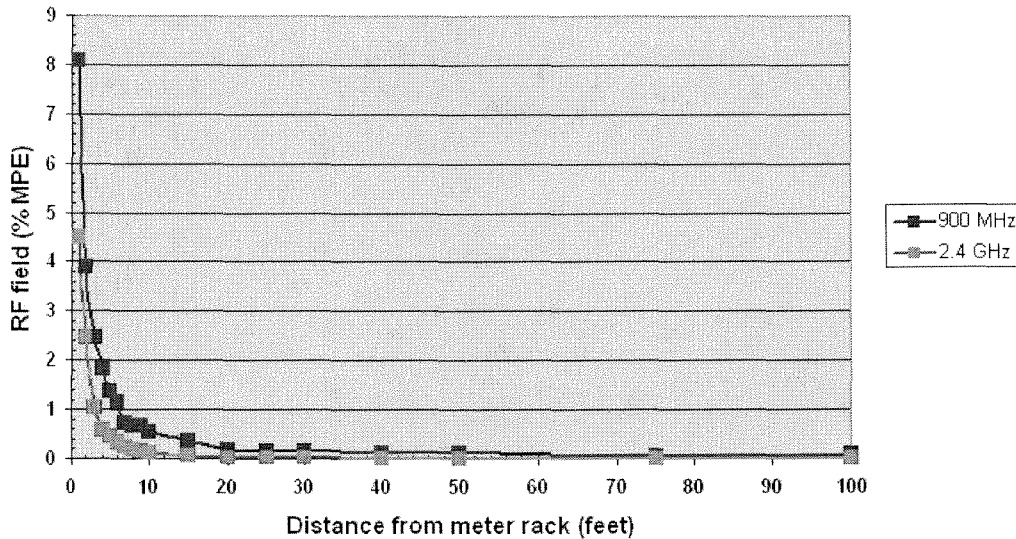


Figure 9-11
Integrated, total composite RF field obtained in meter farm for emissions from the 900 MHz RF LAN and 2.4 GHz Zigbee transmitters operating simultaneously in the vicinity of a meter rack (linear plot).

**RF Fields vs Distance in Meter Farm
with 10 Meters Operating Continuously**

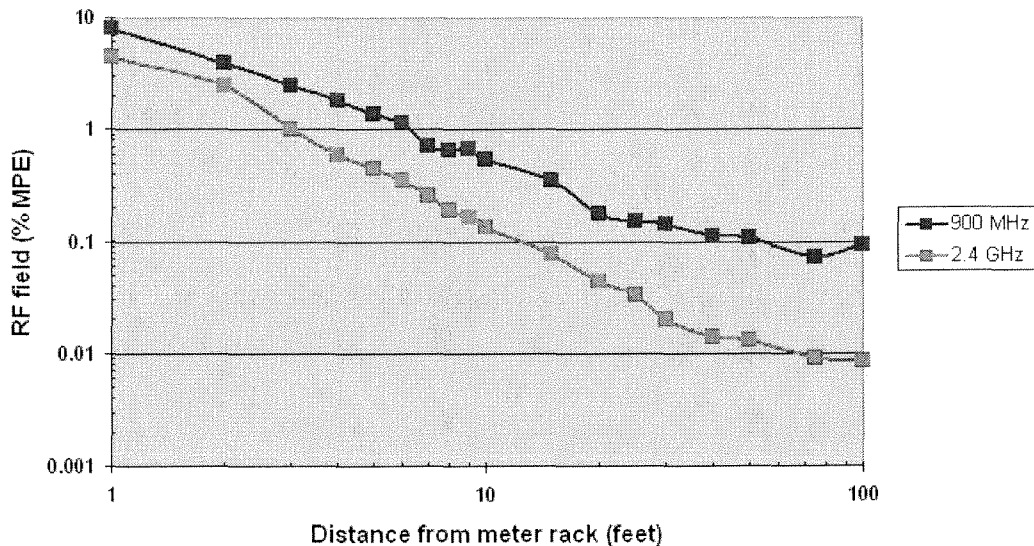


Figure 9-12
Integrated, total composite RF field obtained in meter farm for emissions from the 900 MHz RF LAN and 2.4 GHz Zigbee transmitters operating simultaneously in the vicinity of a meter rack (logarithmic plot).

Residential settings

Homes

In the interest of gathering data on RF fields from Smart Meters in a realistic residential environment, additional measurements were performed in a Downey, California neighborhood. On August 19, 2010, measurements were conducted at two different residences at which SCE Smart Meters had been previously deployed. Two different Smart Meters were used to facilitate the measurements, one that had been programmed to operate in continuous transmit mode on the lowest frequency in the 900 MHz band and the other programmed to operate in continuous transmit mode on the lowest frequency in the 2.4 GHz band. Each meter was temporarily installed at each of the two

homes during which a series of RF measurements were taken at the meter service box on the home, within the front, side and backyards, and throughout the home in all rooms of the home. Figure 9-13 shows an SCE meter technician in the process of installing one of the special “test” meters in place of the meter normally present.

At the first residence, designated residence A, measurements of the maximum, instantaneous peak RF field were conducted by scanning a planar region at 1, 2, 3, and 5 feet in front of the meter. The measurements are summarized in Table 9-5. The region near the service box for residence A was somewhat cramped and measurements were not possible beyond five feet from the face of the Smart Meter.

Table 9-5

Summary of planar area scans performed with the SRM-3006 in front of residential meter installation at residence A, Downey, CA, with transmitters operating continuously.

Location relative to meter (feet)	900 MHz RF LAN		2.4 GHz Zigbee	
	RF field (% public MPE)	Time of measurement (PDT)	RF field (% public MPE)	Time of measurement (PDT)
Surface	9.67	9:49	7.93	11:19
1	0.875	9:54	0.615	11:22
2	0.361	9:56	0.258	11:22
3	0.186	9:58	0.142	11:23
5	0.096	10:00	0.071	11:25

With each of the two specially programmed Smart Meters installed in the home’s service box meter socket, spectrum measurements were performed throughout the home including some outside areas. Figure 9-14 shows the measurement of a planar scan at the residence. Procedurally, the 900 MHz band measurements were performed first, followed by the 2.4 GHz measurements. Table 9-6 summarizes the measurements taken at residence A including a few outdoor measurements. The RF field reading recorded

for each room or area represents the overall peak value of field obtained through a spatial scan of the room or area. It is noted that directly behind the service box with the Smart Meter, inside bedroom 1, the greatest field detected corresponded to 0.01% of the FCC general public MPE. Overall, the greatest RF fields found were in the home office area, where a wireless router was installed for Internet connectivity and in the kitchen when the microwave oven was operating.



*Figure 9-13
SCE meter technician replacing existing Smart Meter with specially programmed meter for residential measurements.*



Figure 9-14
Planar scans were performed at several distances in front of a residential Smart Meter by slowly moving the SRM-3006 within a plane at a fixed distance.

Table 9-6

Spectrum scan measurements of Smart Meter fields in the 900 MHz and 2.4 GHz bands in residence A, Downey, CA. RF field is peak value obtained from a spatial scan of the room interior or area in percent of FCC general public MPE.

Location at residence	RF field (% MPE)	
	900 MHz	2.4 GHz
Front yard	0.00014	0.00611
Bedroom 1	0.00355	0.00876
Bedroom 1 (directly behind meter)	0.010	
Bath	0.009	0.00941
Bedroom 2	0.00909	0.00637
Master bedroom	0.00056	0.00644
Family room	0.00055	0.00627
Dining room/Living room	0.00057	0.00651
Kitchen	0.00057	0.00616
Kitchen (microwave at 6.5 feet)		0.016
Kitchen (microwave at 2 feet)		22.04
Laundry room	0.00053	0.00588
Bath	0.00054	0.00723
Office (Wi-Fi on)	0.00052	0.0288
Garage	0.00055	0.00622
Back side yard	0.00053	0.00653
Backyard	0.00059	0.00658
Pool	0.00058	0.00647

Figure 9-15 shows an interior measurement taken at residence A in a bedroom directly opposite to the mounting location of the Smart Meter on the outside of the house. Outdoor measurements at residence A are shown in Figures 9-16 and 9-17.

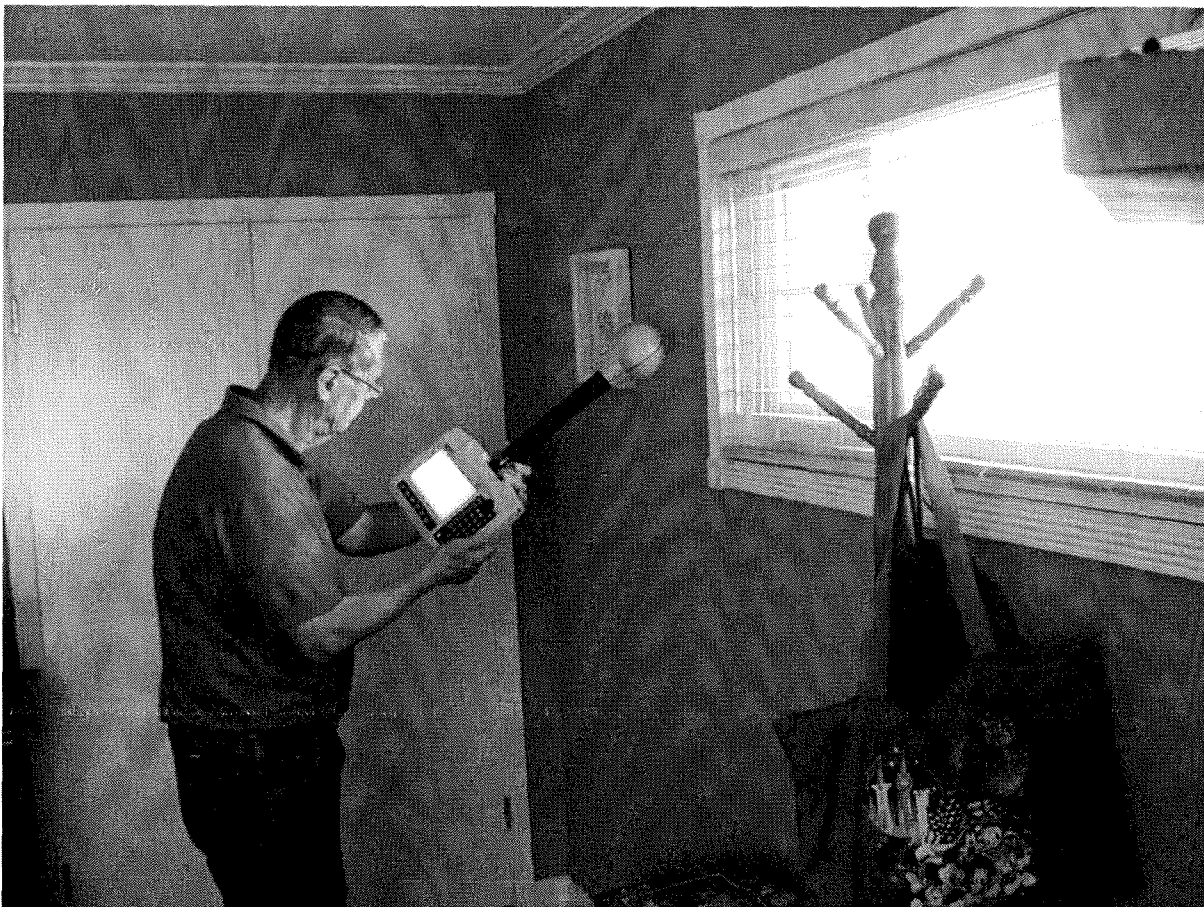
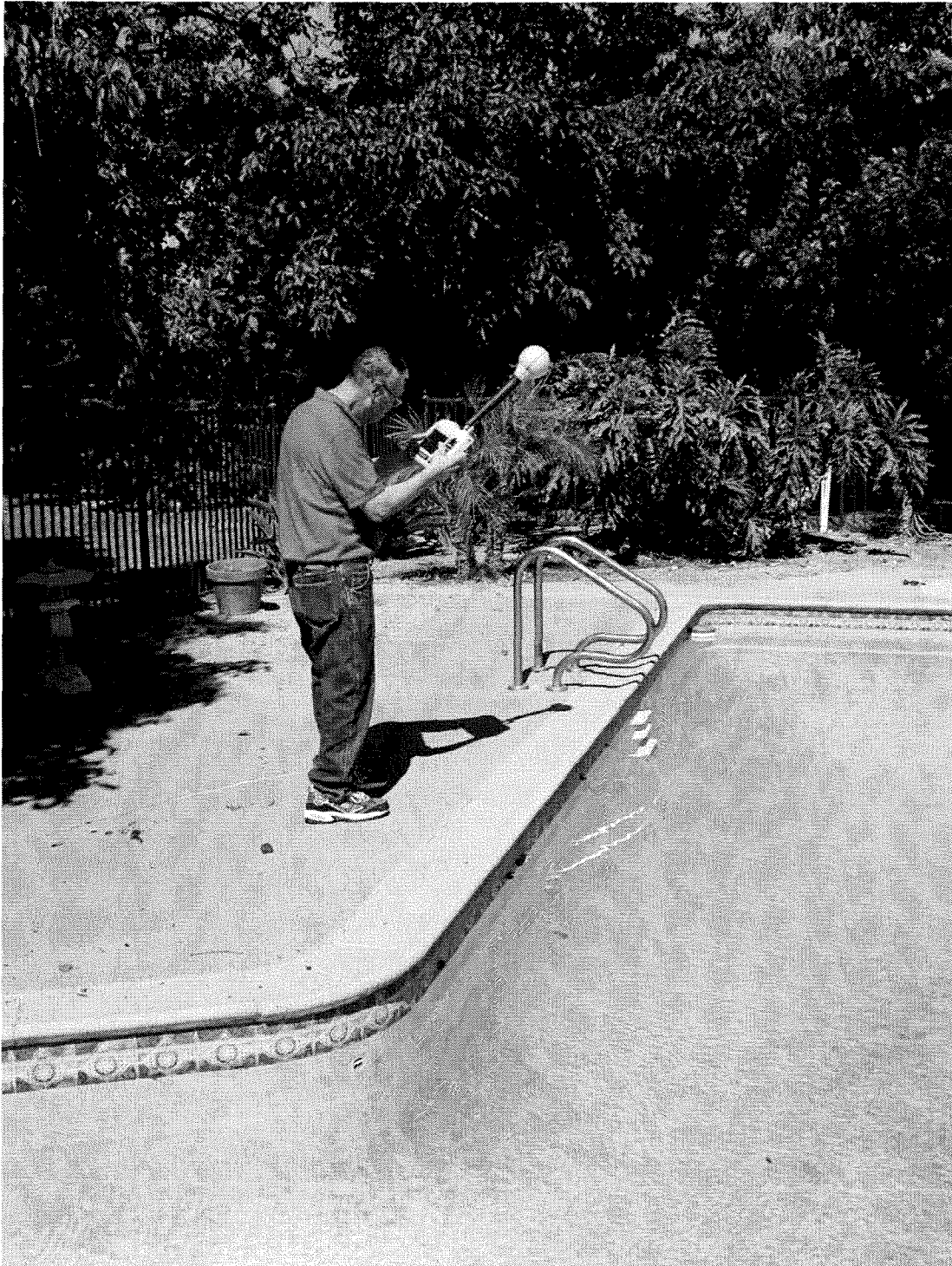


Figure 9-15
Interior residential measurements included measurements on the opposite side of the wall where the Smart Meter was installed at the home.



Figure 9-16
Residential measurements at residence A included both outdoors and indoors measurements of RF fields in both the 900 MHz and 2.4 GHz bands.



*Figure 9-17
Measurements at residence A included exterior locations in the backyard.*

At the second residence (Figure 9-18), designated residence B, also in the same neighborhood of Downey, CA as residence A, the measurement process again included scanning a planar region at 1, 2, 3, 4, 5, 6 and 10 feet in front of the meter. The measurements for residence B are summarized in Table 9-7. The specially programmed Smart Meters were used to facilitate

measurements throughout the property. Figure 9-19 shows the Smart Meter installed at residence B and a planar scan being performed. Within residence B, similar to residence A, a wireless router for Internet connectivity was found in a home office (Figure 9-20). Field measurements acquired within and around the residence are listed in Table 9-8.



*Figure 9-18
Residence B in Downey, CA where indoor and outdoor measurements were made with specially programmed Smart Meters installed to facilitate measurements.*



*Figure 9-19
Performing a planar scan of RF fields adjacent to a Smart Meter at residence B.*

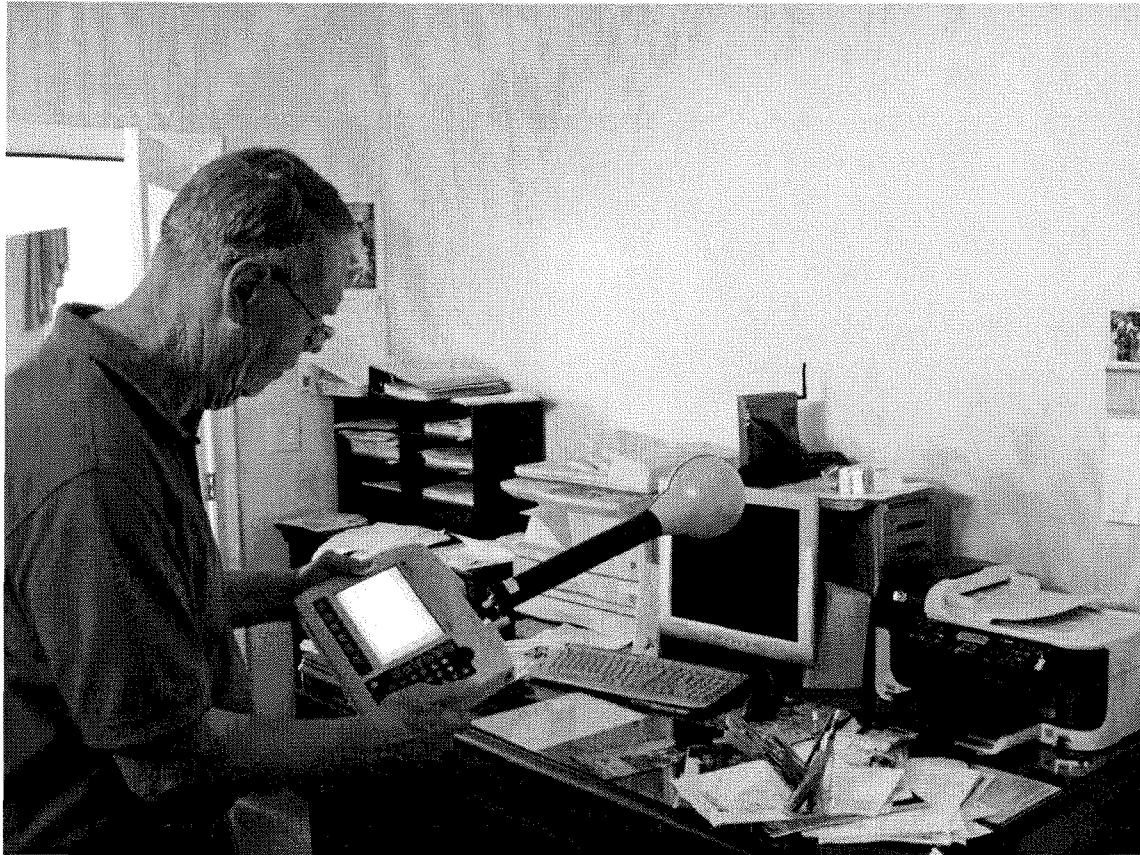


Figure 9-20
 Measured RF fields inside residence B, similar to residence A, tended to be predominated by signals produced by wireless routers used for Internet connectivity throughout the home.

Table 9-7
 Summary of planar area scans performed with the SRM-3006 in front of residential meter installation at residence B, Downey, CA.

Location relative to meter	900 MHz RF LAN		2.4 GHz Zigbee	
	RF field (% public MPE)	Time of measurement (PDT)	RF field (% public MPE)	Time of measurement (PDT)
Surface	10.84	1:34	10.02	1:34
1	1.386	1:35	0.985	1:35
2	0.351	1:36	0.290	1:36
3	0.159	1:37	0.160	1:37
4	0.104	1:38	0.117	1:38
6	0.048	1:40	0.053	1:40
10	0.020	1:41	0.026	1:41

Table 9-8

Spectrum scan measurements of Smart Meter fields in the 900 MHz and 2.4 GHz bands in residence B, Downey, CA. RF field is peak value obtained from a spatial scan of the room interior or area in percent of FCC general public MPE.

Location at residence	RF field (% MPE)	
	900 MHz	2.4 GHz
Front yard	0.00056	0.00659
Bedroom 1	0.00053	0.0063
Bath	0.00056	0.00597
Bedroom 2	0.00052	0.00618
Bedroom 3	0.0015	0.00638
Bedroom 3 (closet behind meter)	0.00872	0.00755
Master bedroom	0.00060	0.00643
Family room	0.00057	0.00753
Dining room/Living room	0.00063	0.00641
Kitchen	0.00056	0.012
Study (with Wi-Fi)	0.00055	0.015
Bath	0.0011	0.00596
Backyard	0.0051	0.015

Residential apartment setting

The use of the specially programmed Smart Meters allowed for relatively quick and definitive measurements of the peak RF fields produced by the internal 900 MHz and 2.45 GHz transmitters. In an effort to acquire data on neighborhood RF fields that might be produced by existing in-place meters, a Downey, CA neighborhood was explored to identify apartment complexes that had obvious groups of meters installed in easily accessible areas for measurement. Measurements with the SRM-3006 instrument were subsequently accomplished in front of meter banks at two apartment buildings on August 20, 2010. Figures 9-21 and 9-22 show the two apartment meter banks with nine and eleven Smart Meters respectively.

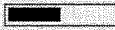
At each of the two meter banks, the SRM-3006 was held at a distance of 1 foot from the frontal plane of the meters and moved back and forth and up and down in this plane to maximize the probability of capturing the peak value of any meter emissions. This process was continued for a period of five minutes at each of the two meter banks. Captured spectra were integrated to obtain the composite RF fields in terms of the instantaneous peak values and average values over the five minute monitoring period. Figure 9-23 shows the resulting observed spectrum of peak values at the nine meter bank with the integrated value of 4.6% of the public MPE. The corresponding integral of the average field was 0.00105% of the MPE.



Figure 9-21
A nine-meter bank at an apartment house in Downey, CA.



Figure 9-22
An eleven-meter bank at an apartment house in Downey, CA.

Battery:		GPS:	33°57'01.5" N	Ant:	3AX 50M-3G SrvTbl:	Ger.Funkd.
08/20/10	12:18:51 PM		118°7'40.5" W	Cable:	--- Stnd:	FCC GP
Integration over Frequency		Min:	902.000 0 MHz	Max:	928.000 0 MHz	Result Type:
		Cent:	915.000 0 MHz	Span:	26.000 0 MHz	Int. Val:
						4.648 %

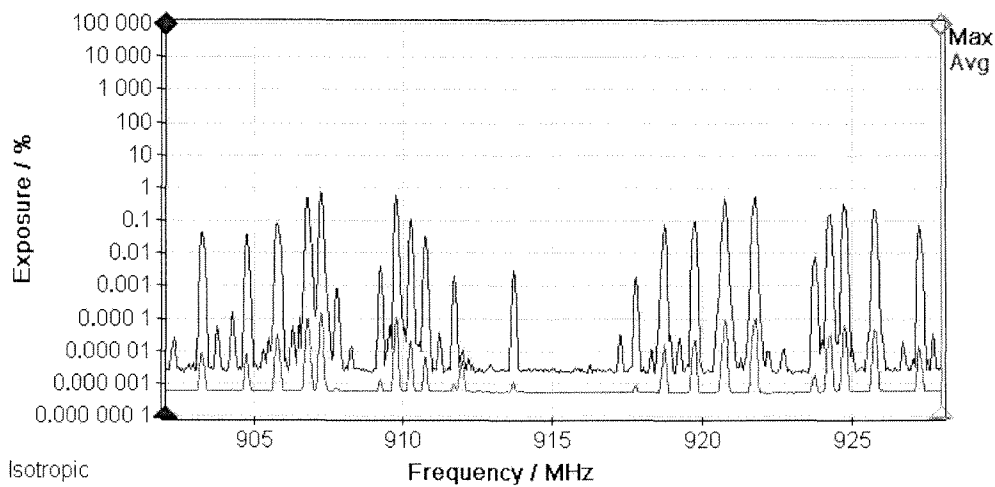


Figure 9-23
Measured maximum (peak) and average RF fields in the 900 MHz band at one foot in front of a nine-meter bank of Smart Meters.

Figure 9-24 provides the measured spectrum of fields at the second meter bank consisting of eleven meters. In this case the integrated composite peak field was 4.9% of the MPE with an integrated composite average field of 0.00124% of MPE.

Battery:		GPS:	33°56'59.9" N	Ant:	3AX 50M-3G SrvTbl:	Ger.Funkd.
08/20/10	12:32:01 PM		118°7'42.0" W	Cable:	--- Stnd:	FCC GP
Integration over Frequency		Min:	902.000 0 MHz	Max:	928.000 0 MHz	Result Type:
		Cent:	915.000 0 MHz	Span:	26.000 0 MHz	Int. Val:
						4.912 %

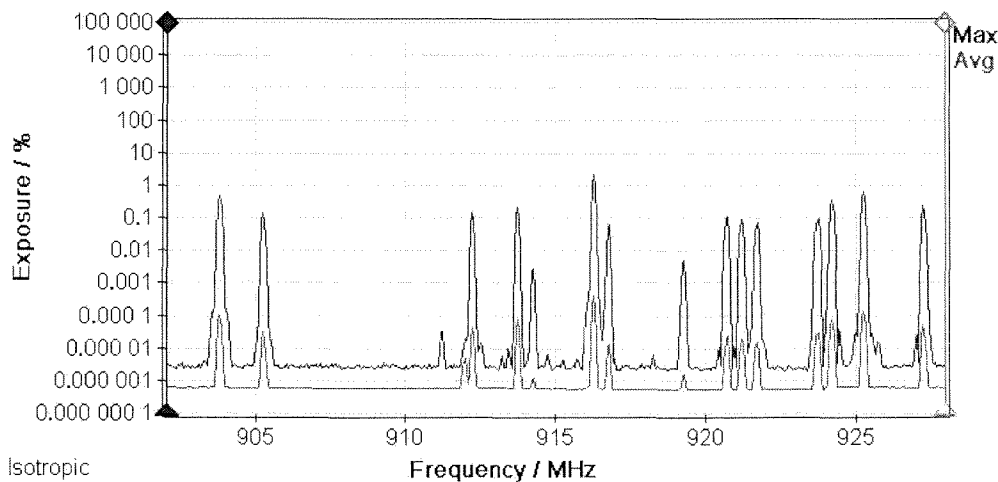


Figure 9-24
Measured maximum (peak) and average RF fields in the 900 MHz band at one foot in front of an eleven-meter bank of Smart Meters.

Neighborhoods with and without Smart Meters

A driving survey of a Downey neighborhood where SCE had deployed Smart Meters was also conducted. Figure 9-25 illustrates the route followed by slowly driving in an automobile with the SRM-3006 probe held out of the front passenger window (see Figure 9-26). The objective of this exercise was to see if Smart Meter RF fields could be detected with the instrumentation used under these conditions and to see if a neighborhood with installed Smart Meters could be distinguished from another neighborhood in which Smart Meters had not been deployed. The resulting accumulative spectrum of peak fields is shown in Figure 9-27. It must be noted that these integrated values of RF field represent the instantaneous peak values of RF fields that were observed on the spectrum analyzer, even

if the field existed for a fraction of a second; for proper comparison to RF exposure standards, time-averaged values of RF fields must be used. Hence, the indicated integrated values are extremely conservative estimates of actual time-averaged exposure. A peak value corresponding to 0.00686% of the FCC MPE was found from the 34 minute drive. Because of the intermittent nature of the Smart Meter signals, peaks would appear from time to time but quickly vanished. While a large number of apparent Smart Meter signals could be observed, the average value of these signals is nearly vanishingly small. This activity was somewhat similar to walking through the Itron meter farm in that signals from the many meters occur randomly, making it difficult to definitely identify any particular meter's emission but relatively easy to observe signals when originating from many different meters.

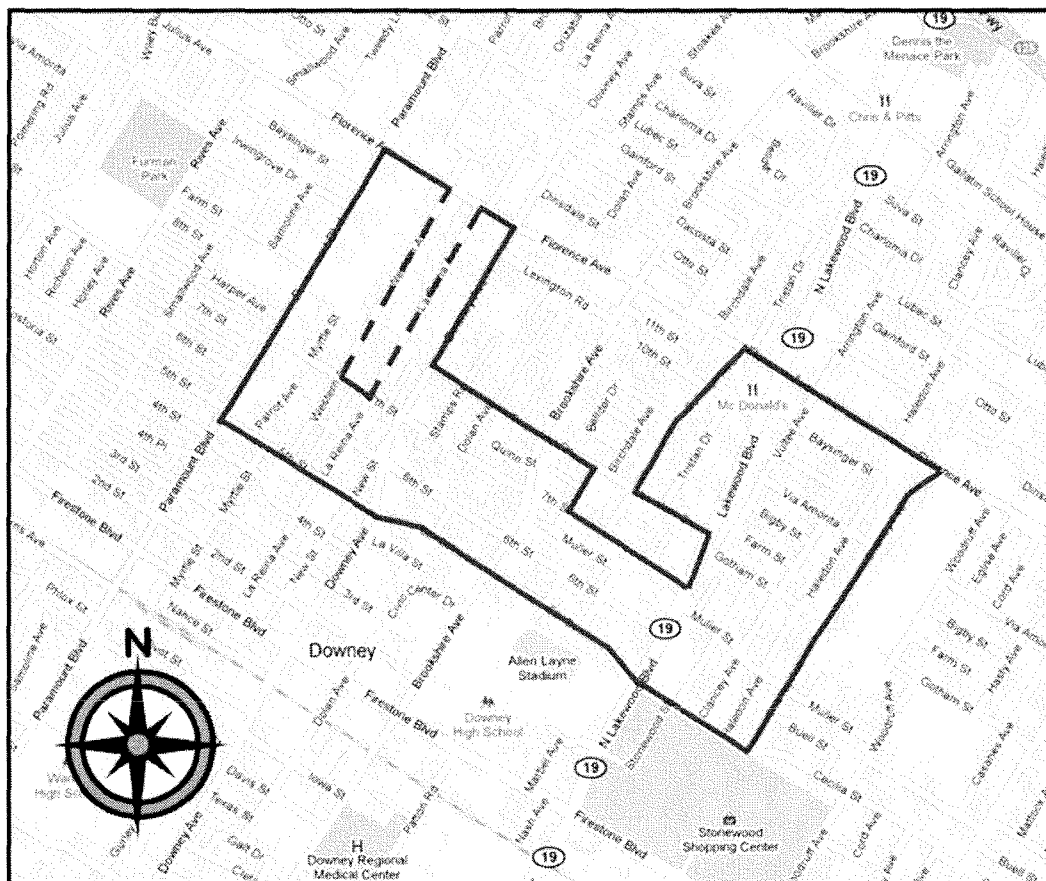
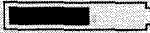


Figure 9-25
Route in Downey, CA neighborhood with SCE deployed Smart Meters over which a driving survey was conducted to test the ability to detect RF signals associated with residential meter installations.



*Figure 9-26
Conducting a "driving survey" of a Smart Meter deployed neighborhood.*

Battery: 	GPS: 33°56'38.9" N	Ant: 3AX 50M-3G	SrvTbl: Ger.Funkd.
08/20/10 11:54:17 AM	118°7'50.9" W	Cable: ---	Stnd: FCC GP
Integration over Frequency	Min: 902.000 0 MHz	Max: 928.000 0 MHz	Result Type: Max
	Cent: 915.000 0 MHz	Span: 26.000 0 MHz	Int. Val: 0.006 86 %

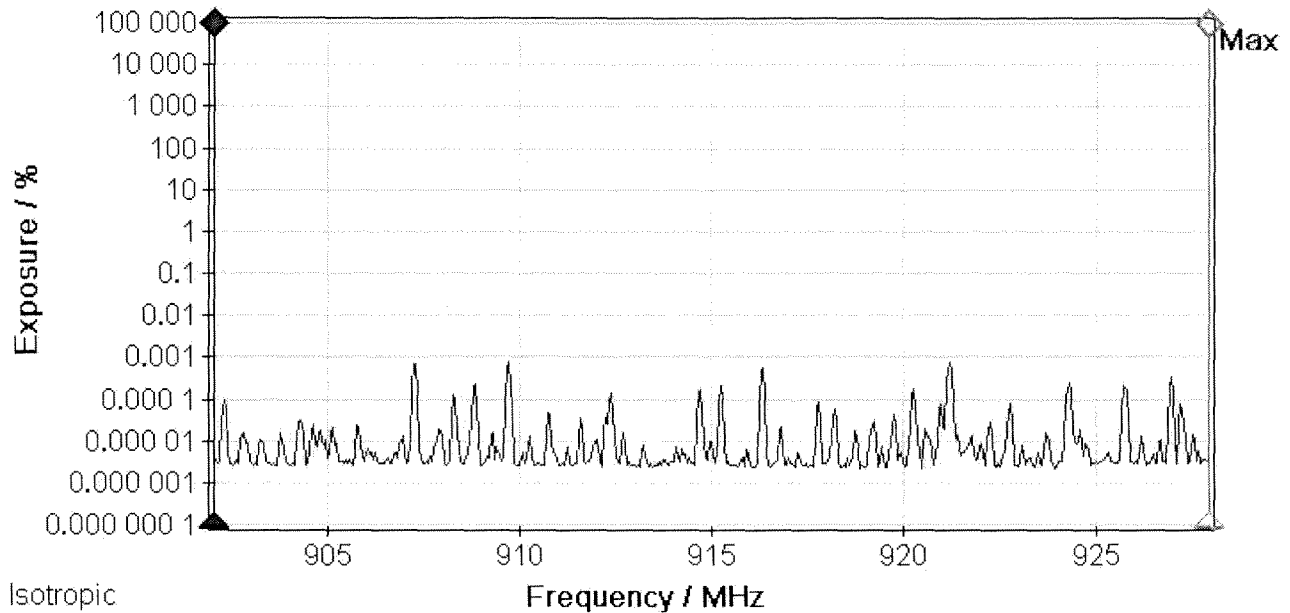


Figure 9-27
 Measured peak spectrum of RF fields detected with the SRM-3006 during traveling the route mapped in Figure 9-25. Fields were monitored for a total of approximately 34 minutes.

To develop a comparative view of neighborhood ambient RF fields in the 900 MHz band, a driving survey through a portion of Santa Monica was conducted in the afternoon of August 20, 2010 (see route map in Figure 9-28). SCE had not yet deployed Smart Meters in Santa Monica at that time. The results of two spectrum scans in which the instantaneous peak fields were monitored are shown in Figures 9-29 and 9-30. These scans reveal a lack of 900 MHz signal activity other than for an occasional emission, perhaps related to

cordless telephones. While the residential neighborhood areas were essentially absent of 900 MHz activity, such was not the case for a commercial district in Santa Monica, as shown in Figure 9-31. As the survey vehicle turned onto a main street in the commercial district, signals were almost immediately noted to appear on the spectrum analyzer. None of these signals were exceptionally strong but they were plentiful during the few minutes spent within the commercial district.

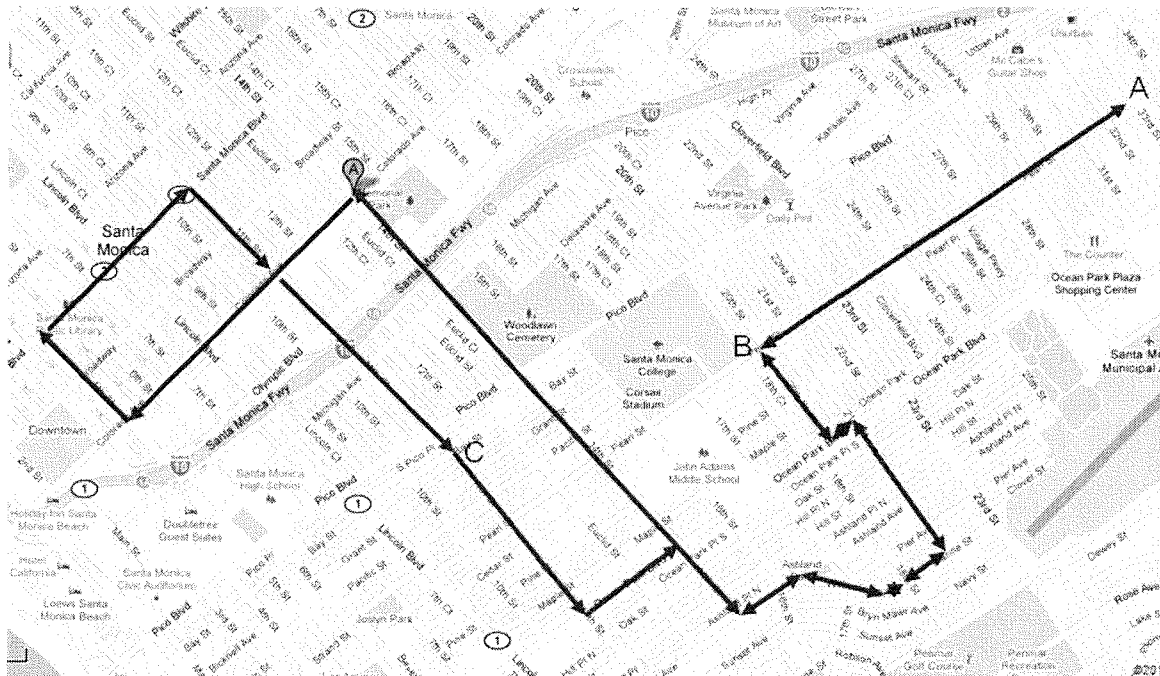


Figure 9-28
Route in Santa Monica, CA neighborhood where SCE Smart Meters have not been deployed over which a driving survey was conducted to test the ability to detect RF signals that might exist in the 900 MHz band.

Battery:		GPS:	33°56'29.2" N Ant:	3AX 50M-3G SrvTbl:	Ger.Funkd.	
08/20/10	12:41:37 PM		118°6'54.4" W Cable:	---	Std: FCC GP	
Integration over Frequency	Min:	902.000 0 MHz	Max:	928.000 0 MHz	Result Type:	Max
	Cent:	915.000 0 MHz	Span:	26.000 0 MHz	Int. Val:	0.000 60 %

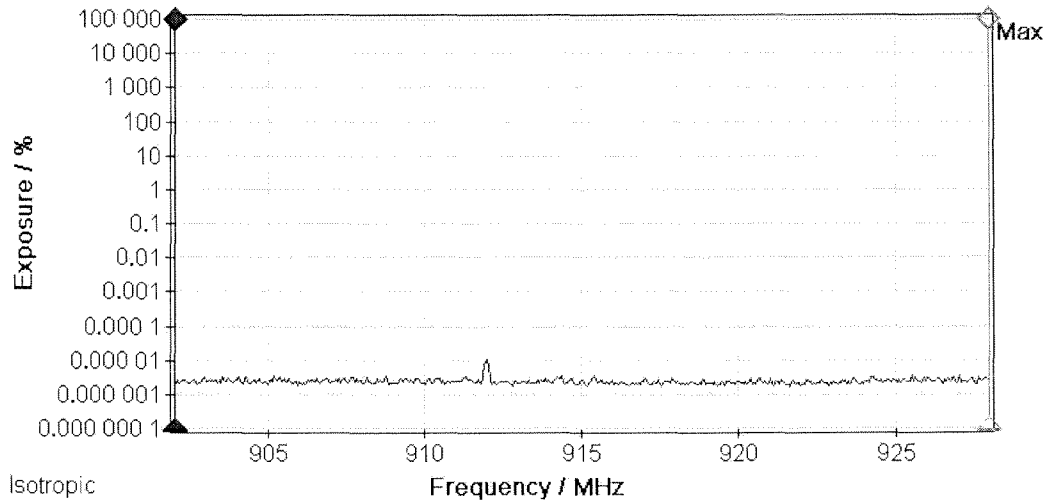


Figure 9-29
Spectrum scan in residential neighborhood of Santa Monica, CA consisting of an approximately 20 minute drive.

Battery:	Ext. Power	GPS:	34°0'37.6" N Ant:	3AX 50M-3G SrvTbl:	Ger.Funkd.
08/20/10	03:14:22 PM		118°27'37.0" W Cable:	--- Stnd:	FCC GP
Integration over Frequency		Min:	902.000 0 MHz	Max:	928.000 0 MHz
	Cent:	915.000 0 MHz	Span:	26.000 0 MHz	Int. Val:
				Result Type:	Max
					0.000 93 %

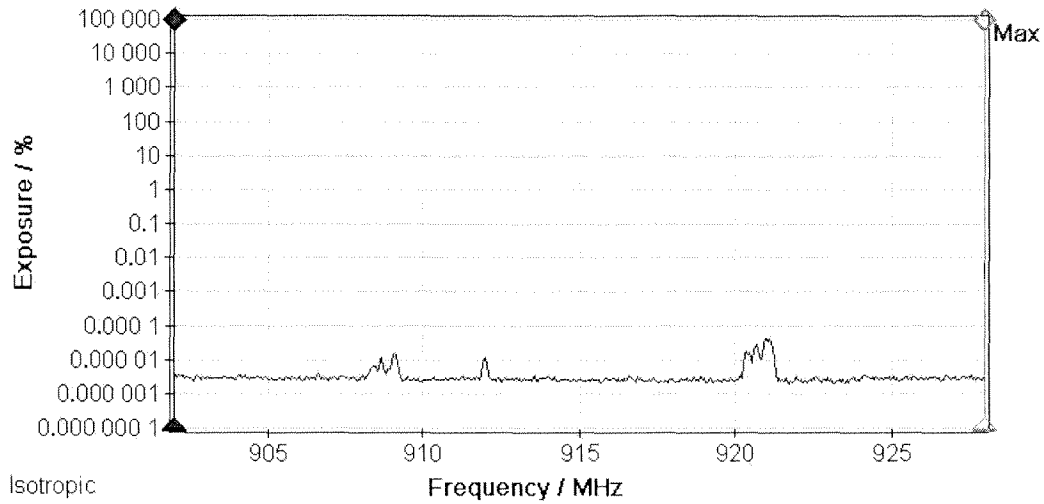


Figure 9-30
Spectrum scan in residential neighborhood of Santa Monica, CA showing weak signals, apparently caused by 900 MHz cordless telephones.

Battery:	Ext. Power	GPS:	34°0'48.6" N Ant:	3AX 50M-3G SrvTbl:	Ger.Funkd.
08/20/10	02:53:02 PM		118°28'44.4" W Cable:	--- Stnd:	FCC GP
Integration over Frequency		Min:	902.000 0 MHz	Max:	928.000 0 MHz
	Cent:	915.000 0 MHz	Span:	26.000 0 MHz	Int. Val:
				Result Type:	Max
					0.001 96 %

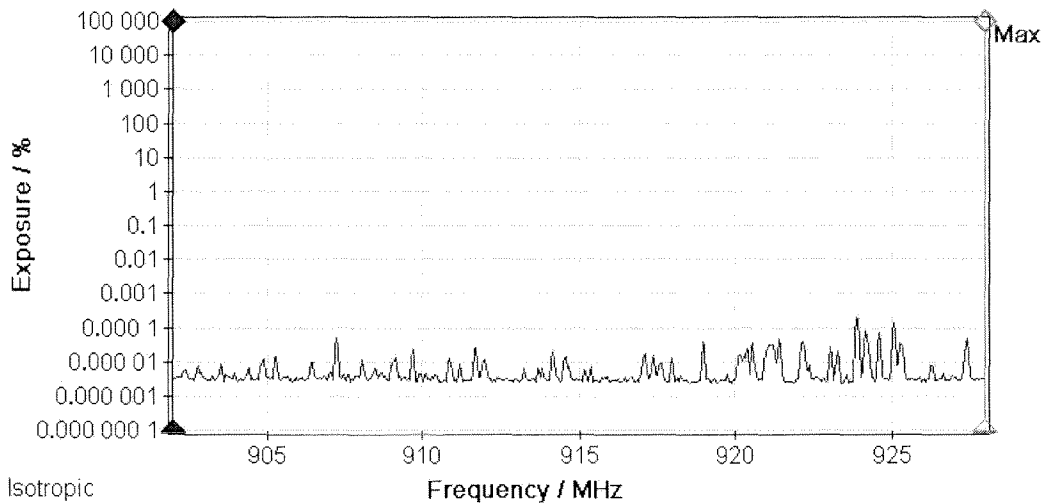


Figure 9-31
Spectrum scan in a commercial district of Santa Monica, CA showing noticeable activity from devices other than Smart Meters.

A second SRM-3006 was used to measure RF fields in several other frequency bands in Santa Monica, CA (The calibration certificates are contained in Appendix A). Measurements included the:

- FM radio broadcast band of 88-108 MHz (Figure 9-32),
- spectrum of 800 to 900 MHz band (Figure 9-33),
- PCS band from 1.9 to 2.0 GHz (Figure 9-34).
- VHF spectrum of 50 MHz to 216 MHz (Figure 9-35), and
- 2.4 to 2.5 GHz band which includes Wi-Fi and microwave ovens (Figure 9-36)

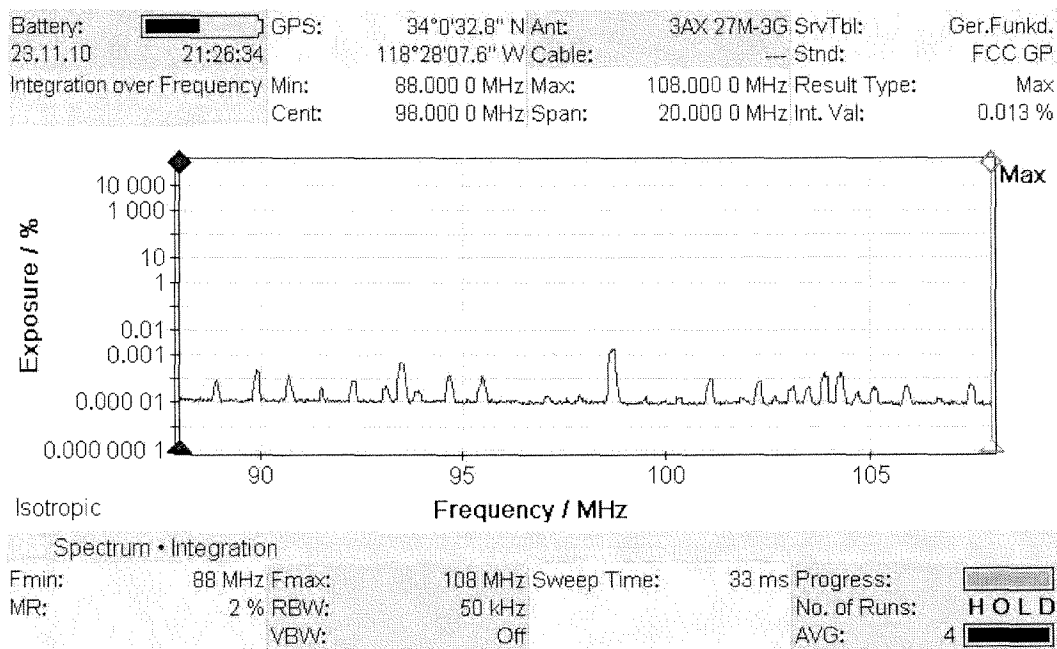


Figure 9-32
Spectrum scan of the FM radio broadcast band in Santa Monica, CA with a band integrated RF field equivalent to 0.013% of the FCC MPE for the public.

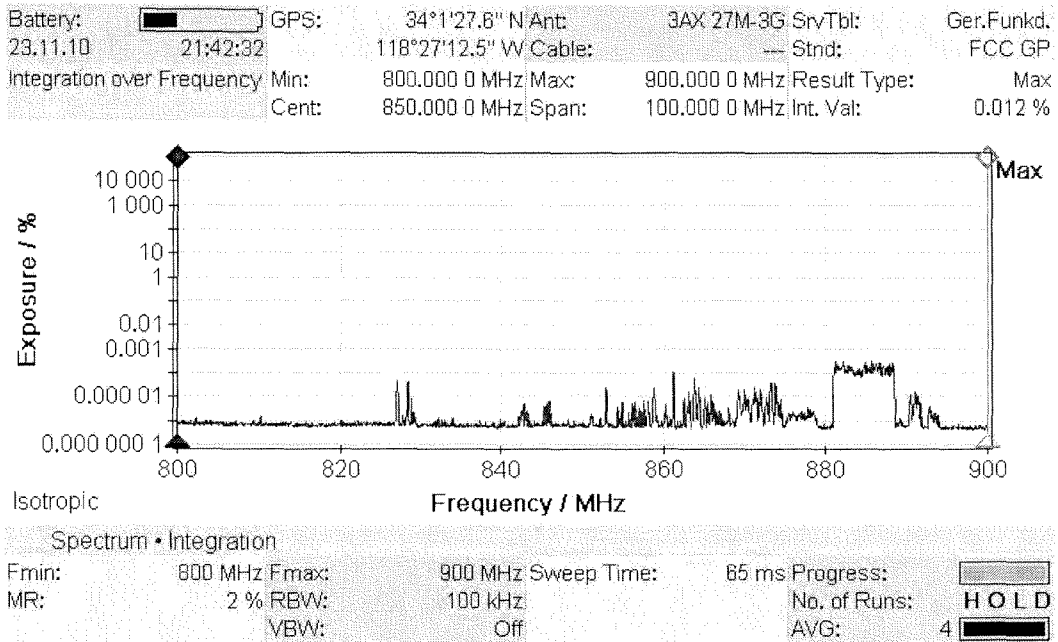


Figure 9-33
Spectrum scan of the 800 MHz to 900 MHz band in Santa Monica, CA, with a band integrated RF field equivalent to 0.012% of the FCC MPE for the public.

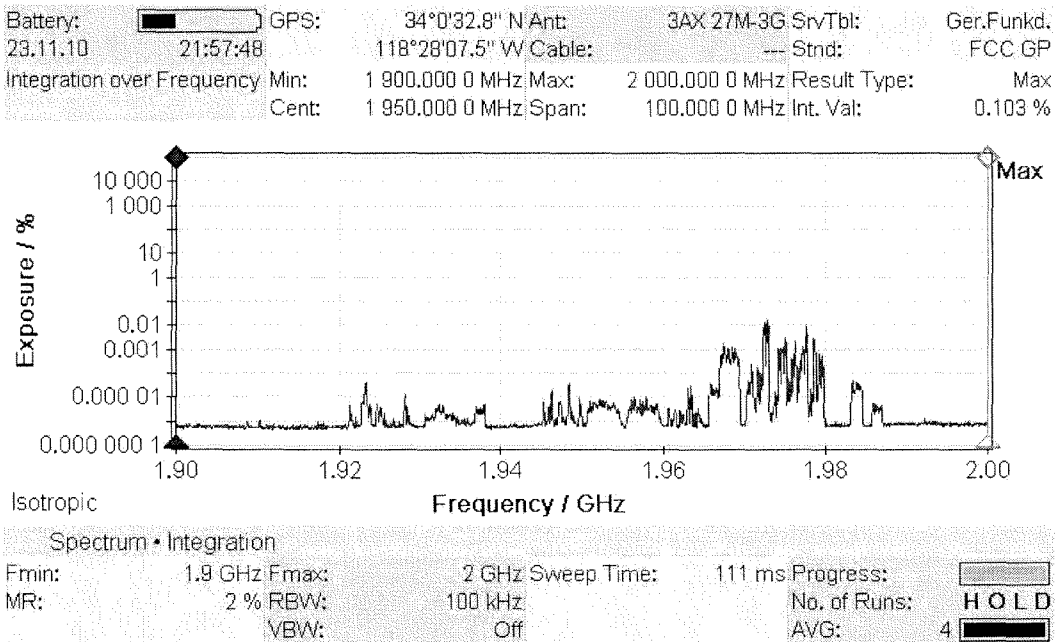


Figure 9-34
Spectrum scan of the 1.9 GHz to 2.0 GHz band in Santa Monica, CA, with a band integrated RF field equivalent to 0.103% of the FCC MPE for the public.

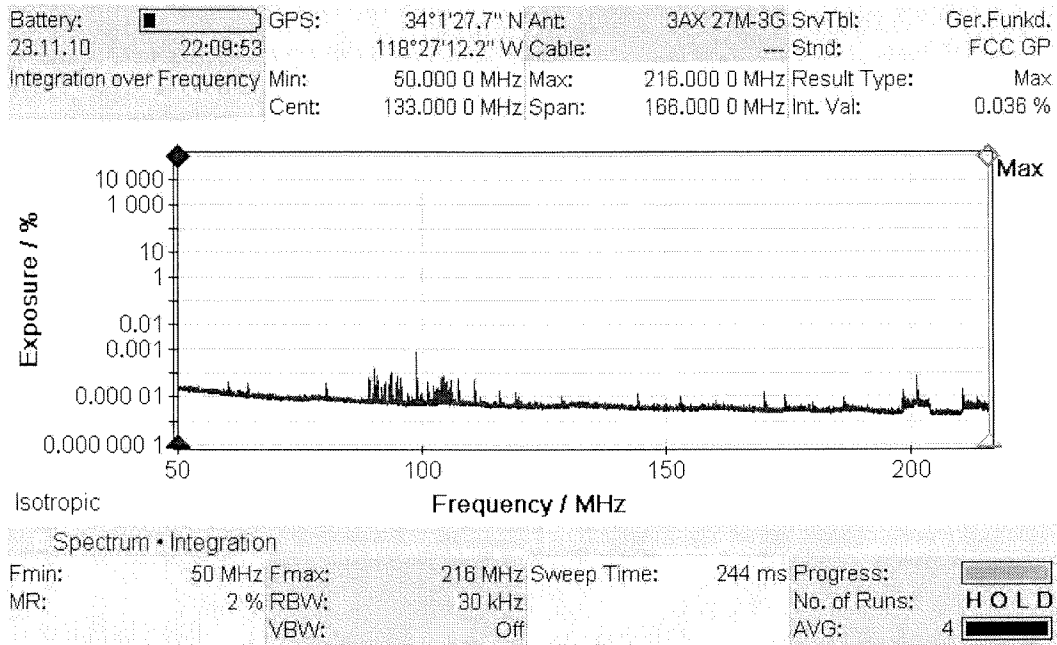


Figure 9-35
Spectrum scan of the 50 MHz to 216 MHz band in Santa Monica, CA, with a band integrated RF field equivalent to 0.036% of the FCC MPE for the public.

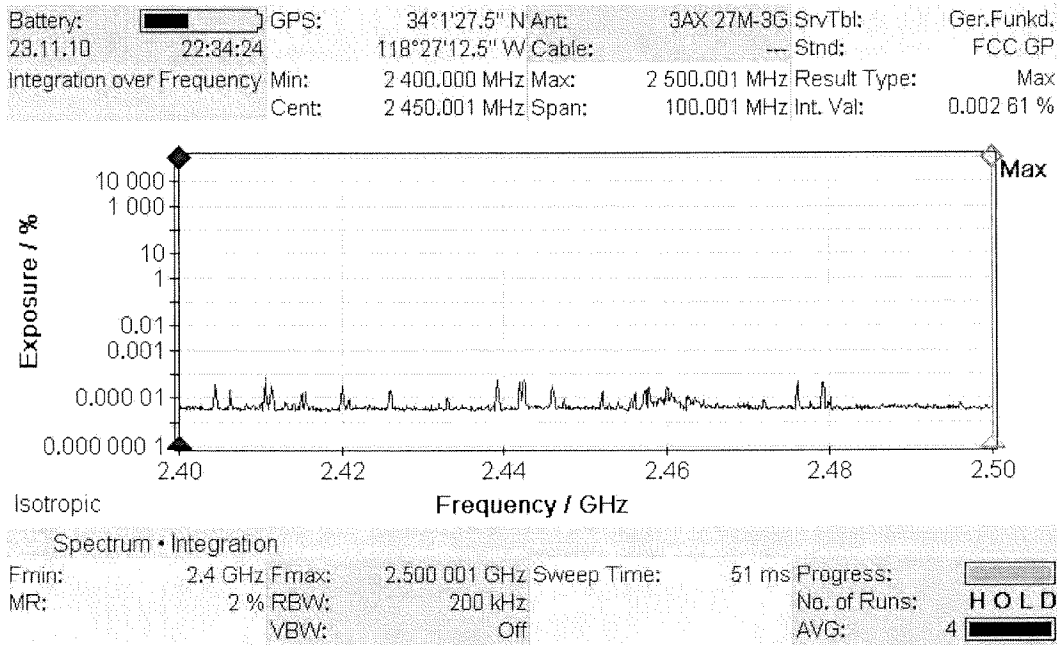


Figure 9-36
Spectrum scan of the 2.4 GHz to 2.5 GHz band in Santa Monica, CA, with a band integrated RF field equivalent to 0.0026% of the FCC MPE for the public.

The spectrum measurements represented in Figures 9-32-9-36 provide some perspective on environmental levels of RF from sources other than Smart Meters. The FM radio broadcast band has, historically, been determined to be a primary contributor to ambient RF fields¹⁵. Because most of the FM broadcasting within the LA region originates from atop Mt. Wilson, a considerable distance from many parts of the metropolitan area, median RF fields, in 1980, were found to be somewhat lower than in some other large

cities. However, with the introduction of cellular telephone base stations, ambient RF fields have likely increased somewhat simply due to the density of cellular and PCS base stations and their distribution among the population. Interestingly, Figure 9-34, which illustrates activity in the PCS band (cellular telephones), indicated the greatest value of peak RF field contribution of the several bands measured in this neighborhood set of measurements with a value equivalent to 0.1% of the FCC MPE.

¹⁵ Tell, R. A. and E. D. Mantiplay (1980). Population exposure to VHF and UHF broadcast radiation in the United States. *Proceedings of the IEEE*, Vol. 68, No. 1, January, pp. 6-12.

Section 10: Shielding Effectiveness Measurements

RF fields can be reduced in strength by introducing conductive materials between the field source and the area to be shielding from the emissions. For example, the metallic meter box within which all electric power meters are installed will attenuate RF fields that may be directed to the back of the meter. This is partially responsible for the reduction in radiated power directly behind Smart Meters tested found in this investigation. While performing the measurements of RF fields associated with Smart Meters in California, a series of measurements of insertion loss afforded by three different types of metal lath was conducted. Metal lath is commonly used in construction of stucco homes, typical of southern California and it was of interest to examine what influence such material might have on Smart Meter RF fields.

Shielding effectiveness of different metal meshes

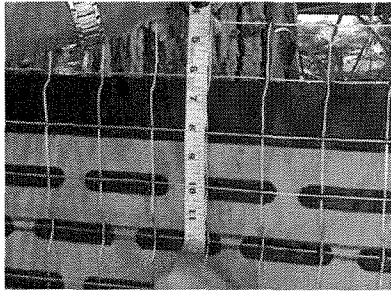
An impromptu measurement of three different metallic meshes was conducted by setting up the specially programmed Smart Meters, one for the 900 MHz band and the other for the 2.4 GHz Zigbee band, measuring the RF field with the SRM-3006 instrument and then placing a sheet of the different meshes between the

Smart Meter and the measurement probe. Figure 10-1 shows this process where the Smart Meter is installed in a specially designed socket to allow convenient operation of the meter in different locations.

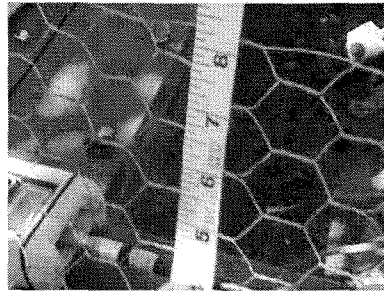
Three different forms of metal lath (mesh/netting) were evaluated at both the 900 MHz and 2.4 GHz frequencies associated with the Smart Meter emissions. Figure 10-2 shows these lath samples. The lath shown in panel A consisted of a square shape, measuring 2 inches on a side. The lath in panel B is what is commonly known as “chicken wire” consisting of hexagonal shaped openings approximately one inch by one inch. The lath in panel C was comparatively, significantly smaller in dimension, measuring approximately one-quarter inch by one-half inch for the openings. The lath in panel C is more commonly used in plaster work as opposed to exterior stucco application but is also used in application of exterior rock surfacing in some areas of the country. Insertion loss measurement results for the different types of metal lath are given in Table 10-1. Insertion loss is expressed in linear units as a reduction factor and logarithmically as decibels (dB). These data are presented graphically in Figure 10-3.



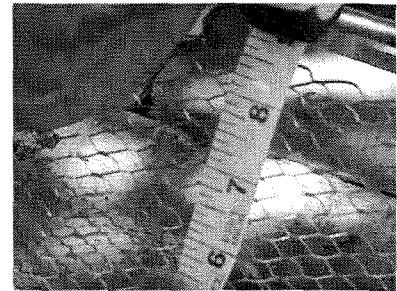
Figure 10-1
Measurement setup to determine the insertion loss presented by a conductive mesh (chicken wire in this case).



2" x 2"



1" x 1"



0.25" x 0.5"

Figure 10-2
Measurement setup to determine the insertion loss presented by a conductive mesh (chicken wire in this case).

Table 10-1
Insertion loss measurement results for three different types of metal lath expressed as a reduction factor (F) and in decibels (dB).

Frequency band	Panel A lath		Panel B lath		Panel C lath	
	F	dB	F	dB	F	dB
900 MHz	2.5	4.1	8.9	9.5	82	19.1
2.4 GHz	1.3	1.2	2.6	4.2	14	11.4

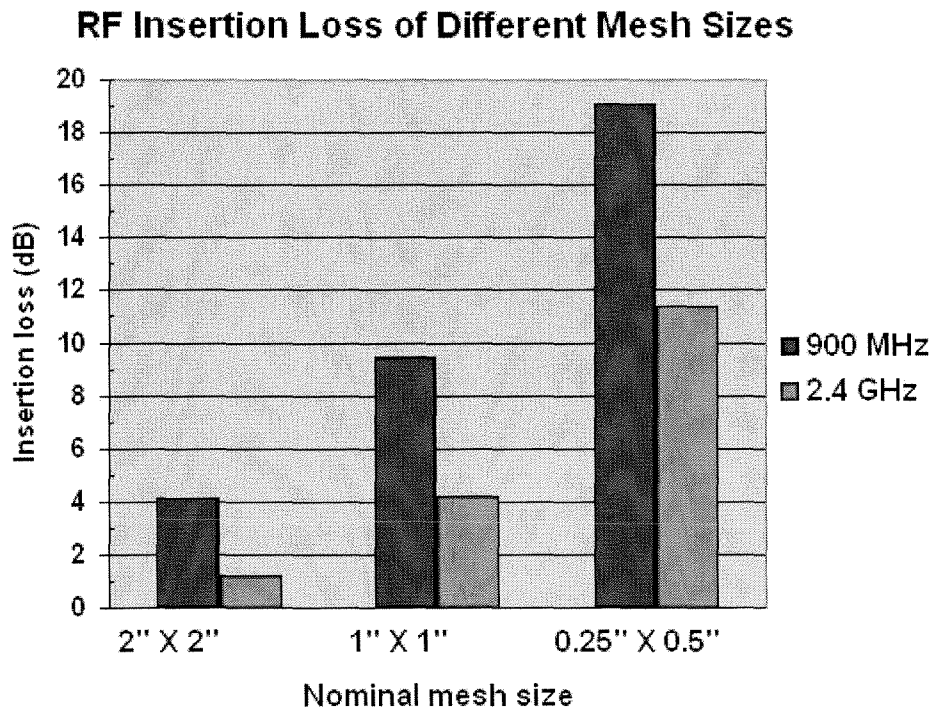


Figure 10-3
Insertion loss of three different metal mesh sizes.

The data given in Table 10-1 and shown in Figure 10-3 show an expected increase in insertion loss (attenuation) of RF fields with decreasing mesh size and a decrease in insertion loss with the higher frequency band. With the relatively large 2" by 2" mesh, the least insertion loss was associated with the 2.4 GHz band. The greatest insertion loss was for the longer wavelength emission in the 900 MHz band and the finest mesh size. The data suggest that the chicken-wire type netting commonly used in stucco home construction can afford significant reductions in RF fields that may enter the home ranging from 4.2 dB to 9.5 dB. This range corresponds to mesh transmissions of 38% in the 2.4 GHz band and 11% in the 900 MHz band.

Shielding effectiveness of a simulated stucco wall

To more completely evaluate the attenuation exhibited by a typical stucco wall, as might be found in southern California homes, a simulated wall section was constructed in Colville, WA. The wall was built as a 4 feet wide by 8 feet tall section on a support with casters to allow mobility. The wall was constructed with 2x4 dimensional lumber with studs on 16 inch centers with the "outside" wall sheathed with 7/16" OSB (oriented strand board). This sheathing was then covered with one layer of underlayment paper (Davis Wire All Purpose Super Kraft Asphalt Sheathing Paper) followed with the "chicken wire" lath being stapled onto the wall section (Davis Wire "self-furr" stucco netting, woven 17 gauge, 1.5 inch by 2.25 inch mesh opening). Two coats of stucco (Spec Mix® Scratch & Brown Preblended Stucco), including a base scratch coat followed with a brown coat, were applied to the lath. Each coat was allowed to set for several days. R-13 fiberglass insulation (Owens Corning with Kraft facing) was placed between the studs and the "interior" side of the wall was then covered with half-inch sheetrock (dry wall). Appendix F shows the wall during construction and Figures 10-4 and 10-5 show it set up with a Smart Meter positioned on a shelf on the "outside" wall surface with the two different measurement antennas supported on a tripod.

Measurements were conducted using the Wi-Spy spectrum analyzer device described earlier. The Wi-Spy unit was evaluated prior to its use by injecting swept signals from a communications monitor (IFR Model 2975) and using the Wi-Spy to acquire a large number of scans of the 900 MHz and 2.4 GHz bands. The Wi-Spy was determined to exhibit a response across each band that was within the range of ± 0.5 dB. A yagi antenna was established on a support and directed toward a Smart Meter programmed for continuous operation without the wall in place. The Smart Meters¹⁶ were positioned approximately 1 inch from the stucco surface of the wall to the rear surface of the meter and 58 inches from the ground to the center of the meter. RF field strength was then measured without the wall and with the wall in place to assess insertion loss. The measurement antenna and the Smart Meter was not moved during this process; only the wall was removed and replaced for the measurements with and without the wall. For the 900 MHz band, the five element yagi antenna was an M² Antenna Systems, Inc. Model 911-ISP (with 11 dBi gain) set 37 inches from the backside of the simulated wall to the end of the antenna boom and at the same height as the center of the Smart Meter. For the 2.4 GHz band, the yagi antenna was an Air802, LLC Model ANYA2412 (with 12 dBi gain) set 47 inches from the backside of the simulated wall to the end of the antenna boom. Figure 10-4 shows the 900 MHz yagi antenna in place for measuring the RF field behind the simulated wall. The 2.4 GHz yagi is shown during measurements of the attenuation of the wall in the higher frequency band in Figure 10-5.

For each frequency band, a series of five repeated measurements were performed of the received signal strength, measured in dBm, for horizontal and vertical polarizations. Table 10-5 summarizes the measurement data from which insertion loss values for the 900 MHz band and 2.4 GHz bands were determined. A representative view of the Wi-Spy spectrum analyzer display is seen in Figure 10-6.

¹⁶ Model CL200, 902.25 MHz, SCE# 222010-273722. Model CL200, 2405 MHz, SCE# 222010-273720.

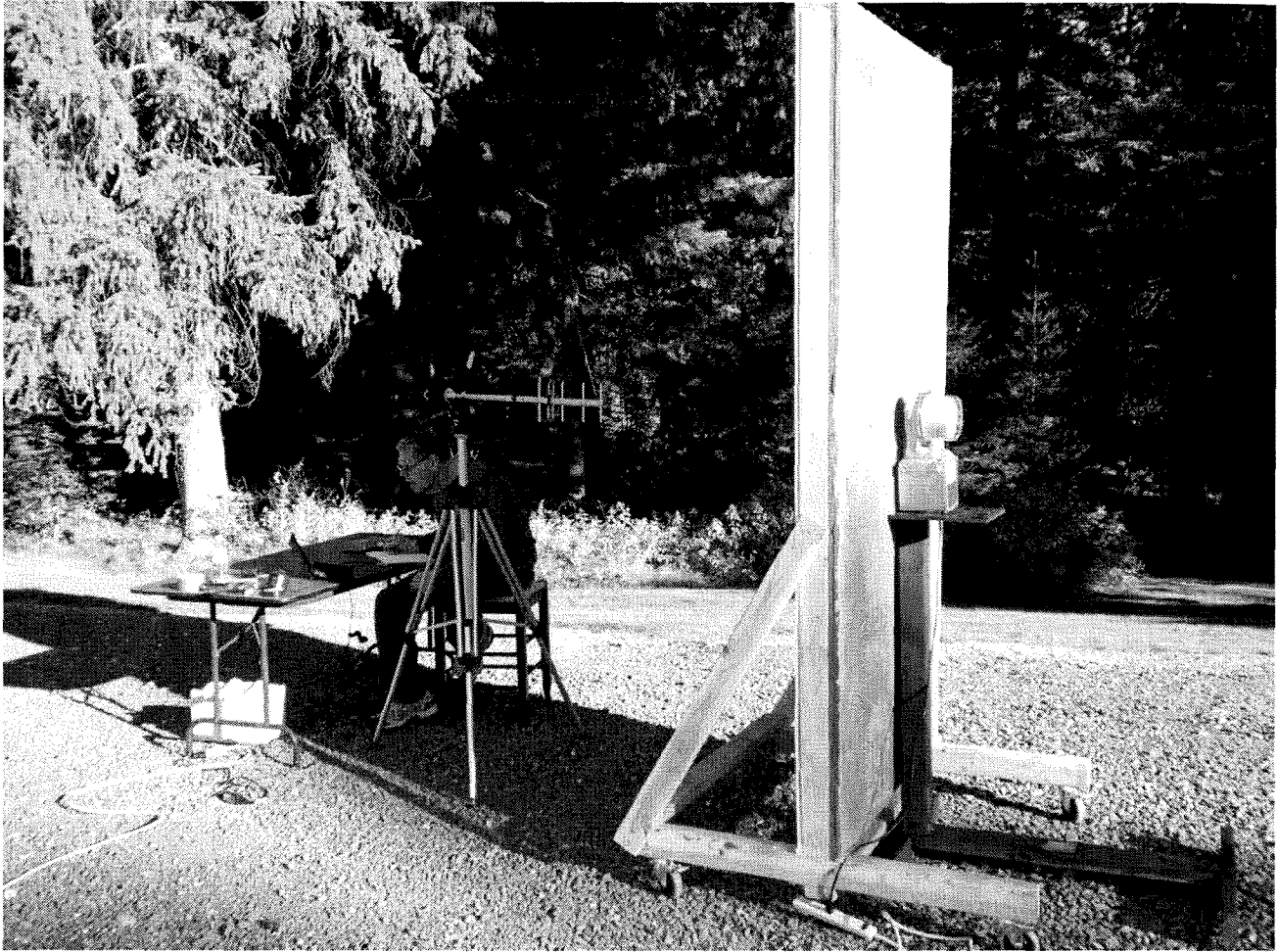


*Figure 10-4
Measurement setup for determining insertion loss of simulate stucco wall shown with the 900 MHz yagi antenna.*

The data in Table 10-2 show that, under the measurement conditions used, the simulated stucco wall offered an overall average insertion loss (attenuation) of the Smart Meter RF fields of 6.1 dB in the 900 MHz RF LAN band and 2.5 dB in the 2.4 GHz Zigbee band. These data are consistent with the earlier measurements of insertion loss of different dimension metallic lath materials using the isotropic probe of the SRM-3006 instrument. Differences between the two sets of measurements are likely due to the different dimensions of the wire netting (1.5 inches in this case), inclusion of the wall building materials and the different measurement distances used. In the case of the earlier

described measurements, the measurement probe was located 6 inches from the various mesh materials compared to between 37 and 47 inches in the simulated wall measurements. Further, the isotropic measurements were made with the Smart Meter source placed 6 inches from the mesh and directed toward the mesh; some degree of interaction with the RF transmitters could be expected that could also contribute to differences in measured values of insertion loss. In the simulated wall measurements, the back of the meter was placed within 1 inch of the stucco with its underlying metallic netting.



*Figure 10-5
Measurement setup for determining insertion loss of simulate stucco wall shown with the 2.4 GHz yagi antenna.*

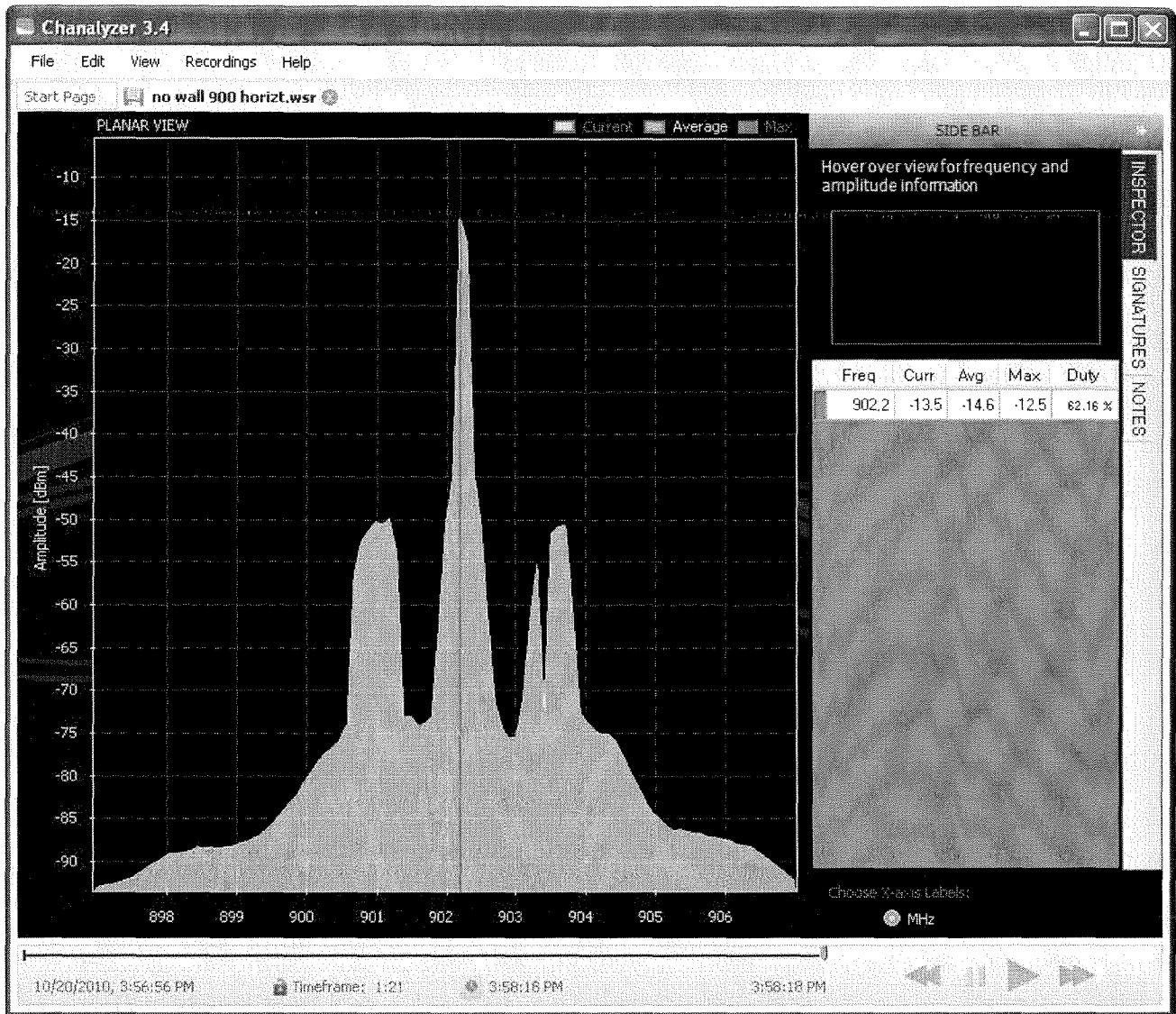


Figure 10-6
 Illustrative display of the Wi-Spy spectrum analyzer display showing the captured average signal measured over a period of 81 seconds from a 900 MHz RF LAN Smart Meter transmitter. In this measurement, the simulated wall was not present. Marker readout data are shown on the right side of the display.

Table 10-2

Insertion loss measurement data for simulated wall in 900 MHz and 2.4 GHz bands.

Frequency (MHz)	Trial	Signal level (dBm)				Insertion loss (dB)
		No wall		With wall		
		Horizontal	Vertical	Horizontal	Vertical	
902.25	1	-14.5	-18.2	-22.5	-21.8	6.2
902.25	2	-14.5	-18.0	-22.5	-21.5	6.1
902.25	3	-14.5	-18.3	-22.6	-21.4	6.0
902.25	4	-14.5	-18.0	-22.5	-21.6	6.1
902.25	5	-14.5	-18.1	-22.5	-21.6	6.1
					Mean±SD	6.1±0.1
2405	1	-30.7	-34.7	-34.7	-35.6	2.9
2405	2	-30.5	-35.0	-34.8	-35.2	2.8
2405	3	-30.7	-35.3	-34.5	-34.5	2.1
2405	4	-30.3	-35.2	-34.6	-33.8	2.1
2405	5	-30.3	-35.2	-34.4	-34.6	2.4
					Mean±SD	2.5±0.4